Sussex Research Online

Recent advances in the coordination chemistry of benzotriazole-based ligands

Article (Accepted Version)

Loukopoulos, Edward and Kostakis, Georgios E (2019) Recent advances in the coordination chemistry of benzotriazole-based ligands. Coordination Chemistry Reviews, 395. pp. 193-229. ISSN 0010-8545

This version is available from Sussex Research Online: http://sro.sussex.ac.uk/id/eprint/84085/

This document is made available in accordance with publisher policies and may differ from the published version or from the version of record. If you wish to cite this item you are advised to consult the publisher's version. Please see the URL above for details on accessing the published version.

Copyright and reuse:
Sussex Research Online is a digital repository of the research output of the University.

Copyright and all moral rights to the version of the paper presented here belong to the individual author(s) and/or other copyright owners. To the extent reasonable and practicable, the material made available in SRO has been checked for eligibility before being made available.

Copies of full text items generally can be reproduced, displayed or performed and given to third parties in any format or medium for personal research or study, educational, or not-for-profit purposes without prior permission or charge, provided that the authors, title and full bibliographic details are credited, a hyperlink and/or URL is given for the original metadata page and the content is not changed in any way.

http://sro.sussex.ac.uk

Recent advances in the coordination chemistry of benzotriazole-based ligands

Edward Loukopoulos and George E. Kostakis*

Department of Chemistry, School of Life Sciences, University of Sussex, Brighton BN1 9QJ, UK.

e-mail: G.Kostakis@sussex.ac.uk

Keywords: benzotriazole, nitrogen ligands, coordination clusters, coordination polymers, magnetic properties, catalysis

Contents

Abstract

With the use of *N*-donor ligands in coordination chemistry receiving significant interest and attention in the last few decades, benzotriazole has emerged as an ideal molecule that provides many synthetic advantages and reliable routes towards polynuclear coordination clusters and coordination polymers. In order to fully realise this potential, the current work provides a systematic study of the recent advances on the use of benzotriazole and its derivatives as ligands in coordination chemistry. The reported complexes have been primarily categorized in regards to the exact linker used and its role in the resulting architecture (either as a main or as a secondary ligand). Important structural information, as well as notable properties (such as magnetism, catalysis, luminescence, bio-applications) are also mentioned for the compounds.

1. Introduction

Benzotriazole (Hbta) is an aromatic heterocyclic compound that has been widely popular in organic as well as inorganic chemistry. It belongs in the general category of azoles, along with other well-known heterocyclic molecules such as pyrazole, imidazole, 1,2,3-triazole, 1,2,4-triazole and tetrazole. Hbta contains a benzene ring that is fused with a five-membered aromatic ring which incorporates the 1,2,3-triazole moiety. Since the proton in this moiety can easily relocate between the nitrogen atoms, Hbta can exist in two tautomeric forms, 1H- and 2H-Benzotriazole (Scheme 1, Forms **A** and **B** respectively). Investigation of this phenomenon has been the subject of multiple studies[1–6] throughout the years, which showed that the 1H-tautomer (**A**) is the predominant species in solution. This has been attributed to its high dipole moment (μ = 4.3 D in **A**, 0.38 D in **B**, according to theoretical calculations) which favours interactions with the solvent and therefore provides better solvation than in the case of the 2H-tautomer[7]. These spectroscopic studies as well as X-Ray crystallography[8] have also shown that the 1H-tautomer is the only stable isomer found in the solid state.

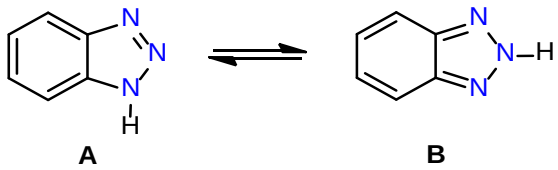

Scheme 1. The two tautomeric forms in Hbta.

Historically, the synthesis of the first benzotriazole derivative dates back to the late 19th century. A study by Zinin in 1860 reports efforts towards the nitration of azoxybenzene[9]. One of the afforded products was 2-phenylbenzotriazole-1-oxide, although this was not recognised until 1899 by Werner and Stiasny[10]. Other studies in that period by Hofmann[11] and Ladenburg[12] investigated the effect of nitrous acid on various phenylenediamines, noting that the use of o-phenylenediamines resulted in products with unique properties compared to the rest. These products were later found to be benzotriazole derivatives and the synthetic method to obtain Hbta remains similar today (Scheme 2), albeit with certain improvements in the reaction conditions[13].

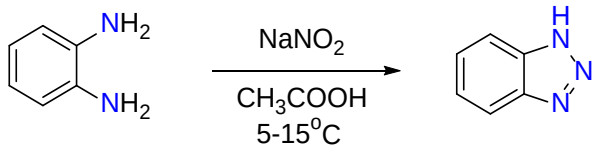

Scheme 2. Common synthetic method to obtain benzotriazole.

The popularity of benzotriazole derivatives amongst organic chemists is in no small part due to their attractive properties. Hbta is an odourless, non-toxic, non-sensitive chemical that shows excellent solubility in a variety of organic solvents and is almost insoluble in water. Additionally, it is inexpensive and easy to synthesize. More importantly, Hbta exhibits both electron donating and electron attracting capabilities; it can either act as a weak acid (pKa = 8.2) through proton loss, or as a very weak Brønsted base (pKa < 0) through accepting a proton using the lone pair electrons available on the nitrogen atoms. As such, it is also soluble in aqueous Na_2CO_3 as well as HCl, meaning that it can be easily separated from reaction mixtures. Finally, its ring system shows remarkable thermal (up to 400°C) and chemical (in the presence of H_2SO_4, KOH, $LiAlH_4$ etc.) stability. For these reasons, benzotriazole and its derivatives have been extensively used in synthetic organic chemistry as auxiliary tools towards a great range of reactions and syntheses. Relevant work by Katritzky should be noted in particular, as his group contributed more than 600 research papers as well as multiple reviews and books related to this field in the span of three decades. This enormous work revolving around the synthetic utilities of benzotriazole derivatives extends well beyond the scope of this review. Characteristic examples include benzotriazole-mediated alkylation reactions or the synthesis of heterocycles, peptides and amino-acid derivatives[14,15].

However, the unique properties and synthetic versatility of Hbta are not limited within the realm of synthetic organic transformations. In 1947, Procter and Gamble Ltd submitted a patent[16] on the use of Hbta as a corrosion inhibitor for metallic copper. In particular, subjection of copper to a solution containing Hbta formed a barrier layer that was insoluble in water and many organic solvents, protecting the metal from potential surface reactions. Subsequent studies[17] by Cotton and co-workers in the 1960s suggested that this protective layer consisted of a polymeric Cu^{I}-bta complex in which each benzotriazole molecule is deprotonated and uses its two non-central

nitrogen atoms of the 1,2,3-triazole moiety to coordinate to two different copper centres, forming a linear polymeric structure (Scheme 3).

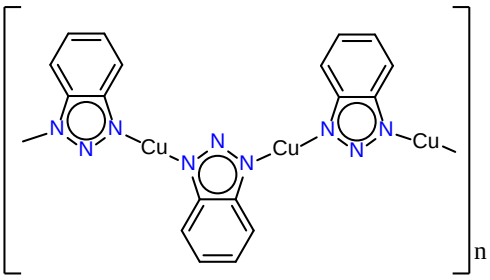

Scheme 3. Proposed structure of the formed copper-benzotriazole complex as suggested by Cotton and co-workers.

As a result of these reports Hbta was introduced in inorganic synthesis as a potential ligand towards the formation of coordination complexes. The first related coordination compound that was characterized by X-Ray crystallography was presented in 1976 when Meunier-Piret and co-workers reported[18] the structure of a Ni^{II}/benzotriazole coordination complex, while studies in the 1980s also investigated the coordination capabilities of Hbta with other transition metals[19,20]. However, the increased popularity of *N*-donor linkers in the late 1990s allowed researchers to fully realize the advantages that benzotriazole-based ligands could offer in coordination chemistry: (i) being *N*-donor ligands, they can provide dynamic and flexible frameworks[21]; (ii) the 1,2,3-triazole moiety provides multiple potential coordination modes and allows Hbta to be utilized as a terminal or a bridging ligand (Scheme 4); (iii) they can participate in various interactions (e.g. hydrogen bonds, $\pi\cdots\pi$ stacking) which stabilize the resulting structures and provide a better understanding of the system; (iv) due to the synthetic versatility of Hbta it is very easy to synthesize benzotriazole-based ligands with various levels of flexibility, although in some cases it can be difficult to separate the resulting 1H- and 2H-isomers.

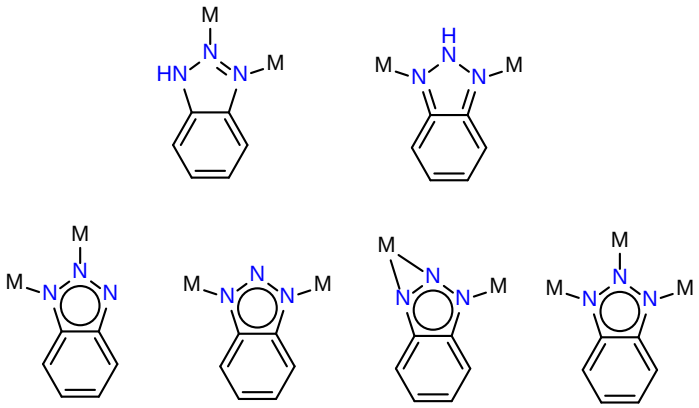

Scheme 4. Bridging coordination modes of benzotriazole (top, modes $\mu_{2,3}$, $\mu_{1,3}$) and benzotriazolate (bottom, modes $\mu_{1,2}$, $\mu_{1,3}$, μ-η^2:η^1, $\mu_{1,2,3}$).

As a result of the above, a search in the Cambridge Structural Database (CSD)[22] for coordination compounds based on benzotriazole-derived ligands reveals a high number of studies with the majority published after 2000. However, the relevant reviews on this subject are surprisingly scarce. In 2010 Mohamed reported[23] the coordination chemistry of various *N*-donor ligands employing coinage metals, yet only complexes based on 1,2,4-triazole are mentioned. A review by Aromí and co-workers in 2011 presents the use of triazole and tetrazole ligands in coordination chemistry and includes some examples of benzotriazole-based complexes[24]. Similarly, a 2012 review[25] by Zhang covers the subject of metal azolate frameworks, however only a few selected cases are mentioned in regards to benzotriazolate compounds. Notably, Shi and Cheng recently reviewed the chemistry of N-heterocyclic carboxylic acids, providing significant synthetic coordination aspects of this particular framework. [26] In order to fully realise the potential of benzotriazole-based linkers in coordination chemistry, as well as update the existing bibliography, this review will present a more detailed, non-exhaustive list of related coordination complexes covering the literature as of February 2019. This list will include certain structural information on the compounds as well as notable reported applications. In order to facilitate this presentation, the complexes have been primarily categorized in regards to the exact linker used (Hbta or some derivative) and its role in the resulting architecture (either as a main or as a supporting co-ligand).

2. Benzotriazole as a Main Ligand

2.1. Polynuclear Coordination Clusters

Long-time investigations of the coordination capabilities of Hbta using M^{II} transition metals have shown that the system frequently leads towards polynuclear coordination complexes with similar structural motifs. Notably, a family of pentanuclear compounds with the general formula $[M_5(OH)_x(bta)_{6-x}(acac)_4(H_2O)_{4x}]$ (where M = Cu^{II}, Ni^{II}, acac = acetylacetonate, x = 0, 1) have been commonly reported[27–29] in previous decades. These compounds consist of four penta-coordinated M^{II} centres that are found in the corners of an imaginary tetrahedron, while the fifth M^{II} ion is found at the centre of this arrangement and is hexa-coordinated. These metal centres are bridged exclusively by deprotonated benzotriazole (bta) molecules in a $\mu_{1,2,3}$-bridging fashion, as the N1, N3 nitrogen atoms coordinate to metal ions of the tetrahedron while the six N2 atoms coordinate to the central octahedral metal. The remaining coordination sites are occupied by oxygen atoms deriving from acetyloacetonate units, which simply act as chelating terminal ligands. In 2008, Biswas and co-workers reported[30] the synthesis of a Zn_5 complex with the same structural characteristics (Figure 1), formulated as $[Zn_5(bta)_6(acac)_4]$ (**1**), based on the room temperature reaction of $Zn(acac)_2$ and Hbta in CH_2Cl_2.

Interestingly, a study[31] by Raptopoulou and co-workers in 2009 showed that the same reaction in DMF yields the analogous compounds $[Zn_5(bta)_6(acac)_4(DMF)]\cdot DMF$ and $[Zn_5(bta)_6(acac)_4(DMF)]\cdot 3.7DMF$ (**2** and **3**), however higher nuclearity may be achieved when the reaction takes place at high temperature and in the presence of pyrazine. The afforded product in this case is a nonanuclear compound, formulated as $[Zn_9(bta)_{12}(acac)_6]\cdot 6DMF$ (**4**). Its structure contains seven Zn^{II} centres that are found at the corners of two corner-sharing imaginary tetrahedra, and a Zn^{II} ion at the centre of each tetrahedron (Figure 2). As such, this motif may be best described as the addition of two tetrahedral units from **1** with the abstraction of one Zn^{II} centre and two $acac^-$ molecules. The benzotriazole molecules also exhibit a similar coordination mode. Further efforts[32] by Volkmer's group resulted in the construction of two more nonanuclear complexes with similar structural motif and coordination characteristics, formulated as $[Ni_9(bta)_{12}(NO_3)_6(MeOH)_6]\cdot 4THF$ (**5**) and $[Co_9(bta)_{12}(MeOH)_{18}]\cdot(NO_3)_6\cdot 9C_6H_6$ (**6**). Instead of pyrazine, the authors employ a very large excess of Hbta during the synthetic procedure, with metal:ligand ratios of 1:4 and 1:8 respectively. Due to this, the excess ligand acts as the base to

deprotonate the coordinated bta molecules. Additionally, magnetic measurements were also performed for **5 – 6**, revealing the presence of antiferromagnetic interactions between the metal ions in each case. A pseudopolymorph of **5**, formulated as $[Ni_9(bta)_{12}(NO_3)_6(DMA)_6]\cdot 3DMA$ (**7**) was also reported recently by Zhang and co-authors[33]. In this case, the compound was synthesized through the use of solvothermal conditions. Expectedly, **7** showed similar magnetic behaviour compared to **5**, with antiferromagnetic interactions among the Ni^{II} ions.

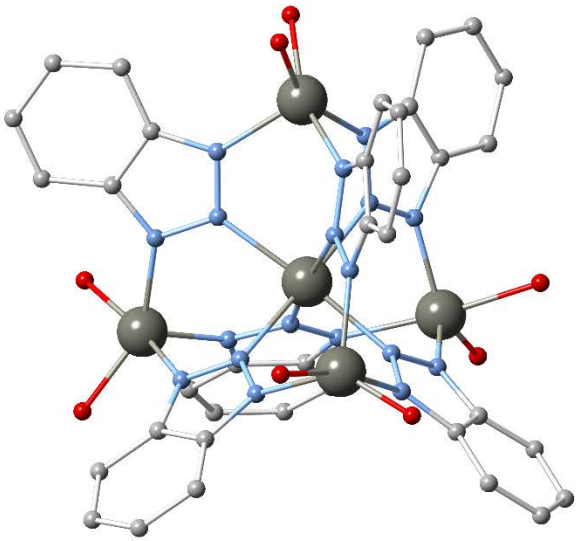

Figure 1. The pentanuclear motif as observed in compound **1**. Hydrogen atoms and parts of the acetyloacetonates are omitted for clarity. Colour code Zn (grey), C (grey), N (light blue), O (red).

Another example of the pentanuclear structural motif was reported by Yuan and co-workers, who synthesized a mixed valent complex that contains four Cu^{I} ions in the corners of the imaginary tetrahedron and a Cu^{II} ion in the centre[34]. The resulting compound is formulated as $[Cu^{II}Cu^{I}_4(bta)_5Cl(PPh_3)_4]$ (**8**). The bta molecules exhibit a similar coordination mode as they bind to the Cu^{II} ion through the N2 atom and bridge two Cu^{I} centres with the remaining nitrogen atoms. In this case, four PPh_3 molecules and one chloride act as the terminal ligands, with the latter also contributing to the charge balance of the complex.

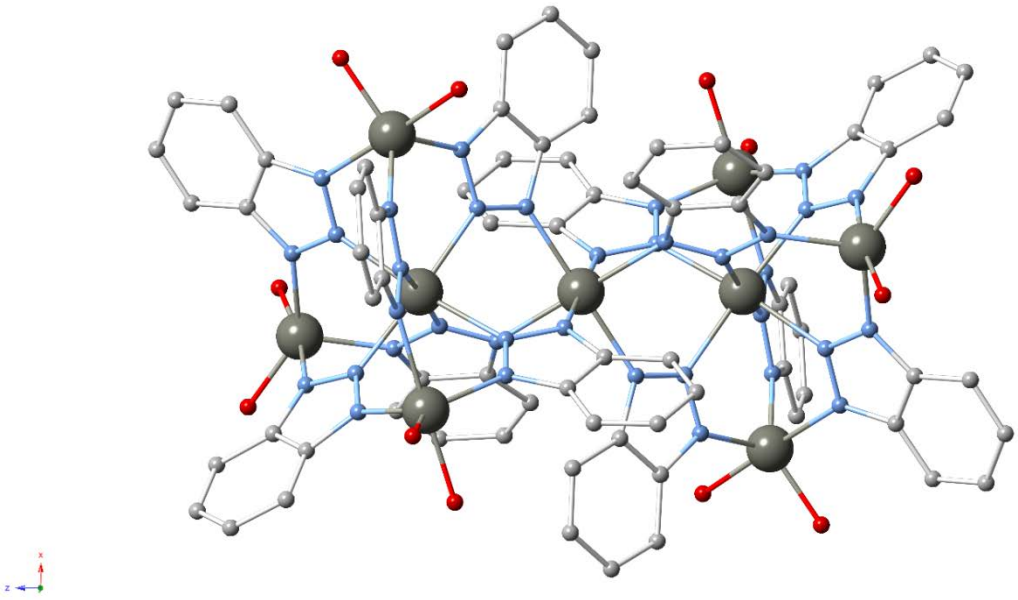

Figure 2. The nonaanuclear motif as observed in compound **4**. Hydrogen atoms and parts of the acetyloacetonates are omitted for clarity. Colour code Zn (grey), C (grey), N (light blue), O (red).

The mixed-metal design approach utilizing benzotriazole was also adopted in a series of reports[35,36] by Sulway and others, who further expanded their studies to include s- and p-block metals. These efforts resulted in compounds with different nuclearities, affording the polynuclear cage complexes $[Fe^{II}\{(Me_3Si)_2N\}_2Li(bta)]_2$, $[(hmds)_8Sn_8(bta)_{12}Li_8Cl_4]\cdot 8PhMe$, $[(hmds)_8Sn_8(bta)_{12}Li_8Br_4]\cdot 3PhMe$, $[Li_2(bta)_3(THF)_3]_2[SnI_4]\cdot(THF)$ (**9-12**, where PhMe = toluene, hmds = hexamethyldisilazide). Notably, the synthesis of all compounds involves a one-pot, air-sensitive reaction in which all metal salts and Hbta are added in solid form and cooled to -78ºC. Solvent is then added and the mixture is slowly heated to room temperature. **9** consists of a $[Li_2(bta)_2]$ unit in which each bta coordinates to two Li centres in a $\mu_{1,2}$–bridging mode. This core is then capped on each end by a $[Fe^{II}\{(Me_3Si)_2N\}_2]$ moiety while additional $\{(Me_3Si)_2N\}$ molecules complete the structure of the dimer. Magnetic susceptibility experiments for **9** point towards very weak antiferromagnetic exchange between the dinuclear Fe^{II} units. On the other hand, employment of Sn^{II} halides leads to different structures depending on the source used. $SnCl_2$ and $SnBr_2$ in toluene lead to the isostructural polynuclear cages **10** and **11**; they exhibit highly asymmetric molecular structures in which each of the deprotonated bta ligands coordinates to three metal centres. For ten of the twelve benzotriazolates this consists of one tin and two lithium centres, while the opposite occurs in the remaining two bta molecules. In contrast, the use of SnI_2 yielded

compound **12** which contains a trimeric lithium benzotriazolate unit and a rare tetraiodostannate dianion.

Even more different motifs and nuclearities may be achieved when M^{III} metal sources are introduced into the synthetic procedure; this has led to the reports of several benzotriazole-based coordination clusters with interesting magnetic properties. In a series of studies[37–39] Jones and co-workers utilize the physical properties and multimodal capabilities of Hbta with MnF_3 to generate tri-, deca-, and hexaicosametallic Mn^{III} coordination complexes. To overcome the general insolubility of MnF_3 the authors employ Hbta as the solvent; all reactions are performed at 100°C to generate "melt" Hbta, in which the metal is soluble. This results in a simple synthetic route that does not require oxidation of Mn^{II} sources. The trinuclear species $[NHEt_3]_2[Mn_3O(bta)_6F_3]\cdot 2MeOH$ (**13**) consists of an anionic $[Mn_3O(bta)_6F_3]^{2-}$ unit in which a central μ_3-bridging oxide links three Mn^{III} centres which are found in a triangular arrangement (Figure 3, upper left). Deprotonated benzotriazole units provide further bridging in a $\mu_{1,2}$-fashion as each bta molecule coordinates to two Mn^{III} ions along the edge of the imaginary triangle. The unbound nitrogen atoms form strong O-H···N hydrogen bonds with the lattice methanol solvents to further stabilize this architecture. The use of pyridine, a weaker but coordinating base, increases the aggregation of these units into larger fragments and results in the formation of a decanuclear complex with its core formulated as $[Mn_{10}O_6(OH)_2(bta)_8(py)_8F_8]$ (**14**). This compound contains eight edge-sharing $\{Mn_3O\}^{7+}$ triangular units as described before (Figure 3, upper right), with py molecules as terminal ligands and the benzotriazolate units participating again in $\mu_{1,2}$-bridging and hydrogen bonding. A protonated Hbta molecule is also found in the lattice, forming a strong hydrogen bond to increase framework stability. When no base is used during synthesis, aggregation of the $\{Mn_3O\}^{7+}$ units increases even further and results in a hexaicosanuclear compound $[Mn_{26}O_{17}(OH)_8(OMe)_4F_{10}(bta)_{22}(MeOH)_{14}(H_2O)_2]$ (**15**, Figure 3, bottom). The versatility and role of the benzotriazole units is critical for the formation of **15**. All 22 units are deprotonated, contributing to the charge balance; four of these exhibit a $\mu_{1,2,3}$-bridging coordination mode, using all nitrogen atoms to coordinate to Mn^{III} ions. The remaining eighteen molecules participate in $\mu_{1,2}$-bridging instead, as the third nitrogen atom forms hydrogen bonds with nearby MeOH, H_2O or OH^- units. Magnetochemical investigations for compounds **13 – 14** showed that the respective $\chi_M T$ values decrease as temperature decreases, indicating the presence of dominant

antiferromagnetic exchange interactions between the metal ions. Additional studies for **15** showed that the compound displays single-molecule magnet (SMM) behaviour, i.e. exhibiting magnetization which is of molecular origin, thus retaining it even after the removal of the external field. In particular, **15** showed magnetisation relaxation at low temperatures below 1.2 K.

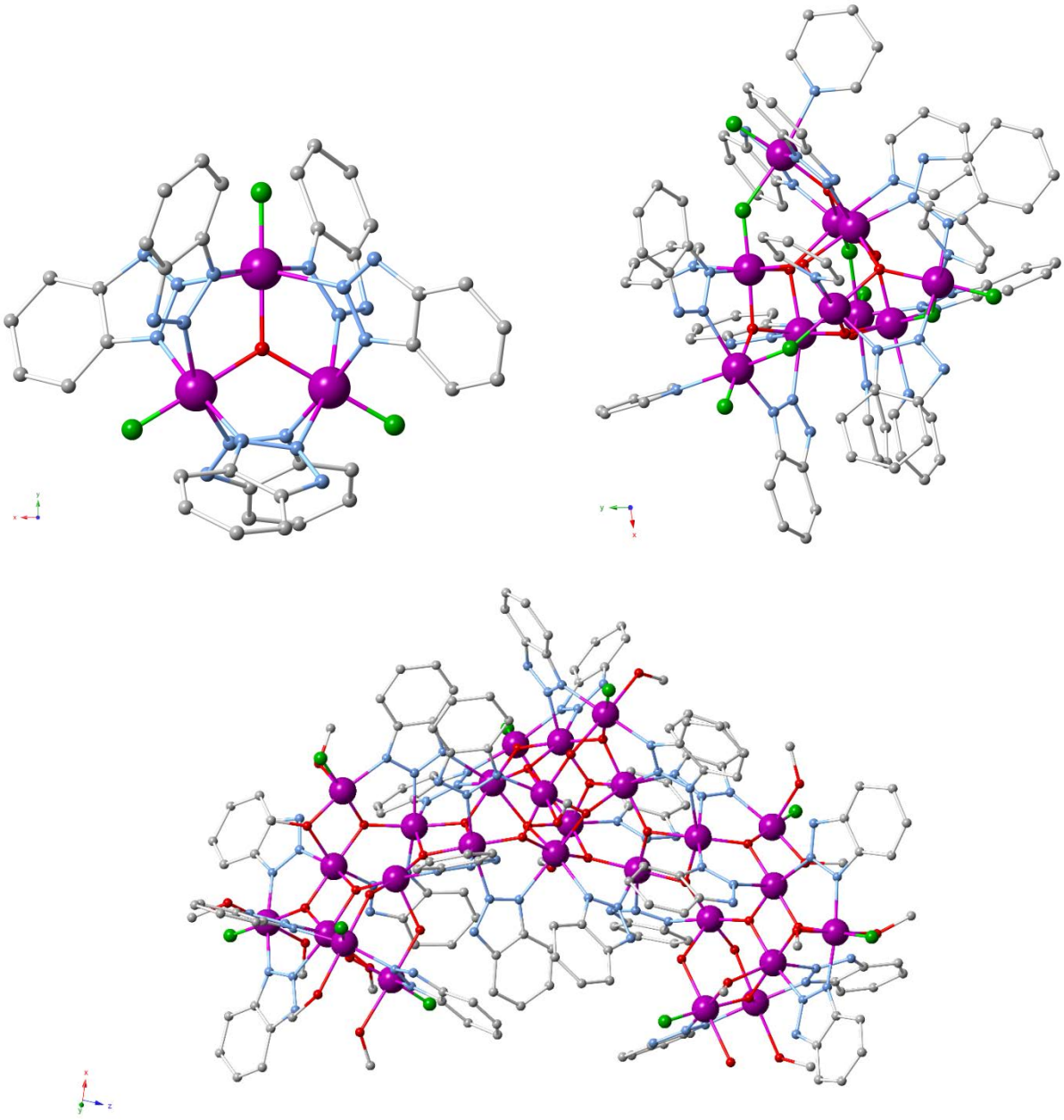

Figure 3. (upper left) The anionic trinuclear unit found in compound **13**. (upper right) The structure of the decanuclear complex **14**. (bottom) The structure of the hexaicosanuclear compound

15. Hydrogen atoms and all lattice molecules are omitted for clarity. Colour code Mn^{III} (dark magenta), C (grey), N (light blue), O (red), F (green).

Similar investigations with various Fe^{III} sources led to the construction of two more polynuclear complexes, formed as $[Fe_5O_2(OMe)_2(bta)_4(Hbta)(MeOH)_5Cl_5]$ (**16**) and $[Fe_{14}(bta)_6O_6(OMe)_{18}Cl_6]$ (**17**) respectively[40–42]. The former compound exhibits a structural motif that is similar to the one described in compound **1**; however, in this case a protonated Hbta unit is also observed, acting as a terminal ligand to one of the Fe^{III} centres. All benzotriazole molecules participate in extensive hydrogen bonding as well as $\pi\cdots\pi$ interactions with other Fe_5 clusters in the lattice. Magnetic studies point to an antiferromagnetic coupling of the central Fe^{III} ion to the peripheral metal ions which gives rise to a spin ground state of S = 15/2. In contrast, the tetradecanuclear compound **17** was afforded under solvothermal synthetic conditions and shows a completely different motif, consisting of a central hexagonal Fe_6 ring that is linked to a $[Fe_4(bta)_3Cl_3]$ unit on either side through methoxide and oxide bridges (Figure 4). All benzotriazolate units exhibit a $\mu_{1,2,3}$-bridging mode, while chloride anions are also present and act as terminal ligands. **17** exhibits a very large ground spin state of S = 25, which is attributed by the authors to the competition of antiferromagnetic exchange interactions within the cluster. In a follow-up study, an analogous synthetic procedure (reaction of M^{III} chloride with NaOMe and Hbta in MeOH at 150 °C) was performed using Cr^{III} and V^{III} sources to generate the isoskeletal compounds $[Cr_{14}(bta)_6O_6(OMe)_{18}Cl_6]$ (**18**) and $[V_{14}(bta)_6O_6(OMe)_{18}Cl_6]$ (**19**). However, the magnitude of the exchange interactions appears to be much smaller in this case as both complexes were found to have S = 0 spin ground states[41]. To overcome this issue, the authors utilized $[N^nBu_4]_3[V_2Cl_9]$ as the starting material in an attempt to influence the nuclearity of the resulting complex. Indeed, reaction with Hbta in THF and Me_3CCO_2H afforded in that instance an octametallic V^{III} cluster formulated as $[N^nBu_4]2[V_8O_4(bta)_8(O_2CCMe_3)_4Cl_6]$ (**20**), as reported in a subsequent study[43]. As seen in Figure 5, the complex exhibits a butterfly-like $\{V_8O_4\}^{16+}$ structure with four central and four peripheral oxo-bridged vanadium sites; further bridging occurs through $\mu_{1,2,3}$-bta ligands. While **20** does not display any single-molecule magnet (SMM) characteristics, it shows remarkably strong ferromagnetic coupling behaviour (J > +100 cm^{-1}) and significant magnetic anisotropy (D = 0.297 cm^{-1}) with a large S = 4 ground state.

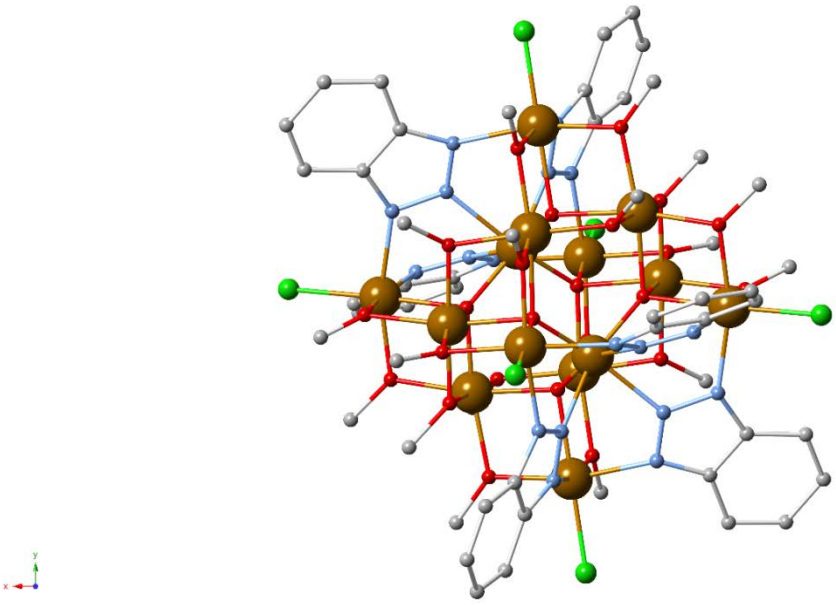

Figure 4. The structure of the tetradecanuclear complex **17**. Hydrogen atoms are omitted for clarity. Colour code Fe^{III} (brown), C (grey), N (light blue), O (red), Cl (green).

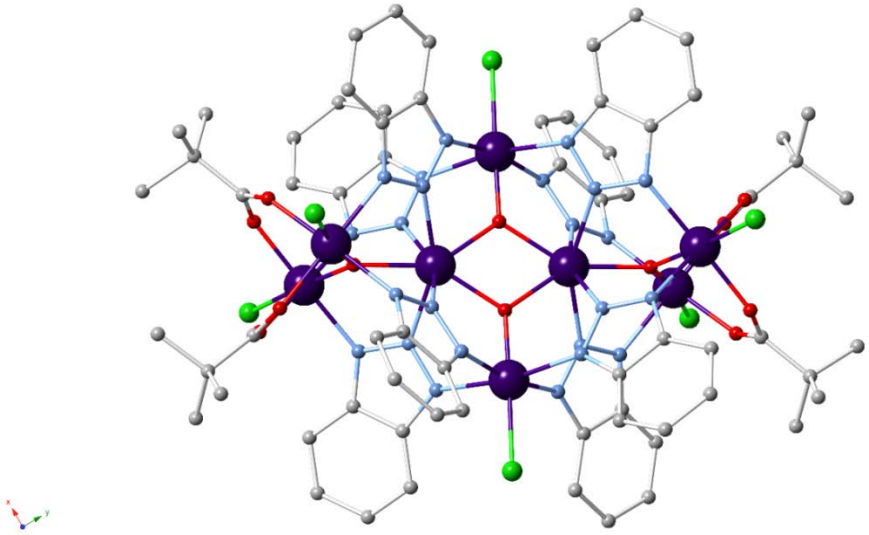

Figure 5. The octavanadium complex **20**. Hydrogen atoms are omitted for clarity. Colour code V^{III} (purple), C (grey), N (light blue), O (red), Cl (green).

In order to obtain compounds with improved SMM behaviour, Layfield and co-authors explored the capabilities of benzotriazole using lanthanide sources[44]. More specifically, reactions with $DyCp_3$ (Cp = cyclopentadienyl) and Hbta resulted in a dimeric compound formulated as

$[Cp_2Dy(bta)]_2$ (**21**), which was found to behave as a SMM in temperatures below ~12 K. It consists of Dy^{III} centres that are bridged by deprotonated bta ligands. Each of these ligands coordinates to one metal centre through two nitrogen atoms and to the other one through the remaining nitrogen in a μ-η^2:η^1 bridging mode (Figure 6). Notably, **21** is one of the first benzotriazole-based complexes in organolanthanide chemistry.

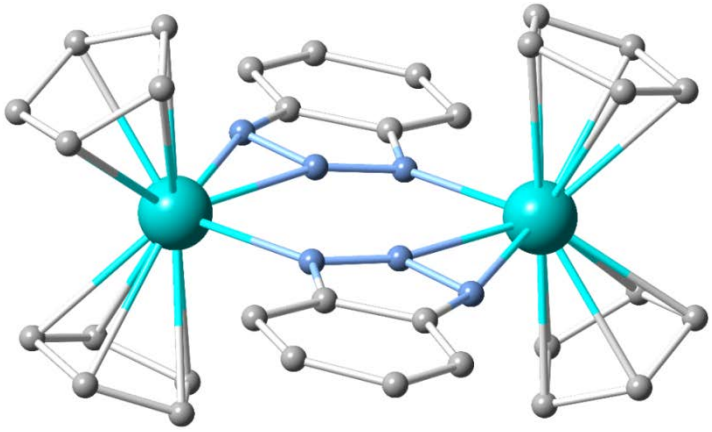

Figure 6. The structure of compound **21**. Hydrogen atoms are omitted for clarity. Colour code Dy (cyan), C (grey), N (light blue).

While the majority of the above studies focused on the magnetic properties of the resulting clusters, other directions are also possible. Recently, Shestopalov *et al.* reported two novel hexanuclear rhenium clusters with potential luminescent and biological uses[45]. Formulated as $K_4[\{Re_6(\mu_3\text{-}S)_8\}(bta)_6]$ and $K_{2.75}H_{1.25}[\{Re_6(\mu_3\text{-}Se)_8\}(bta)_6]$ respectively (**22** - **23**), these compounds contain a robust $\{Re_6(\mu_3\text{-}X)_8\}^{2+}$ core that is already known for its photoluminescence capabilities in the ~550 - 1000 nm emission window, making it particularly interesting for bioimaging and biolabeling purposes. From a structural point of view, both complexes consist of a nearly regular Re_6 octahedron residing inside a X_8 cube; each rhenium centre is also coordinated to a terminal η^1–bta ligand. Moreover, the use of benzotriazole is crucial in this study, as its pseudoamphiphilic nature makes both **22** and **23** water-soluble, allowing them to easily penetrate through cell membranes for potential medical and biological applications. Indeed, both compounds showed cellular uptake activity without acute cytotoxic effects at concentration levels of practical biological applications; in addition, their red phosphorescence lifetime and quantum yield values

were found to be among the highest reported for analogous complexes, highlighting their promising potential as bioimaging agents.

2.2. Coordination Polymers

Apart from the formation of zero-dimensional polynuclear coordination clusters, Hbta has also been identified as a suitable linker towards the design of coordination polymers under appropriate synthetic parameters. Few examples of such compounds exist in the literature. For instance, Shao and co-authors report the isolation of a three-dimensional CP with helix-like network, formulated as $[Zn(bta)_2]$ (**24**) under harsh hydrothermal conditions[46]. The framework in **24** comprises of tetrahedral zinc centre nodes that are considered asymmetrical, as they are linked through bridging $\mu_{1,3}$-bta molecules with different directions (Figure 7).

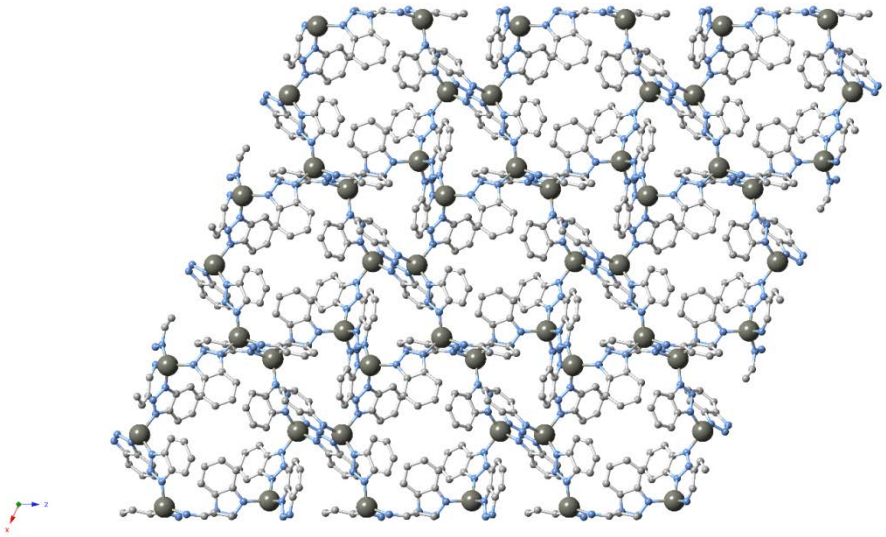

Figure 7. Part of the 3D architecture in compound **24**. Hydrogen atoms are omitted for clarity. Colour code Zn (grey), C (grey), N (light blue).

Later, Han and co-workers reported[47] the synthesis of an unusual hexamanganese complex, $H[Mn_6(bta)_8Cl_5]\cdot(H_2O)_4$ (**25**), that extends to three dimensions. **25** was prepared through an intense solvothermal reaction of $MnCl_2\cdot4H_2O$ and Hbta in the presence of triethylamine and 1H-benzimidazole-2-carboxylic acid (H_2bic). This coordination polymer contains Cl-centered tetragonal $[Mn_4(bta)_8]$ building units bridged by monomeric manganese centres to give rise to the resulting 3D architecture, with the $\mu_{1,2,3}$-bta molecules playing an important role in the formation

of the structure. Additionally, magnetic characterization experiments for **25** revealed the presence of antiferromagnetic coupling between the Mn^{II} ions. Below 46 K, the complex shows a steep increase in the $\chi_M T$ value, indicating spin-canting behaviour.

In another notable example Lin and co-authors presented[48] the first crystal structure of a coordination polymer containing Cu^{I} sources and Hbta, a feat of significant importance as it could shed light in the mechanistic investigations of the aforementioned corrosion inhibiting effect of benzotriazole in metallic copper. The compound is formulated as $[Cu^{I}_2(bta)_2]$ (**26**) and its structure contains crystallographically independent Cu centres that exhibit linear, trigonal and tetrahedral geometry respectively. These metal ions are linked by $\mu_{1,2,3}$-bridging type deprotonated benzotriazole molecules, as the framework extends to form a 1D chain which is presented in Figure 8. The formation of $\pi\cdots\pi$ stacking interactions between these bta units further increases the stability of the architecture.

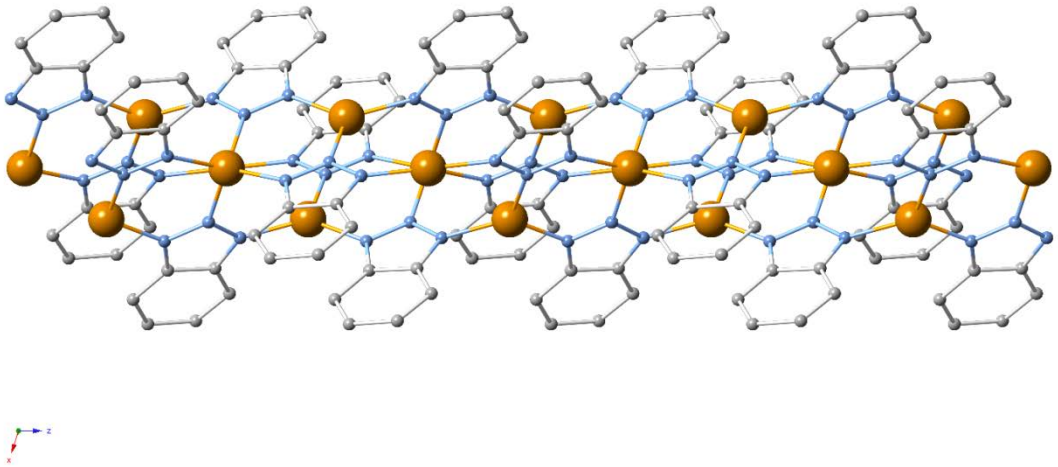

Figure 8. Part of the polymeric 1D network in compound **26**. Hydrogen atoms are omitted for clarity. Colour code Cu^{I} (orange), C (grey), N (light blue).

Furthermore, in a series of studies by Müller-Buschbaum's group various lanthanide sources are employed to produce several CPs with different dimensionalities as the coordination capabilities of Hbta are utilized in full effect[49–52]. In this synthetic procedure the reactants are first heated to 100-120°C to form "melt" Hbta and are then subjected to solvothermal conditions for several days. The method affords 1D CPs that exhibit a chain framework based on a $[Ln(bta)_x(Z)]$

backbone, where Z is a neutral ligand species that is either Hbta or one of its thermal decomposition products, in this case phenylene-diamine or ammonia. These CPs are $[La(bta)_3(Hbta)]$, $[Ce(bta)_3(Hbta)]$, $[Pr(bta)_3(Hbta)]$, $[Nd(bta)_3(Ph(NH_2)_2)]$, $[Tb(bta)_3(Ph(NH_2)_2)]$, $[Yb(bta)_3(Ph(NH_2)_2)]$, $[Ho_2(bta)_6(Hbta)(NH_3)]$ and $[Eu^{II}(bta)_2(Hbta)_2]$ (**27 – 34**). **27 – 32** exhibit deca-coordinated lanthanide centres and two different coordination modes are seen in the benzotriazole ligands. In the first one, the ligand shows a μ-η^2:η^1 binding mode, coordinating to one Ln centre through two nitrogen atoms while the third nitrogen coordinates to a neighbouring Ln ion. In the second type of bta ligands the third nitrogen atom does not coordinate and instead participates in hydrogen bond interactions. The coordination sphere of the Ln ion is filled by either Hbta of $Ph(NH_2)_2$ molecules which bind through two nitrogen atoms. **33** exhibits a ladder-like framework which contains nona-coordinate holmium centres; the bta ligands are either in a similar μ-η^2:η^1 binding mode or a $\mu_{1,3}$-bridging type. **34** presents a rare case of a divalent lanthanide compound and its Eu^{II} centres are octa-coordinated. To add to this structural variety, crystal transformations of **27**, **28** and **33** were induced in temperatures up to 350°C: in these conditions the neutral ligands are removed from the frameworks and are replaced by symmetry related bta molecules which increase the dimensionality, leading to the 3D CPs $[La(bta)_3]$, $[Ce(bta)_3]$ and $[Eu^{II}(bta)_2]$ (**35 – 36**).

2.3. Polyoxometalate-Based Structures

Another strategy in the synthesis of coordination compounds involves the use of polyatomic metal-oxo cluster anions, commonly known as polyoxometalates (POMs). Such moieties can exhibit a significant variety in shapes, sizes and compositions[53,54], making them very promising candidates for the design of sophisticated building blocks towards unique and functional architectures. As a result, the development of POM-based frameworks has become increasingly popular in recent years[55,56]. Benzotriazole has also been utilized during the design of such compounds due to its excellent crystal engineering capabilities that include ease of coordination as well as multiple coordination modes. The first example of such efforts is presented by Wang and co-workers, who reported[57] the synthesis of two high-nuclearity copper coordination polymers based on Hbta and Keggin-type polyanions. These hybrid compounds are formulated as $[Cu^{I}_8(bta)_4(Hbta)_8(SiMo_{12}O_{40})]\cdot 2H_2O$ and $[Cu^{II}_6(OH)_4(bta)_4(SiW_{12}O_{40})(H_2O)_6]\cdot 6H_2O$ (**37** – **38**). In both cases, the use of Hbta is crucial as the ligand appears in both its protonated and

deprotonated forms towards the formation of multicopper clusters which are then linked by the polyanions to induce a 1D (**37**) or a 2D (**38**) architecture respectively. The compounds were also tested for their catalytic properties in the photodegradation of methylene blue (MB), showing excellent activity (91.5% conversion of MB for **37**, 96.5% for **38**) after 140 minutes.

Incorporation of silver acetate and NaOH using similar Keggin-type anions by Zhou and co-authors[58] resulted in the synthesis of the two-dimensional Hbta-based compound $[Ag_4(bta)_2(Hbta)_2(H_2O)Na(PMo_{12}O_{40})]\cdot H_2O$ (**39**). In this case, the main building block is a one-dimensional chain consisting of $[Ag_4(bta)_2(Hbta)_2]$ units with the benzotriazolates exhibiting various coordination modes; the POM anions also coordinate to the Ag centres to link these chains and extend the architecture to the resulting 2D layer. In similar fashion, Wang and co-workers reported[59] the synthesis of two isostructural heptanuclear hybrid compounds, $[\{Ag_7(Hbta)_2(bta)_4\}\{PW_{12}O_{40}\}]\cdot H_2O$ and $[\{Ag_7(Hbta)_2(bta)_4\}\{PMo_{12}O_{40}\}]\cdot H_2O$ (**40** - **41**), through the use of silver nitrate. Once again, in these 2D structures the ligand presents two different coordination modes, as it appears either as $\mu_{1,2,3}$-bridging bta or as monodentate η^1-Hbta to terminate the extension of the cluster. It also participates in various ($Ag^I\cdots\pi$, $\pi\cdots\pi$, H-bonding) interactions that influence the resulting architecture and crystal packing. Two more isostructural heptanuclear compounds, $[\{Cu^I_7(Hbta)_2(bta)_4\}\{PMo_{12}O_{40}\}]$ (**42**) and $[\{Ag_7(Hbta)_2(bta)_4\}\{AsW_{12}O_{40}\}]$ (**43**), were recently reported by Cao and co-authors[60]. Both these compounds were found to be excellent photocatalysts towards the degradation of Rhodamine B (after 100 minutes under UV irradiation, **42** and **43** showed 96.7% and 97.5% conversion respectively).

Finally, an interesting article[61] by Ruan *et al*. reports the design of POM-based 3D coordination polymer $[Cu^{II}_{12}(bta)_{12}(\mu_3\text{-}OH)_5(\mu_2\text{-}H_2O)_6]\cdot PMo_{12}O_{40}\cdot 2HPMo_{12}O_{40}\cdot 18H_2O$ (**44**), which due to symmetry forms a nanosized hexagonal Cu_{30} wheel (Figure 9) containing a $[PMo_{12}O_{40}]^{3-}$ anion in its cavity. Notably, the high size and nuclearity of this wheel is attributed to the steric effect of the benzotriazole ligand. Two different building blocks, a triangular $[Cu_3(bta)_3(\mu_3\text{-}OH)]^{2+}$ and a dicopper $[Cu_2(bta)_2(\mu_2\text{-}OH)]^{1+}$ are found; in both these units the benzotriazolate ligands are found in a $\mu_{1,2,3}$-bridging mode. Magnetic studies for **44** pointed towards antiferromagnetic behaviour, with the $\chi_M T$ values measured at 4.21 and 0.31 cm^3 K/mol at 300 and 2 K respectively.

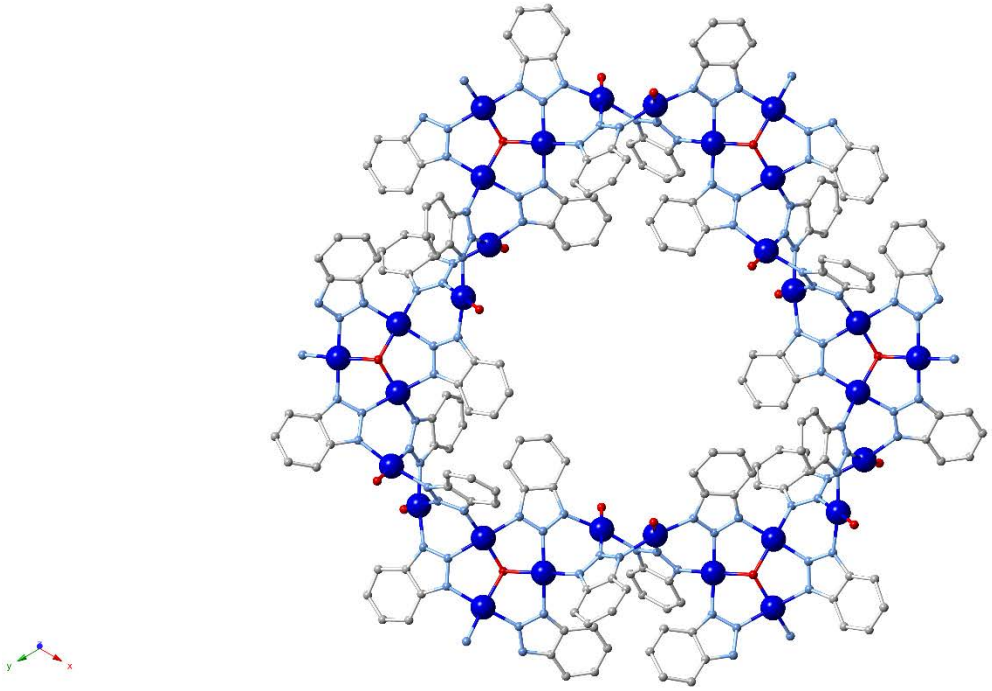

Figure 9. The hexagonal Cu_{30} wheel in **44**. All hydrogen atoms and polyanions have been omitted for clarity. Colour code Cu (dark blue), C (grey), N (light blue), O (red).

3. Benzotriazole as a co-Ligand

A significant portion of coordination chemistry studies have incorporated Hbta as a potential secondary ligand. More specifically, it has been primarily used as a supporting linker in the construction of CPs due to its versatility in coordination modes and bridging capabilities. From a structural point of view, the role of Hbta falls under one of the following categories: (i) it forms stable polynuclear coordination clusters which in this case are used as building blocks and are linked by a second ligand (usually of *O*-donor type), forming multi-dimensional materials, (ii) it acts as a supporting pillar in otherwise existing metal:ligand frameworks, occupying the remaining coordination sites and increasing the dimensionality of the structure. Examples of both categories will be presented herein.

Several attempts have been made to utilize the well-established $[M^{II}_5(bta)_6]^{4+}$ unit as a secondary building block and introduce a polytopic bridging co-ligand. The first relevant report came from Bai and co-authors who used $[M_5(bta)_6(NO_3)_4(H_2O)_4]$ (M = Co^{II} or Ni^{II}) as the node, then introduced LiTCNQ (TCNQ = 7,7,8,8-tetracyano-p-quinodimethane) for its radical anions to

replace the nitrate and water molecules and occupy their coordination sites[62]. This stepwise assembly led to the synthesis of 3D diamond-like networks (**45** and **46**) based on the $[M_5(bta)_6(TCNQ^{\cdot-})_4]$ backbone (Figure 10). It is worth noting that this benzotriazolate polynuclear node retains its structural stability during this procedure.

Subsequently, employment of the analogous Zn^{II} cluster as precursor along with the introduction of linear polycarboxylates as co-ligands led to additional CPs of similar fashion. Wang and co-workers report the compounds $[Zn_5(bta)_6(bdc)_2(H_2O)_2]$, $[Zn_5(bta)_6(abdc)_2(H_2O)_2]$ and $[Zn_5(bta)_6(bpdc)_2(H_2O)_2]$ (**47** – **49**, where H_2bdc = 1,4-benzenedicarboxylic acid, H_2abdc = 2-amino-1,4-benzenedicarboxylic acid and H_2bpdc = 4,4'-biphenyldicarboxylic acid), which also exhibit similar 3D microporous diamondoid networks[63]. Similar rational synthesis using 1,4-naphthalenedicarboxylic acid (H_2ndc) by Deng *et al*. led to $[Zn_5(bta)_6(ndc)_2(H_2O)]$ (**50**), which exhibits a 3D framework with different topology due to the added steric hindrance of the naphthalene-based co-linker[64]. **50** was also tested for its luminescent properties, showing solvent-dependent activity. Another diamond-like 3D interpenetrated framework, $[Zn_5(bta)_6(tda)_2]$ (**51**, H_2tda = thiophene-2,5-dicarboxylic acid) was reported by Zhang and co-authors, showing selective gas sorption of C_2H_2 or CO_2 over CH_4 at room temperature[65]. Remarkably, this step-wise synthetic approach can still be employed using ligands of increased length and number of carboxylate groups. In a comprehensive study, Lan and co-authors[66] use the Zn_5 precursor cluster along with a series of tetratopic polycarboxylate ligands of increasing size and with modified functional groups to generate analogous $[Zn_5(bta)_6(L)(H_2O)_x]$ microporous 3D frameworks (compounds **52** – **57**, x = 0 or 1, ligand L = 4,4'-(2,2-bis((4-carboxyphenoxy)methyl)propane-1,3-diyl)bis(oxy)dibenzoic acid for **52**, 4,4'-(2,2-bis((4-carboxy-2-methoxyphenoxy)methyl)propane-1,3-diyl) bis(oxy)bis(3-methoxybenzoic acid) for **53**, 6,6'-(2,2-bis((6-carboxynaphthalen-2-yloxy)methyl)propane-1,3-diyl)bis(oxy) di-2-naphthoic acid for **54**, 3,3'-(4,4'-(2,2-bis((4-(2-carboxyvinyl)phenoxy)methyl)propane-1,3-diyl)bis (oxy)bis(4,1-phenylene))diacrylic acid for **55**, 3,3'-(4,4'-(2,2-bis((4-(2-carboxyvinyl)-2-methoxyphenoxy)methyl)propane1,3-diyl)bis (oxy)bis(3-methoxy-4,1-phenylene))diacrylic acid for **56**, 4',4''-(2,2-bis((4'-carboxybiphenyl-4-yloxy)methyl)propane-1,3-diyl)bis (oxy)dibiphenyl-4-carboxylic acid for **57**). The resulting diamond-like frameworks retain their topological features, allowing for a rational design and control of the CP synthesis. Additional N_2 and H_2 adsorption

studies for **52 – 57** revealed that compound **52** exhibits the highest uptake values (131.9 and 118.9 cm^3g^{-1} respectively) at 77 K.

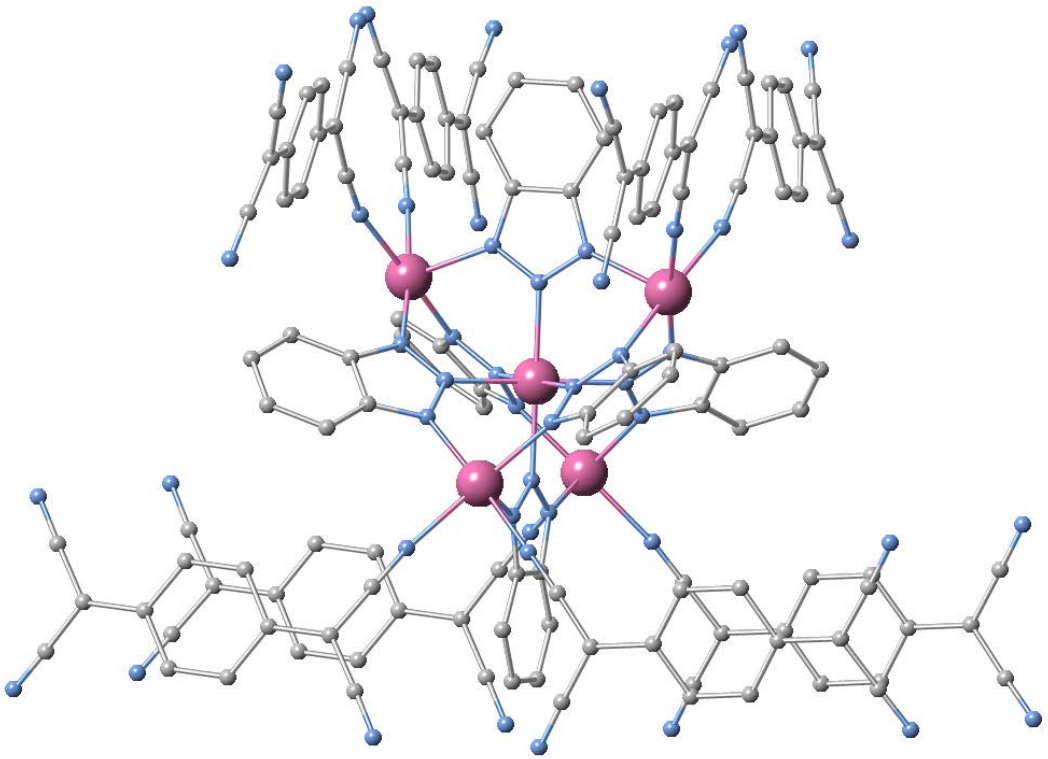

Figure 10. The $[Co^{II}_5(bta)_6(TCNQ^{\cdot-})_4]$ building unit found in compound **45**. Hydrogen atoms are omitted for clarity. Colour code Co (pink), C (grey), N (light blue).

More recently, Chen and others employed tritopic polycarboxylates (H_3qbtcb = 4,4´,4´´-[1,3,5-benzenetriyltris(carbonylimino)]tris(benzoate) and H_3tbtcb = 3,3´,3´´-[1,3,5-benzenetriyltris(carbonylimino)]tris(benzoate)) as co-linkers using a one-pot synthesis instead of the step-wise assembly[67]. This resulted in compounds $[Zn_5(bta)_6(qbtcb)(H_2O)(NO_3)]$ and $[Zn_9(bta)_{12}(tbtcb)_2]$ (**58** and **59**). The structural characteristics of these cluster building blocks and the behaviour of the bta molecules are similar to the pentanuclear and nonanuclear clusters **1** and **4** respectively, indicating that the formation and stability of such species is heavily favoured regardless of the synthetic method. In both products the structure extends to form microporous 2D networks which exhibited selective uptake of CO_2 over CH_4 and N_2 at room temperature, when guest solvents are removed.

A similar one-pot synthesis was also used by Tan and co-authors[68] to generate a compound based on the analogous pentanuclear nickel analogue and isonicotinic acid (H_2ina). $[Ni_5(bta)_6(ina)_3(H_2O)(CH_3COO)]$ (**60**) reveals a porous 2D layer as the co-linker coordinates to metal centres through both its pyridinic and carboxylic groups (Figure 11). **60** also showed selective CO_2 adsorption over CH_4 in its framework.

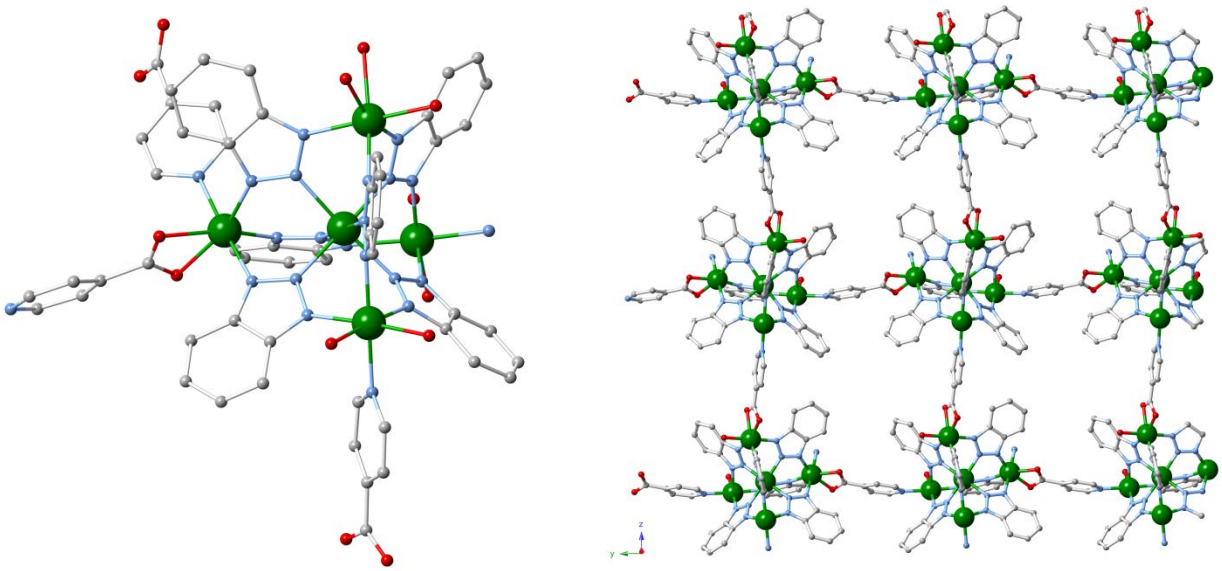

Figure 11. The building unit (left) and the porous 2D layer in compound **60** along the *b0c* plane (right). Hydrogen atoms and certain solvent molecules are omitted for clarity. Colour code Ni (green), C (grey), N (light blue), O (red).

Other types of building block clusters (and consequently, different resulting frameworks) may also be achieved depending on parameters such as the synthetic conditions, the type of co-linker or the binding preference and available coordination sites of the selected metal. For example, Zhong and co-workers report[69] the construction of a 2D layered compound $[Cd_5(bta)_6(bdc)_2(DMF)_4(H_2O)_2]$ (**61**) which contains the common pentanuclear motif and the co-ligand H_2bdc, synthesized in room temperature. However, a similar reaction under intense solvothermal conditions promotes the coordination of more bdc molecules over bta and affords the heptanuclear complex $[Cd_7(bta)_2(bdc)_6(DMF)_8]$ (**62**). In this case the compound contains two inner trinuclear $[Cd_3(bta)]^{5+}$ cluster units in which the Cd centres are found in a triangular arrangement and are bridged by $\mu_{1,2,3}$-bta molecules (Figure 12, upper). These units are linked by bdc ligands as the framework

extends to form a CP with 3D architecture. Furthermore, the addition of 1,2,4-triazole (Hta) as a third co-ligand in the reaction promotes the formation of a polynuclear CP formulated as $[(CH_3)_2NH_2]_2[Cd_5(bdc)_4(ta)_2(bta)_2]$ (**63**); this pentacadmium cluster-based compound also exhibits a rare *gpu* topology, as demonstrated by Wang and co-authors[70]. Li and co-workers reported another 3D CP based on a trinuclear benzotriazole-built unit, using Co^{II} sources and 1,3-benzenedicarboxylic acid (H_2mbdc) under harsh solvothermal conditions[71]. The afforded compound $[Co_4(mbdc)_3(bta)_2(EtOH)_2]$ (**64**) contains tricobalt building blocks bridged by $\mu_{1,2,3}$-bta molecules, with the metal centres forming a rod-shaped chain arrangement (Figure 12, lower).

A different bta-based building block cluster is reported in the cationic framework $[Zn_4(bta)_3(ipa)_6]$ (**65**, H_2ipa = isophthalic acid) constructed by Qin and co-authors[72]. This CP constitutes a rare topological example of a 6-connected uninodal $\{3^3.5^9.6^3\}$-*lcy* net. Synthesized solvothermally at 160°C, its structure contains unusual plate-like $[Zn_4(bta)_3]^{5+}$ units that act as six-coordinated nodes as they are bridged by ipa ligands to form a 3D architecture. Each of these units presents three zinc centres in a triangular arrangement, connecting to the N1, N3 atoms of the bta molecules. A fourth metal ion is found at the centre of this unit, coordinating to the N2 atoms of the benzotriazoles (Figure 13, left). A very similar tetranuclear building unit has been reported in the heterometallic framework $[NH_2(CH_3)_2]_3[N(CH_3)_2][Cd_3Na(bda)_3(bta)_3]$ (**66**) by Li and co-workers[73], with the sodium ion occupying the centre of the unit in this case. The compound also exhibited highly selective gas sorption for H_2 over N_2 (64 and 15 cm^3g^{-1} at 77 K, respectively).

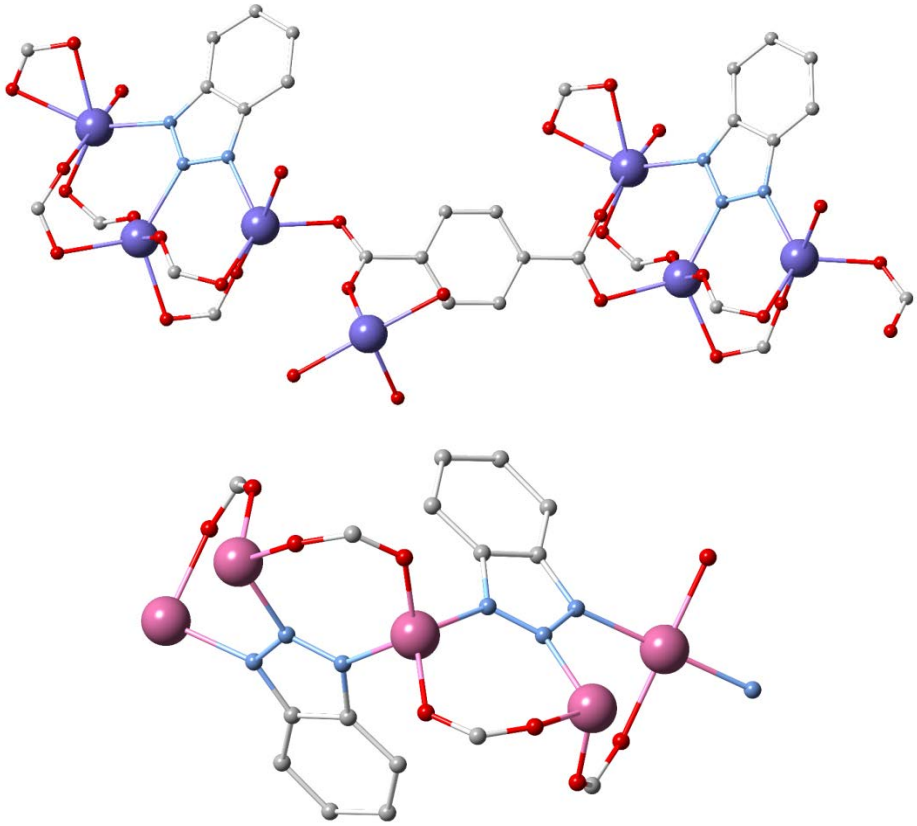

Figure 12. The polynuclear building units observed in compounds **62** (upper) and **64** (lower). Hydrogen atoms are omitted for clarity. Colour code Cd (blue), Co (pink), C (grey), N (light blue), O (red).

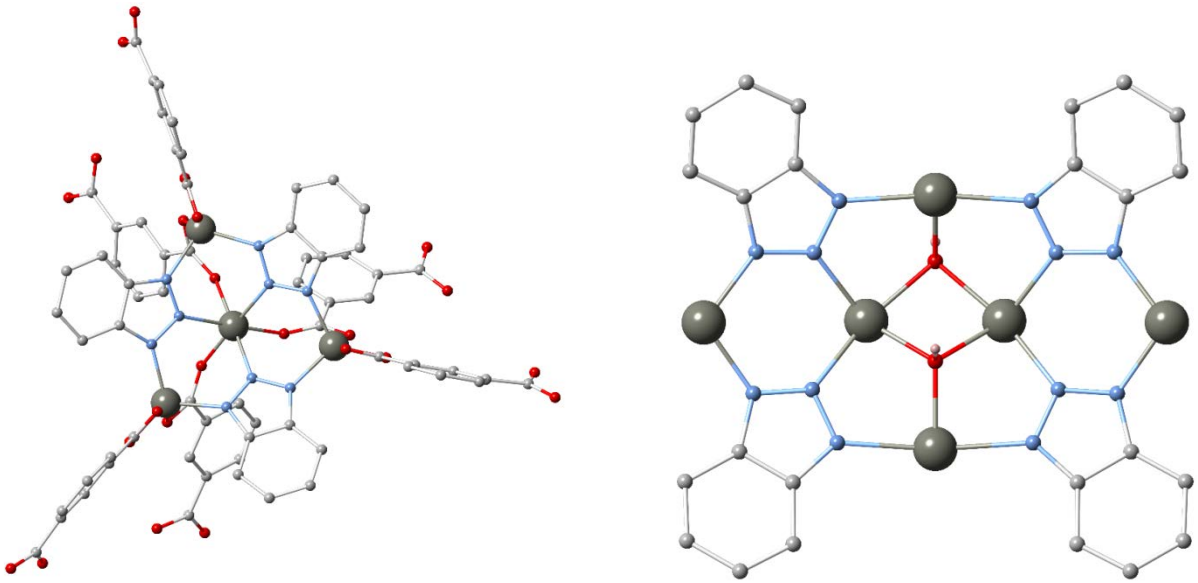

Figure 13. The polynuclear building units observed in compounds **65** (left) and **72** (right). Certain hydrogen atoms are omitted for clarity. Colour code Zn (dark grey), C (grey), H (light pink), N (light blue), O (red).

Compounds of various nuclearities may also be achieved with the use of different types of polycarboxylates such as ligands containing *N*- and *O*-donor atoms or tritopic linkers. For example, a recent study[74] by Kan and co-workers reports the synthesis of 3D interpenetrated CPs $[Zn_9(bta)_{12}(atdbc)_3(DMF)]$ and $[Zn_4(bta)_6(bcpt)]$ (**67** and **68**, where H_2atdbc = 4,4'-(4-amino-1,2,4-triazol-3,5-diyl)dibenzoic acid, H_2bcpt = 3,5-bis(4'-carboxy-phenyl)-1,2,4-triazole). While **67** exhibits the same nonanuclear building block that was mentioned in **59**, **68** demonstrates 1D zig-zag $[Zn_4(bta)_6]^{2+}$ chains that are interconnected by linear bcpt ligands to construct the resulting 3-fold interpenetrated framework. **67** also showed good sorption ability for small gases and notable selectivity to separate CO_2 from CH_4.

Fan and others have reported[75] the solvothermal synthesis of a Cd^{II} CP based on the ligand 1,3,5-benzenetricarboxylic acid (H_3btc): the formulated compound $(NH_3)_2[Cd_3(btc)_2(bta)(DMA)]$ (**69**) exhibits a complicated 3D framework based on trinuclear cadmium units controlled by $\mu_{1,2,3}$-bta molecules. Jiang and co-authors have also demonstrated[76] the importance of these trimetallic building blocks in the solvothermal synthesis of complexes $(Hdma)_3[Zn_3(bta)(btc)_2(DMF)]_3$ and $(tma)_4[Zn_3(bta)(btc)_2(H_2O)]_4$ (**70** and **71**, where Hdma = protonated dimethylamine and tma = tetramethylammonium). The different coordination modes of btc molecules compared to **69** result in the formation of three-dimensional microporous CPs, based on ring-size metallamacrocycles that are constructed by either three (**70**) or four (**71**) trinuclear $[Zn_3(bta)(COO)_4]$ units as seen in Figure 14. The resulting anionic frameworks exhibit large voids occupied by the charge-balancing organic cations.

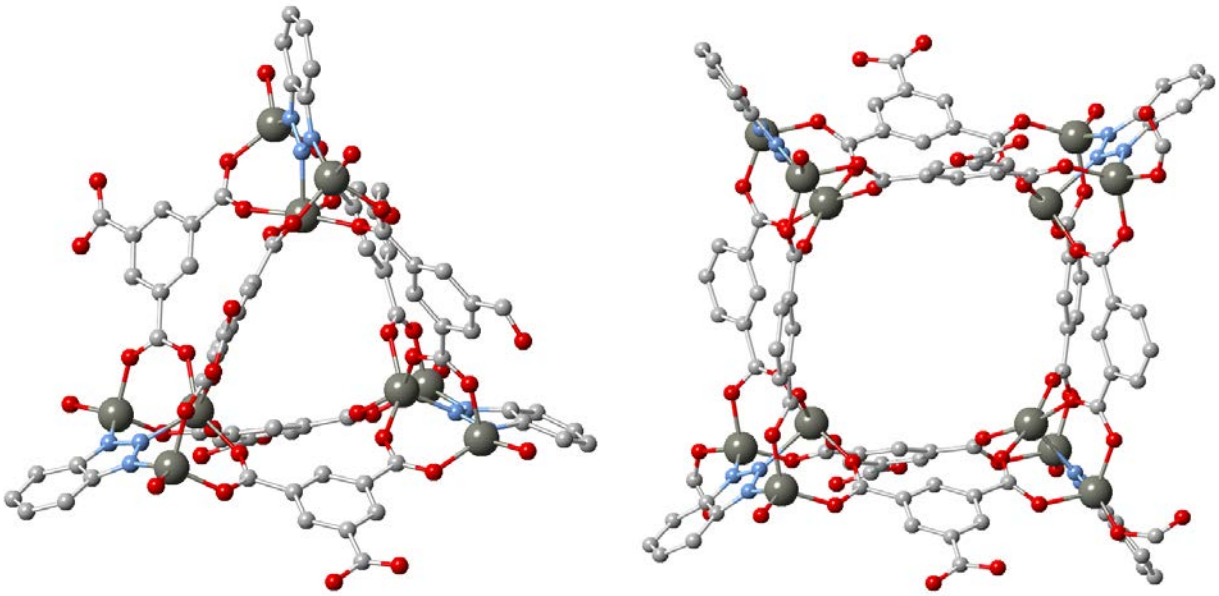

Figure 14. The polynuclear building units found in compounds **70** (left) and **71** (right). Hydrogen atoms and solvent molecules are omitted for clarity. Colour code Zn (dark grey), C (grey), N (light blue), O (red).

Finally, an unusual heptanuclear $[Zn_7(bta)_7(oadbc)(\mu_3\text{-}OH)_2(\mu_2\text{-}OH)_2]$ complex (**72**, H_3oadbc = 5-oxyacetatoisophthalic acid) was synthesized by Shao and co-workers, who reacted zinc acetate and H_3oadbc at 180°C for several days[77]. The structure of **72** is rather complicated and is based on a rare hexa-zinc subunit that is best formulated as $[Zn_6(bta)_4(\mu_3\text{-}OH)_2]$, containing four zinc atoms in a near planar metallomacrocyclic motif as well as two zinc centres inside this cyclic cavity. These ions are connected by $\mu_{1,2,3}$-bta and μ_3-OH moieties (Figure 13, right). The extended framework is three-dimensional as these sub-units are linked by oadbc ligands and $\mu_{1,3}$-bta molecules, while the uncoordinated central N atoms in these benzotriazoles participate in structure-stabilizing hydrogen bonding interactions.

In regards to the latter category, in which Hbta is utilized as a secondary pillar to increase the dimensionality of coordination compounds, most studies employ carboxylate-based ligands as primary linkers. In order to promote this outcome over the formation of benzotriazole-based cluster building blocks, the synthetic method typically involves careful adjustment of the mixture's pH (usually to 7-8) in accordance to the pKa value of the primary linker in each case. The solution is then subjected to solvothermal conditions for several days. Such procedures are reported in the

formation of compounds $[Co_5(\mu_3\text{-}OH)_2(bdc)_3(bta)_2]$, $[Zn_5(\mu_3\text{-}OH)_2(bdc)_3(bta)_2]$, $[Zn_5(\mu_3\text{-}OH)_2(\mu_2\text{-}OH)_2(pqca)_4(bta)_2]$, $[Co(cdc)_{0.5}(bta)]$, $[Zn(cdc)_{0.5}(bta)]$, $[Zn(apa)_{0.5}(bta)]$, $[Zn(gta)_{0.5}(bta)]$, $[Co_3(D\text{-}cam)_2(bta)_2]$, $[Zn_3(D\text{-}cam)_2(bta)_2]$, $[Co_3(sdba)_2(bta)_2]$ and $[Cd_2(bpt)(bta)(DMF)]$ (**73 – 83**, Hpqca = 2-phenyl-4-quinolinecarboxylic acid, H_2cdc = 1,4-cyclohexanedicarboxylic acid, H_2apa = adipic acid, H_2gta = glutaric acid, D-H_2cam = D-camphoric acid, H_2sdba = 4,4´-dicarboxybiphenyl sulfone and H_3bpt = biphenyl-3,4´,5-tricarboxylic acid)[78–82]. In compounds **73 – 79** the bta units bridge metal centres in a $\mu_{1,3}$-fashion to form a M-bta 1D chain, thus increasing the dimensionality of the framework. An example of such a function is presented in Figure 15. The architectures in the remaining compounds are based on $[M_3(bta)_2(CO_2)_4]$ nodes which contain both linkers and are connected by $L_{carboxylate}$ molecules; in these cases, bta adopts a $\mu_{1,2,3}$-bridging coordination mode. Very recently, Zou *et al.* reported[83] the solvothermal synthesis of an anionic Zn^{II} CP formulated as $[(CH_3)_2NH_2][Zn(fda)(bta)_2]$ (**84**, where H_2fda = furan-2,5-dicarboxylic acid). The structure demonstrates a honeycomb-like framework formed by Zn^{II} centres and fda linkers, bridged by $\mu_{1,3}$-bta units to form a 3D architecture. Notably, investigations on the luminescent properties of **84** showed that the compound can be used as a highly sensitive and selective luminescent probe of acetylacetone with a detection limit of 0.647 μmol/L. **84** also demonstrated partial cation exchange capabilities through post-synthetic modifications that resulted in the replacement of some Zn^{II} ions with Cu^{II}, Co^{II} or Ni^{II} centres.

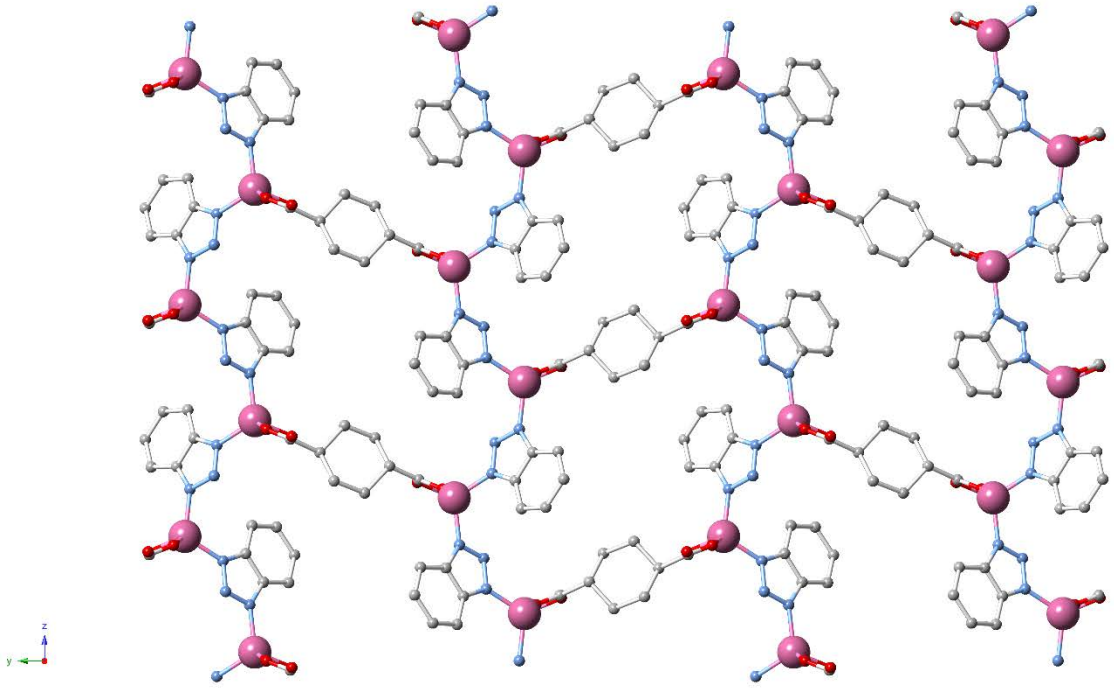

Figure 15. Part of the 2D network in compound **76** along the *b0c* plane. Hydrogen atoms are omitted for clarity. Colour code Co (light purple), C (grey), N (light blue), O (red).

Examples of non-carboxylate linkers as co-ligands have also been reported in the literature, although they are less common. A notable paradigm was presented in 2009 by Herchel and co-workers, who opted to use a 0D metalloligand based on Fe^{III} and the salen ligand (salen = *N*,*N*′-Ethylenebis(salicylimine))[84]. The addition of Hbta induces dimensionality and leads to a 1D chain as the $[Fe(salen)]^{1+}$ nodes are bridged by $\mu_{1,3}$-bta molecules to generate [Fe(salen)(bta)] (**85**). This compound also showed promising anti-tumour activity against various cancer cell lines. In another report[85], Shankar and others employed the *N*-donor co-ligand 1,2,3,4,5,6-hexakis(benzimidazol-1-ylmethyl)-benzene (hbmb) to generate the hexanuclear spheroid metallocavitand $[Re_6(CO)_{18}(bta)_6(hbmb)]\cdot Me_2CO$ (**86**, Figure 16) in a one-step self-assembly procedure. In this case, the $\mu_{1,3}$-bridging bta units are crucial in tuning the depth and size of the cavitand, while its supramolecular architecture allows it to act as a host for guest acetone molecules. Additional attempts to employ *N*-donor molecules as co-ligands have been reported by Han *et al.*, who studied[86] the solvothermal reaction of Co^{II} sources, Hbta and (1H-benzimidazol-2-yl)methanethiol. In this case however, the benzimidazole-based ligand suffers an *in situ* transformation to 1H-benzimidazole-2-carboxylic acid to provide the bonding capabilities of both

N- and *O*-donor atoms. This plethora of coordination sites lead to the formation of three unusual octanuclear compounds (**87** – **89**) that exhibit structural diversities depending on the reaction solvent: the same stoichiometric ratio of reactants yields a cup-shaped Co_8 cluster in MeOH (**87**), while the addition of ethanol/n-propanol and n-butanol affords Co_8 cluster-based 1D chains (**88** and **89** respectively). The presence of benzotriazolates in all of the compounds is important towards the formation of $[Co_4(bta)_3]$ tetramer units that are bridged by bic ligands to generate the resulting octanuclear core. Furthermore, magnetic experiments for **87** – **89** indicate their antiferromagnetic behaviour.

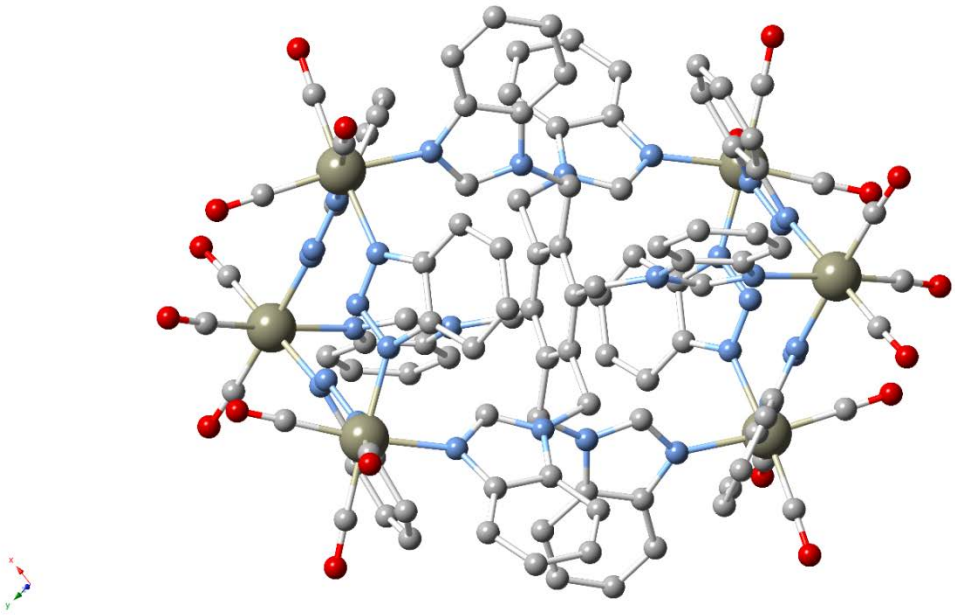

Figure 16. The hexanuclear compound **86**. Hydrogen atoms are omitted for clarity. Colour code Re (grey), C (grey), N (light blue), O (red).

4. Benzotriazole Derivatives as Main Ligands

Many derivatives of Hbta have also been used as ligands in coordination chemistry. This section includes: (i) *C*-substituted benzotriazoles with added functional groups in the 5´ (or 5´,6´) position(s). These compounds retain their triazole moiety intact for coordination and in general are commercially available at low cost. The most common examples are 5-methylbenzotriazole (MebtaH), 5-chlorobenzotriazole (ClbtaH), benzotriazole-5-carboxylic acid (H_2btca), 5,6-dimethylbenzotriazole (Me_2btaH) and 5,6-dimethoxybenzotriazole (OMe_2btaH); (ii) *C*-substituted

molecules incorporating a fused second 1,2,3-triazole moiety, leading to benzo(bis)triazole ligands; (iii) *N*-substituted benzotriazoles in either the 1´ or 2´ position; such molecules may only offer two nitrogen atoms for metal coordination, however they also provide extended options in ligand design and flexibility due to the synthetic versatility of Hbta.

4.1. C-substituted Benzotriazole Derivatives

4.1.1. 5- and 5,6-substituted Benzotriazoles

In regards to this category, employment of M^{II} sources with MebtaH, ClbtaH, Me_2btaH or OMe_2btaH (Scheme 5) as the main ligand once again seems to favour the formation of polynuclear coordination clusters; these complexes show no major differences compared to the analogous Hbta-based compounds mentioned before, despite the presence of additional chemical groups with potential steric hindrance. As a result, the reported[30,41,87–90] penta-, nona- and tetradecanuclear compounds $[Zn_5Cl_4(Me_2bta)_6]$, $[Zn_9(Me_2bta)_{12}(CH_3COO)_6]$, $[Zn_9Cl_6(OMe_2bta)_{12}]$, $[Fe_{14}O_6(Mebta)_6(OMe)_{18}Cl_6]$, $[Fe_{14}O_6(Clbta)_6(OMe)_{18}Cl_6]$, $[Fe_{14}O_6(Me_2bta)_6(OMe)_{18}Cl_6]$ (**90** – **95**) exhibit the same structural features noted in compounds **1**, **4** and **17** respectively. Similar isostructural complexes with a heteronuclear $\{M^{II}Zn_4\}$ (compounds **96** – **103**, where M = Fe, Co, Cu, Ni, Ru) [30,87,88] or $\{M^{II}_3Zn_6\}$ (compound **104**, where M = Fe) [90] core have also been reported; in both cases, the M^{II} ions are located in the centre of the core arrangement.

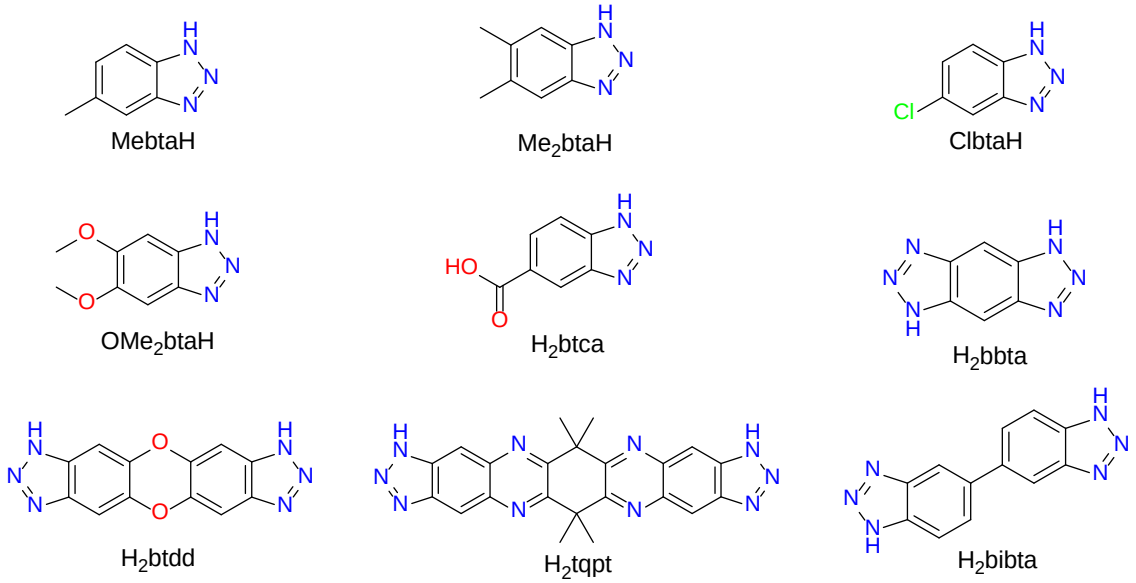

Scheme 5. The *C*-substituted benzotriazole-based ligands mentioned in Section 4.1.

On the other hand, reports on the use of M^{III} sources with Me_2btaH have yielded much more unpredictable results. In an expansion of their work in benzotriazole ligands employing MnF_3 as the metal source, Jones and co-authors synthesized[39,91] one Mn^{III}_8 and one $Mn^{IV}_3Mn^{III}_{10}$ polynuclear cluster, formulated as $[Mn_8O_4(OMe)_2(Me_2bta)_6F_8(Me_2btaH)(MeOH)_8]$ (**105**) and $[Mn_{13}O_{12}(Me_2bta)_{12}F_6(MeOH)_{10}(H_2O)_2]$ (**106**) respectively (Figure 17). These clusters are vastly different to compounds **13** – **15** that were generated with Hbta, although similar synthetic procedures involving the use of "melt" Me_2btaH were utilized; this implies that the steric effects of the additional methyl groups are a crucial factor in the self-assembly of the cluster. The main core of **105** consists of a central $[Mn_4O_2]^{8+}$ butterfly unit, the body atoms of which also connect to two peripheral $[Mn_3O]^{4+}$ triangular units via an O^{2-} ion to form a $[Mn_8O_4]^{16+}$ core. Six deprotonated Me_2Bta ligands bond in a $\mu_{1,2}$-coordination mode, while further bridging and terminal ligation occurs from methoxy groups and fluorine anions. The protonated Me_2btaH ligand bonds in a monodentate fashion to a Mn centre, while stabilizing the framework through hydrogen bonding. **106** contains a centred $[Mn^{IV}_3Mn^{III}_4O_{12}]$ core. Within this unit, the Mn^{IV} ions form a linear $[Mn_3O_4]$ trimer through the centre of the hexagon with the Mn^{III} centres attached on either side. The remaining Mn^{III} ions are located, alternately above and below this plane, connected with the hexagonal core through O^{2-} bridges. Further bridging takes place through $\mu_{1,2}$-Me_2bta ligands to ensure cluster stability. Magnetic experiments for **105** and **106** reveal that both compounds have small spin ground states.

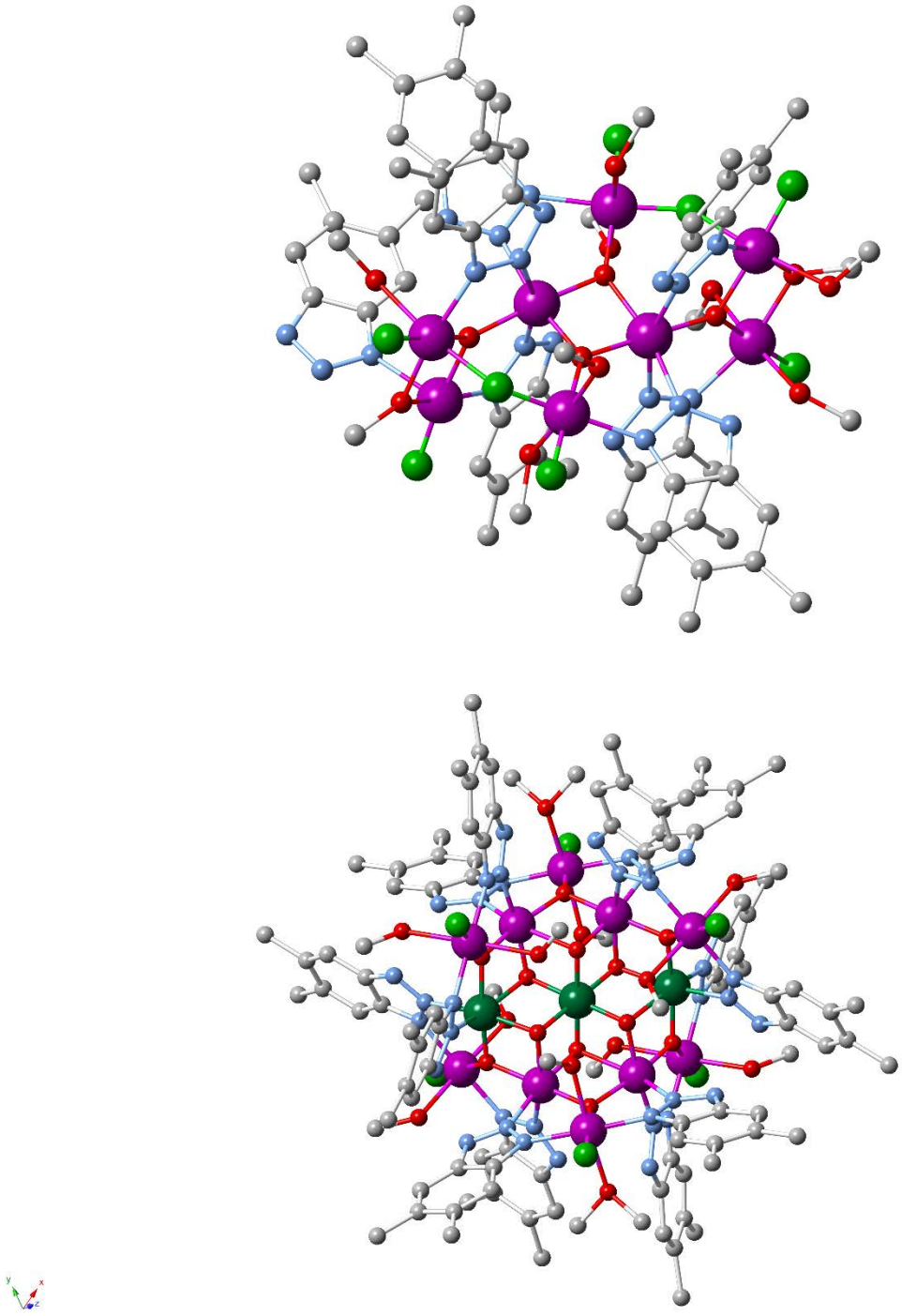

Figure 17. (upper) The octanuclear compound **105**. (lower) The tridecanuclear complex **106**. Hydrogen atoms are omitted for clarity. Colour code Mn^{III} (dark magenta), Mn^{IV} (dark green) C (grey), N (light blue), O (red), F (green).

The same group also explored the vanadium chemistry of Me_2btaH in a subsequent article[92]; notably, the reaction of VCl_3 with Me_2btaH and NaOMe in MeOH at room temperature under an inert atmosphere yielded the mixed-valence $V^{III}/^{IV}$ species $[(V^{IV}O)_8V^{III}_2(Me_2bta)_8(OH)_4(OMe)_{10}]$ (**107**). This unique compound is based on a square prismatic, box-like octanuclear $(V^{IV}O)_8$ cluster which contains a covalently bound V^{III} dimer, resulting in an overall very highly reduced polyoxovanadate. The deprotonated Me_2bta ligands play a critical role in the self-assembly of this cage, with four $\mu_{1,3}$-bridging molecules forming the edges of the square faces of the $(V^{IV}O)_8$ box, and another four also connecting to the central V^{III} ions in a $\mu_{1,2,3}$-coordination mode (Figure 18). Magnetic susceptibility experiments for **107** showed a strong presence of antiferromagnetic interactions, with the room-temperature value of $\chi_M T$ measured at 3.3 cm^3 K mol^{-1} and rapidly decreasing as temperature decreased.

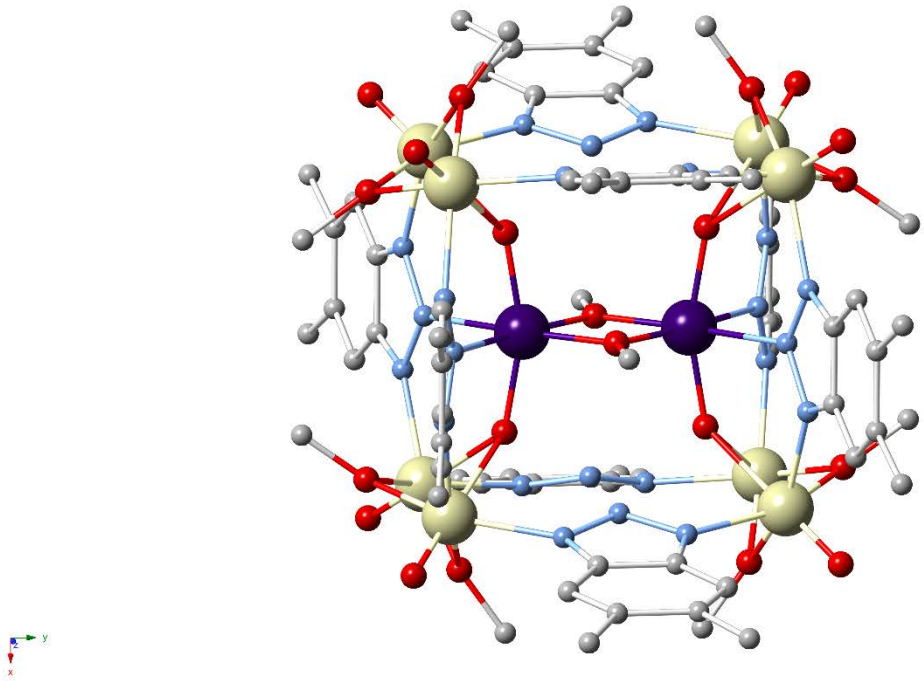

Figure 18. The decanuclear box-like cluster **107**. Hydrogen atoms are omitted for clarity. Colour code V^{III} (pale yellow), V^{IV} (purple), C (grey), N (light blue), O (red).

Perhaps the more interesting ligand in the category of 5-substituted benzotriazoles, however, is H_2btca, as its carboxylate group provides additional coordination sites and accounts for completely different structures with unique features and properties. In a recent study, Lanza and co-workers report[93] the formation of a polymeric framework $[Co_3(OH)_2(btca)_2]\cdot 2DMF$ (**108**) which

contains rhombic pores and extends to 3D as each btca unit bridges in a total of five Co^{II} centres through its carboxylate and triazole moieties as seen in Figure 19. These centres are unsaturated (coordination number 5), as the solvent molecules do not coordinate and are instead found within the pores. This framework appears to be very flexible, showing reversible pressure-induced nucleophilic addition of guest molecules; upon increase of pressure, coordination of DMF to one of the unsaturated metal sites occurs as the framework becomes more rigid, while the introduction of MeOH results in solvent exchange and coordination to all Co sites. After decompression, the framework retains its flexibility as the MeOH molecules are no longer coordinated.

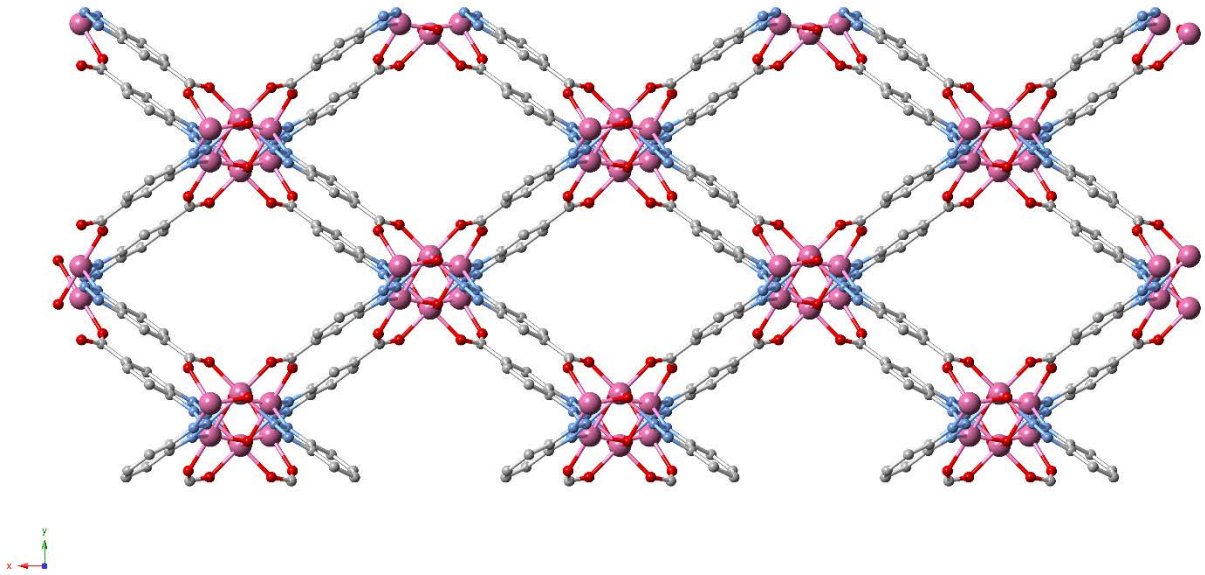

Figure 19. View of the rhombic 3D framework in compound **108**. Hydrogen atoms and solvent molecules are omitted for clarity. Colour code Co (light purple), C (grey), N (light blue), O (red).

A similar solvent exchange phenomenon was demonstrated[94] by Qiao *et al.* in the isoskeletal $[Co_3(OH)_2(btca)_2]\cdot 4H_2O$ (**109**), which upon immersion to EtOH exchanges its guest molecules to generate $[Co_3(OH)_2(btca)_2]\cdot EtOH$. Additionally, sorption properties for the desolvated compound were studied by Ren and co-authors, who showed that the framework exhibits very good CO_2 uptake of 223.7 and 104.7 mg g^{-1} at 273 and 298 K respectively[95]. Xiao and co-workers showed[96] that the isostructural zinc analogue $[Zn_3(OH)_2(btca)_2]\cdot DMF\cdot H_2O$ (**110**) also exhibits large flexibility and a similar "breathing effect". Controlled heating of **110** at 220 or 440°C yielded compounds $[Zn_3(OH)_2(btca)_2]\cdot DMF\cdot 0.5H_2O$ (**111**) and $[Zn_3(OH)_2(btca)_2]\cdot 2H_2O$ (**112**) which

showed increased framework narrowing and pore shrinking as the guest molecules were gradually removed.

Different architectures, however, are obtained with the use of other metals. Han and co-authors have reported[97] a Mn^{II}-based coordination polymer, $[Mn_5(btca)_4(\mu_3\text{-}OH)_2(EtOH)_2]$ (**113**) that extends to three dimensions. **113** features 1D porous channels containing {Mn-OH-Mn} chains and btca linkers; the latter also propagate the structure to its 3D network. Two different bridging modes can be found in the btca ligand: one type adopts a μ_5 mode through three nitrogen atoms and μ_2,η_2-carboxylate group, while the second shows a total μ_4-coordination mode consisting of $\mu_{1,2}$ triazole moiety and μ_2,η_2-carboxylate group. In regards to its potential properties, relevant studies showed that **113** is an unusual example of a 3D metamagnet containing 1D ferrimagnetic chains. Furthermore, the activated framework of **113** was found to absorb CO_2 (at room temperature and 275 K) or H_2 (0.99 wt % at 0.5 atm and 77 K, reaching a maximum of 1.03 wt % at 5.5 atm).

Interestingly, the reaction of Cu^{II} nitrate and H_2btca leads to completely different assemblies depending on the experimental conditions, as shown[98] by Xiao *et al.* The authors report the construction of three Cu^{II} compounds, $[Cu(btca)(H_2O)_2]$, $[Cu(btca)(H_2O)_{3.5}]_8\cdot 16H_2O$ and $[Cu_{2.5}(btca)_{1.5}(Hbtca)_{0.5}(\mu\text{-}Cl)_{0.5}(\mu_3\text{-}OH)(H_2O)]\cdot H_2O$ (**114** – **116**) through the use of solvothermal conditions and various solvents. Synthesized in acetonitrile/ammonia solution/water, **114** exhibits a 2D layer structure with (4.8^2) topology; in this case, the benzotriazolate ligand shows an unusual μ_3-coordination mode that includes a $\mu_{1,2}$ triazole moiety and η_1-carboxylate group. Compound **115** was constructed in a mix of ammonia solution/water and possesses a 0D metallomacrocyclic structure with flat octagonal geometry that is presented in Figure 20: hydrogen bonding between each metallomacrocycle results in an aesthetically pleasing three-dimensional nanotubular architecture. It is worth noting that the carboxylate group of the ligand is not used for coordination in this case. Finally, **116** was afforded in the presence of NaCl/acetonitrile/water and exhibits a 3D porous honeycomb-like structure, with the ligand showing μ_4-coordination mode that contains of $\mu_{1,2,3}$ triazole and η_1-carboxylate moieties. The authors indicate that the diversity of these structures mainly stems from the versatile coordination modes of H_2btca in each compound.

Finally, a novel report[99] from Uhl *et al.* investigates the application of H_2btca in the generation of organometallic frameworks, reacting the ligand with the digallium compound $R_2Ga–GaR_2$, where R = $CH(SiMe_3)_2$. The resulting compound $[Ga_2R_2(btca)]_6$·THF (**117**) generates a dodecagallium cage-like structure with a THF molecule encapsulated in its central cavity. This unprecedented structure contains six Ga-Ga bonds in a single molecule, each bridged by btca carboxylates. The individual bond pairs are further bridged by nitrogen atoms of $\mu_{1,3}$ triazole groups. Notably, the compound retains its cage structure in solution, while the guest solvent molecule cannot be exchanged or be removed *in vacuo*.

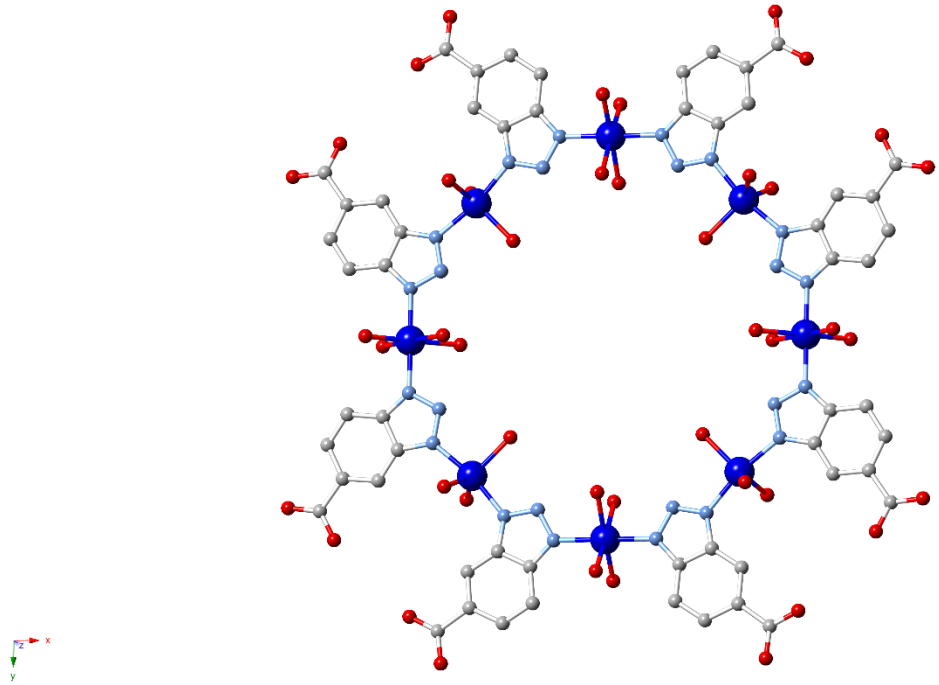

Figure 20. The metallomacrocyclic architecture in compound **115**. Hydrogen atoms and solvent molecules are omitted for clarity. Colour code Cu (blue), C (grey), N (light blue), O (red).

4.1.2. Benzo(bis)triazole Derivatives

In the search for novel *N*-donor ligands towards more unique and functional coordination compounds, a popular design strategy in the last decade has been the incorporation of a second 1,2,3-triazole moiety that is fused within the same benzotriazole unit. These benzo(bis)triazole type of ligands (Scheme 5) can (i) provide plenty of coordination sites, (ii) promote the construction of CPs, easily increasing their dimensionality without the need of additional pillar co-

linkers, (iii) supply the desired level of variety and flexibility depending on the intended use, since they may be attached to either a rigid or a non-rigid backbone.

Seminal work in this field has been performed by Volkmer's group, who attempted to utilize the common $[M_5(ligand)_nX_4]$ motif as a building unit towards high-dimensional CPs without the need of a secondary linker. To achieve this, they introduced[100] the ligand 1H,5H-benzo(1,2-d:4,5-d')bistriazole (H_2bbta). Indeed, the solvothermal reaction of $ZnCl_2$ and H_2bbta in DMF led to the synthesis of compound $[Zn_5Cl_4(bbta)_3]\cdot 3DMF$ (**118**). Notably, the parameters of this synthesis (time, temperature, solvent, base presence) may be further optimized to control the nucleating process in order to produce micro- and nanoscale material[101]. **118** is comprised of cationic pentanuclear $[Zn_5Cl_4]^{6+}$ nodes (four tetrahedral Zn^{II} centres and one octahedral) that are linked through bbta molecules resulting in a 3D porous network (Figure 21). Each bbta ligand shows a $\eta^3{:}\mu^6$ coordination mode similar to the one found in compound **1**. The formed network presents large cavities up to 11.94 Å albeit the aperture of the pores is relatively small (2.52 Å). Due to this, **118** shows highly selective adsorption of H_2 over N_2 at -196^{o}C.

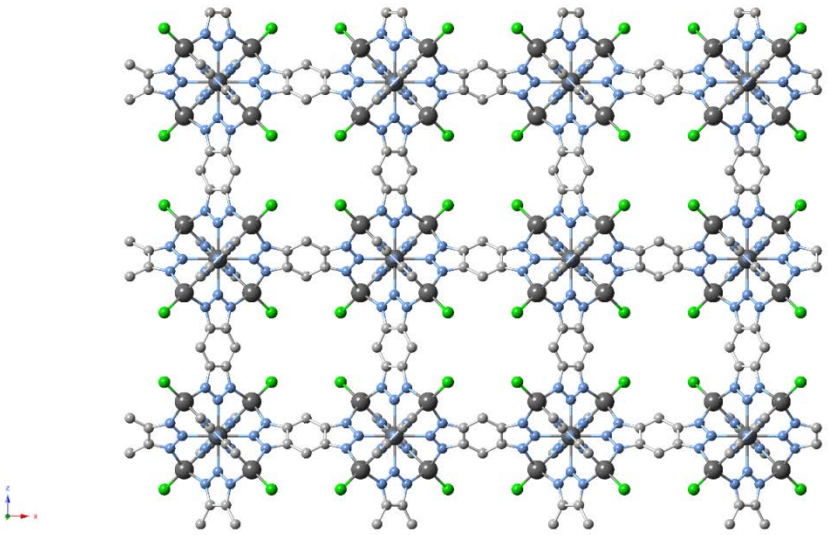

Figure 21. The porous 3D network in compound **118**. Hydrogen atoms and certain solvent molecules are omitted for clarity. Colour code Zn (dark grey), C (grey), N (light blue), Cl (green).

After the introduction of this new type of benzotriazolate ligands several strategic approaches and modifications followed in order to further improve the resulting compounds. Employment of $MnCl_2$ instead of $ZnCl_2$ led to the formation of $[Mn_2Cl_2(bbta)(H_2O)_2]$ (**119**), a 3D porous CP with

a honeycomb-like framework (Figure 22), as reported by Chen and co-authors[102]. While the pentanuclear motif is not observed in this structure, the bbta ligands exhibit a similar binding mode with each molecule coordinating to six Mn^{II} centres. This dynamic framework was then subjected to post-synthetic modifications through removal of all guest molecules and oxidation of the Mn^{II} ions to Mn^{III} by using H_2O_2[103]. Through this method it was made possible to generate a catalytically active porous CP with Mn^{III} sites while avoiding the difficulties of direct synthesis. Indeed, the activated **119** proved to be a suitable heterogeneous catalyst in the oxidation of alkyl benzenes to phenyl ketones as seen in Scheme 6. Average to excellent (21-97%) conversions were afforded when the reaction was performed in MeCN/AcOH/H_2O at 80ºC for 10 hours and under 10 mol% of the compound. The catalyst may also be reused for at least 5 cycles with only marginal decreases in conversion.

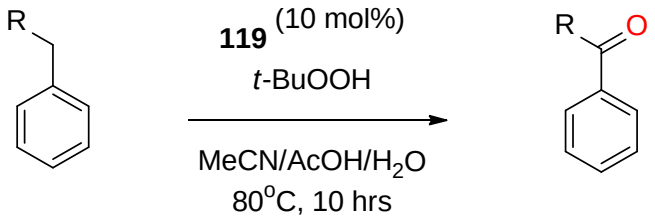

Scheme 6. Oxidation of alkyl benzenes to phenyl ketones as catalysed by **119**.

The presence of open metal sites in this type of frameworks has been extensively utilized leading to several studies of significant importance. The same group reported[104] the synthesis and post-synthetic modification of an analogous Co^{II} compound, [Co_2Cl_2(bbta)] (**120**), in a subsequent study. **120** was then immersed to a solution of 1.0 M KOH for 24 hours resulting to the isostructural [Co_2(μ-OH)$_2$(bbta)] (**121**) through anion exchange while retaining its crystallinity. **121** was found to be a highly efficient electrochemical catalyst towards oxygen evolution reactions, affording a current density of 2.0 mA cm^{-2} at an overpotential of 489 mV. In contrast, compound **120** exhibited much lower activity, indicating that the coordinated hydroxy ligands are crucial in accelerating the reaction process. On the other hand, **120** also presents impressive gas uptake properties as reported by Rieth and co-authors[105], who demonstrated that the compound shows a record NH_3 sorption of 8.56 mmol g^{-1} under conditions suitable to personal protection equipment. This performance was also superior compared to the one of analogous [Cu_2Cl_2(bbta)] and [Ni_2Cl_2(bbta)] (**122** – **123**) porous materials.

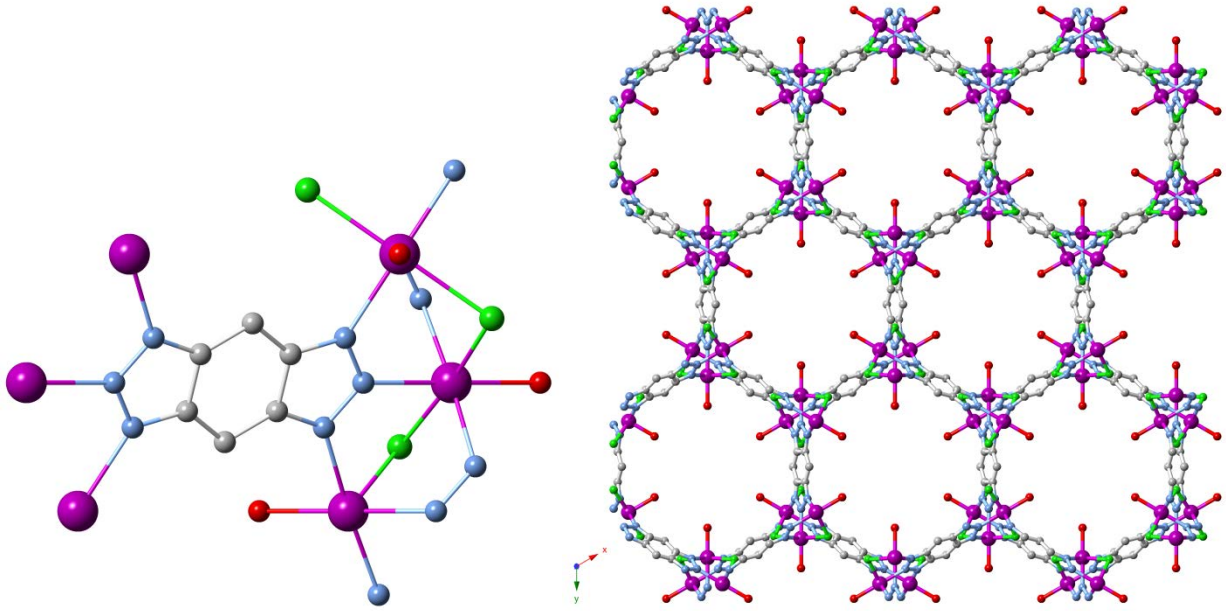

Figure 22. The building unit (left) and the porous 3D honeycomb-like framework (right) in compound **119**. Hydrogen atoms are omitted for clarity. Colour code Mn (dark magenta), C (grey), N (light blue), O (red), Cl (green).

Further investigations of these concepts led to the design of more elongated benzo(bis)triazole ligands in order to extend the eventual frameworks. Denysenko and co-workers synthesized[106] the linker 1,9-dihydrodibenzo[b,e][1,4]dioxino[2,3-d:7,8-d']bis([1,2,3]triazole) (H_2btdd) which contains a benzotriazole moiety fused to each side of a 1,4-dioxane molecule; the use of H_2btdd led to the construction of $[Zn_5Cl_4(btdd)_3]$ (**124**, Figure 23) which contains analogous building units and ligand coordination mode as in **118**. However, due to the longer linker the resulting 3D framework has significantly larger cavities (18.56 Å) and aperture (9.13 Å) sizes, allowing for increased uptake (4 wt%) of H_2 at 20 bar and 77 K.

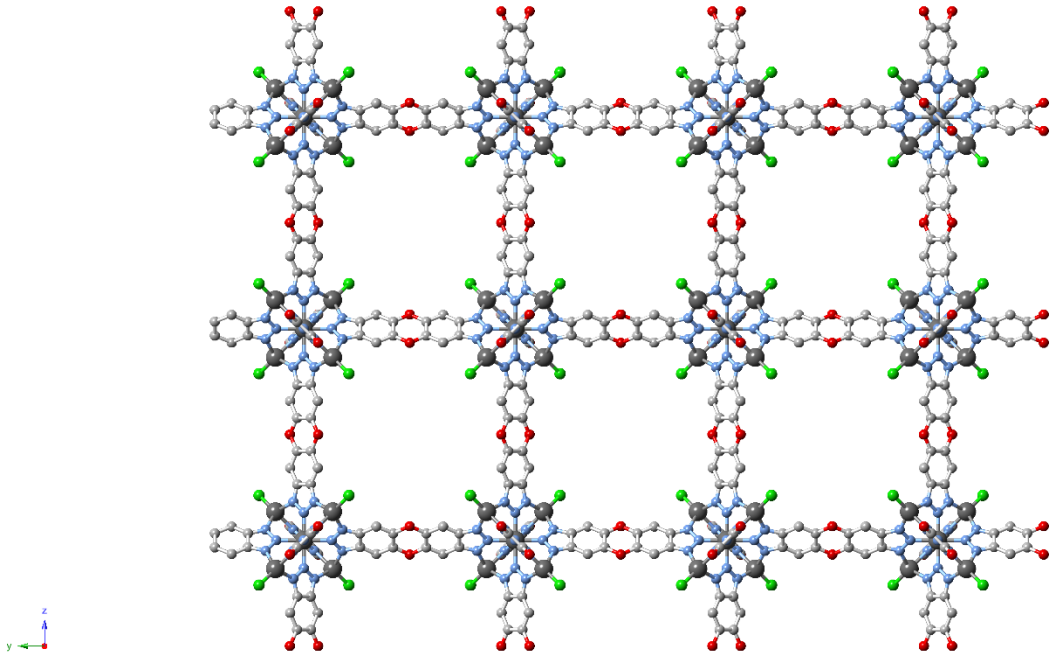

Figure 23. The porous 3D network in compound **124**. Hydrogen atoms are omitted for clarity. Colour code Zn (dark grey), C (grey), N (light blue), Cl (green), O (red).

Remarkably, a significant number of studies have explored the potential of this system through various post-synthetic modifications of **124**. Initial reports by Denysenko *et al.* showed[107] that replacement of the tetrahedral Zn sites with Co^{II} ions is possible when the compound is immersed to a $CoCl_2$/DMF solution under heating, leading to the isostructural mixed metal framework $[ZnCo_4Cl_4(btdd)_3]$ (**125**). Due to its open framework structure, the Co^{II} centres in **125** are catalytically active and thus the compound was found to show reversible CO oxidation capabilities. Notably, the catalyst does not require the high pre-treatment temperatures usually found in such catalysts and can be activated at only 200^oC. The same group demonstrated that an exchange of Zn^{II} centres with Cu^{II} ions is also possible through the use of copper chloride; however, on average only two out of the four tetrahedral Zn sites per unit are replaced with Cu sites in this case. Further ion exchange of the chloride anions with formates led to the corresponding $[Zn_3Cu^{II}_2(formate)_4(btdd)_3]$ compound (**126**), which can be then thermally activated to generate the analogous Cu^{I}-based framework (**127**) that contains free active sites. The authors showed that **127** can bind to small molecules such as C_2H_4 and CO through the formation of stable complexes, suggesting the massive potential of such frameworks.

Additional investigations by Dincă's group based on the above findings have uncovered several applications arising from the ion exchange capabilities of the M^{II}/btdd system. The authors found[108,109] that **124** has a very high water adsorption capacity of 1.05 g g^{-1}; additionally, more controlled replacement of the zinc sites with cobalt is possible, producing a selected number of open metal sites which in turn also provides the ability to control the relative humidity at which water uptake occurs. When nickel centres replaced the peripheral zinc sites of **124**, the resulting analogue **128** was found to be an efficient heterogeneous catalyst for the selective dimerization of propylene[110], resembling the activity of other nickel-based scorpionate compounds with similar coordination environment. Expanding on these concepts, the analogous Ti^{IV}, Ti^{III}, Cr^{II}, Cr^{III}, Fe^{II} complexes were also generated, replacing the peripheral zinc sites in each case to give compounds **129** – **133** respectively; all complexes were then tested for their catalytic activity in olefin polymerization reactions[111]. Notably, the Co^{II} analogue **125** showed[112] extremely high (99.3%) selectivity in the polymerization of 1,3-butadiene towards the corresponding 1,4-*cis*-polymer product.

Treatment of H_2btdd with M^{II} chlorides in DMF/alcohol/HCl at 65 °C afforded[113] the dinuclear compounds $[Mn_2Cl_2(btdd)(H_2O)_2]$, $[Co_2Cl_2(btdd)(H_2O)_2]$ and $[Ni_2Cl_2(btdd)(H_2O)_2]$ (**134** – **136**) which show similar structural features to the bbta-based compound **119**. The activated frameworks were found to show very high NH_3 uptake (15.47, 12.00, and 12.02 mmol of ammonia per gram, respectively, at standard temperature and pressure conditions) that is reversible for at least three cycles. In addition, **135** emerged as an ideal framework for water uptake, capturing 82% water by weight below 30% relative humidity[114]. The unusually high hydrophilicity of these benzotriazolate frameworks can also be utilized as the driving force towards heat transfer. Compounds **123** and **135** were found to exhibit non-overlapping water isotherms that can function in tandem to provide continuous cooling with a record ideal coefficient of performance[115].

Other efforts have concerned the use of such structures in cooperative adsorption studies, in which binding of a guest molecule in one of the framework's open metal sites can lead to alterations in the binding properties at neighbouring metal sites. Such a concept is explored in a recent study by Long and co-workers[116]. The authors employ the combination of Fe^{II} centres with ligands H_2bbta and H_2btdd to examine these phenomena: the resulting compounds $[Fe_2Cl_2(bbta)]$ (**137**)

and [Fe_2Cl_2(btdd)] (**138**) were found to be isostructural to the respective compounds **119** and **134**, exhibiting analogous honeycomb-like frameworks. Indeed, both complexes were found to adsorb CO through a cooperative mechanism involving a spin transition in the Fe^{II} centres. In detail, it was shown that the adsorption of CO in the open metal sites of each framework causes significant contractions in the relevant Fe-N and Fe-Cl bond lengths, consistent with a conversion from high-spin to low-spin Fe^{II}. Interestingly, while both compounds display sharp steps in the adsorption isotherms, the step position shifted considerably in each case (pCO_2 = 170 mbar in **137**, 500 mbar in **138** when T = 25 °C). Additionally, **137** showed high selectivity in potential CO separations when tested in CO/H_2 and CO/N_2 mixtures.

Finally, an interesting strategy that has also been employed using the M^{II}/btdd system is the mimicking of metalloenzymes and their coordination environments in order to generate enzyme-like heterogeneous catalytic activity within metal-organic frameworks. Specifically, recent attempts[117] have been made to functionalize the {N_3ZnCl} coordination sphere that is present in the pentanuclear compound **124** towards compounds which mimic the activity of carbonic anhydrase, an enzyme that catalyses the hydrolysis of carbon dioxide into bicarbonate and protons. **124** was modified through anion exchange experiments to replace Cl sites with OH units, affording the corresponding [$Zn_5(OH)_4$(btdd)$_3$] analogue (**139**) which possesses similar coordination environment to the one of the enzyme. As a result, **139** can bind CO_2 and catalyse the oxygen atom exchange between H_2O and CO_2, in consistency with the activity of carbon anhydrase.

Attempts have also been made to further increase the size of the organic linker while retaining the pentanuclear structural motif. However, utilization of 6,6,14,14-tetramethyl-1,6,11,14-tetrahydro-[1,2,3]triazolo[4',5':6,7]quinoxalino[2,3-b][1,2,3]triazolo[4,5-i]phenazine (H_2tqpt) led to the synthesis of a two-fold interpenetrated 3D network, [Zn_5Cl_4(tqpt)$_3$] (**140**), instead[118]. Interestingly, the additional pyrazine nitrogen atoms do not participate in metal coordination, while the binding mode in the triazole units of tqpt remains the same as in the analogous compounds with shorter ligands. Post-synthetic metal exchange of the peripheral tetrahedral Zn^{II} atoms with redox-active M^{II} ions (Co, Ni, Cu) was also possible. Interestingly, the reaction of Cu^{II} sources with H_2tqpt resulted[119] in the formation of [Cu^{I}_2(tqpt)] (**141**) as the metal centres are reduced during the synthesis. The structure of **141** extends to three dimensions to generate a network with

large (7.8 Å) pores; the three crystallographically independent Cu^{I} ions exhibit different (linear, trigonal, tetrahedral) geometries while tqpt shows the same coordination mode as in **140**. Notably, the compound presents a reversible breathing effect and is able to bind carbon monoxide molecules through its active trigonal Cu^{I} sites.

On the other hand, a report[120] from Schmieder and co-workers documents their efforts towards the synthesis of the shorter-length ligand 1H,1'H-5,5'-bibenzo[d][1,2,3]triazole (H_2bibta). The resulting structure, formulated as $[Zn_5(OAc)_4(bibta)_3]$ (**142**) reveals a 3D microporous architecture with trigonal voids; the building blocks of this frameworks, as well as the binding mode of the linker are analogous as above. Once again, post-synthetic metal exchange of the peripheral tetrahedral Zn^{II} atoms with Co^{II} ions is also possible, depending on the Zn/Co ratio within the suspended solution.

4.2. N-substituted Benzotriazole Derivatives

4.2.1. N1-substituted Benzotriazoles

The use of 1-substituted benzotriazole ligands with various groups or molecules as substituents (Scheme 8) has been prevalent in the literature. One of the first works that incorporated this strategy was by Richardson and Steel, who explored the chemistry of ligands pbta (1-(pyridin-2-yl)-1H-benzotriazole), pmbta (1-(pyridin-2-ylmethyl)-1H-benzotriazole) and ibta (1-(1H-benzotriazol-1-yl)isoquinoline) with Pd^{II}, Cu^{II} and Ag^{I} sources[121]. This strategy mainly afforded 0D complexes and 1D CPs where metal coordination occurs through the N3 atom of the benzotriazole moieties. The resulting compounds, $[Pd_2(pmbta)_2Cl_4]$, $[Cu(pbta)_2(MeOH)_2]\cdot(NO_3)_2$, $[Cu(pbta)_2Cl_2]$, $[Cu(pmbta)_2Cl_2]$, $[Cu_4(ibta)_4Cl_6O]$, $[Ag(pbta)(NO_3)]$, $[Ag(pmbta)(NO_3)]$ (**143** – **149**), were mainly studied for their structural features and to demonstrate the potential of such ligands. A similar linker including the imidazole group, 1-(imidazol-1-yl-methyl)-benzotriazole (imbta), was also explored by An and co-workers in a 2008 study[122]; the authors report the 0D monomeric coordination compound $[Ag(imbta)_2]\cdot(NO_3)\cdot(H_2O)$ (**150**). Although the benzotriazole moiety does not participate in the coordination, it directs the crystal packing and supramolecular architecture through multiple π···π interactions. In addition, **150** demonstrated interesting biological applications, exhibiting radical-scavenging and fungicidal activity. More recently, Hu and co-authors introduced[123] the multiple *N*-donor ligand 1-((2-(pyridin-2-yl)-1-

benzoimidazol-1-yl)methyl)-1-benzotriazole (pbmb) to construct three novel coordination compounds formulated as $[Ag_4(pbmb)_4(BF_4)_4]$, $[Cd_2(pbmb)_4]\cdot(ClO_4)_4$, and $[Cd_4(pbmb)_4I_8(MeOH)_2]$ (**151 - 153**). The former two complexes present dimeric moieties linked by pbmb ligands to form a 1D polymeric chain network, while **153** exhibits a 0D tetrameric structure as the iodine atoms act as terminal ligands and do not extend the architecture further. Photoluminescence measurements for all complexes indicated that **152** exhibits strong fluorescence intensity with a maximum emission wavelength of 387 nm.

In recent years there have also been studies utilizing 1-substituted benzotriazole ligands that have uncovered some notable applications in the field of catalysis. In a series of reports Wang and co-workers investigate the catalytic potential of well-defined 0D complexes that employ the pbta ligand in various organic transformations of importance. In detail, the authors first introduced a Cu^I-based compound formulated as $[Cu^I(pbta)(PPh_3)_2I]$ (**154**, Figure 24, left) that was found to catalyse the reaction of benzyl alcohols and diamines to produce 1-benzyl-2-aryl-1H-benzimidazole and 2-aryl-1H-benzimidazole derivatives[124]. These products were afforded in yields up to 91% when the reactions were performed using 2 mol% of the catalyst and under the conditions presented in Scheme 7. Notably, the presence of the pbta ligand appeared crucial in the catalytic performance as the simple copper salts could not catalyse the reactions. Mechanistic studies revealed that the first step in these transformations involved a reversible alcohol dehydrogenation and the formation of a copper hydride intermediate. A diagnostic copper hydride signal was also observed in solid-state infrared spectroscopy studies, further supporting these findings. In a subsequent article, the authors reported[125] the synthesis of an analogous 0D complex based on gold sources, formulated as $[Au^I(pbta)(PPh_3)]\cdot(CF_3SO_3)$ (**155**). In a similar fashion, **155** was found to be an ideal catalytic precursor in borrowing hydrogen and dehydrogenation reactions of alcohols and amines, resulting in the selective synthesis of substituted amines and ketones as detailed in Scheme 7. Good to excellent yields (67 – 95%) of the relevant substrates were generated under the optimal conditions and using only 1 mol% of the catalytic precursor. The next compound in this family of catalysts was generated from the reaction of pbta with the Ru^{II}(*p*-cymene) chloride dimer, leading to the synthesis of $[Ru^{II}(pbta)$(*p*-cymene)Cl]·Cl (**156**) as reported in a following study[126]. In this case, the Ru^{II} centre coordinates to pbta in a bidentate fashion through the N2 atom of the triazole moiety and the pyridine nitrogen

(Figure 24, right). Under the solvent-free conditions presented in Scheme 7, **156** was successfully tested as a catalyst in the alkylation of 2-oxindole with alcohols for a great range of substrates, affording yields up to 94%. While this reaction took place under N_2 conditions, the same catalytic protocol in the presence of atmospheric air unexpectedly resulted in the C3-hydroxy 2-oxindole products instead, promoting a one-pot C-H hydroxylation reaction (Scheme XX). Once again, the superior catalytic performance of the complex compared to the simple metal salts and other reported catalysts is attributed to the presence of the pbta ligand.

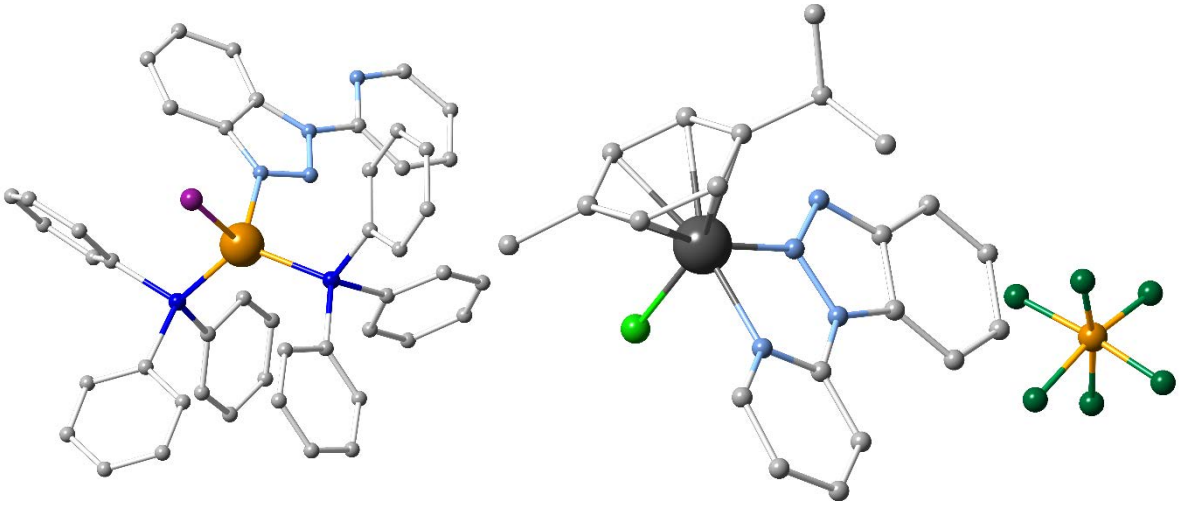

Figure 24. The structures of complexes **154** (left) and **156** (right). Hydrogen atoms are omitted for clarity. Colour code Cu^{I} (orange), Ru (dark grey), C (grey), N (light blue), F (teal), I (purple), Cl (green), P (dark blue).

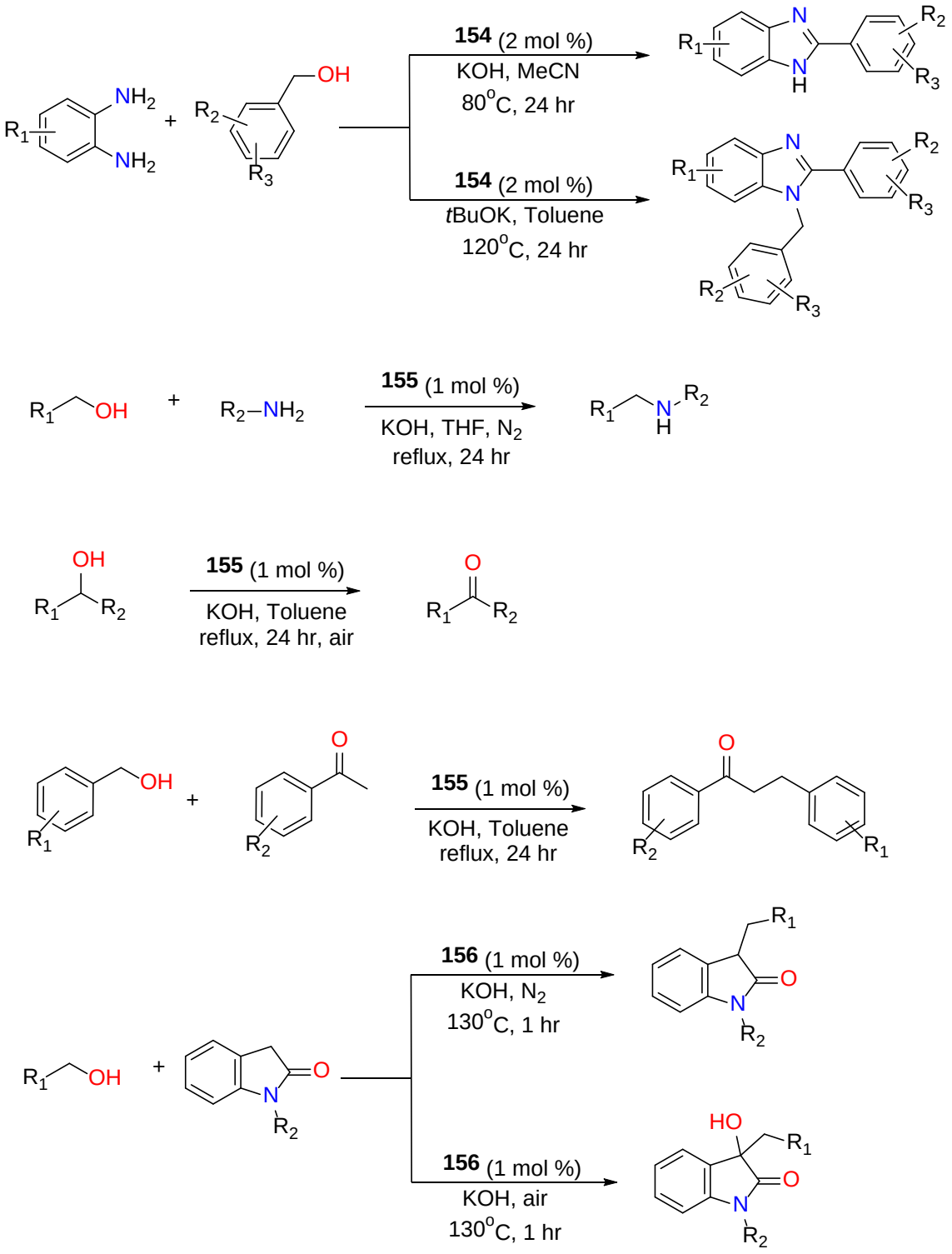

Scheme 7. Overview of the reactions catalysed by **154** – **156**.

Another example in this category of ligands concerns the incorporation of an additional hydroxy group which may provide extra coordination modes and enhance nuclearity to afford CPs and

clusters of interest: A study by Papatriantafyllopoulou and co-workers reports[127] the synthesis of two tridecanuclear Ni^{II} clusters, $[Ni_{13}(OH)_6(OAc)_8(btaO)_{12}(H_2O)_6(n\text{PrOH})_4]$ and $[Ni_{13}(N_3)_6(OAc)_8(btaO)_{12}(MeOH)_{10}]$ (**157** – **158**, Figure 25), utilizing the ligand 1-hydroxybenzotriazole (btaOH). In this case the ligand is coordinated through both nitrogens as well as the hydroxy oxygen atom, adopting a $\eta^1{:}\eta^1{:}\eta^1{:}\mu_3$ bridging mode. While the presence of competitive antiferromagnetic exchange interactions is observed in **157**, the spin frustration disappears with the incorporation of N_3^- ions in **158**. Furthermore, Stoumpos and co-authors synthesized[128] a high nuclearity Mn^{II} CP formulated as $[Mn_3(OAc)_2(btaO)_4(MeOH)_2]$ (**159**). The btaO ligand appears to be crucial in the formation of the resulting architecture, appearing in two different ($\eta^1{:}\eta^1{:}\eta^1{:}\mu_3$ and $\eta^2{:}\eta^1{:}\mu_3$) bridging modes to propagate the structure into two dimensions. Magnetic measurements for **159** indicated an overall antiferromagnetic behaviour. In contrast, lower nuclearity structures are obtained when Zn^{II} and Cd^{II} sources are used: Katsenis and co-authors report[129] the synthesis of 1D CP $[Zn(btaO)_2]$ and 0D monomer $[Cd(btaO)_2(H_2O)_4]$ (**160** – **161**). As expected, the structural simplicity of these compounds compared to **157** – **159** is related to the less complicated coordination modes of btaO ($\eta^1{:}\eta^1{:}\mu$ and η^1 in each case).

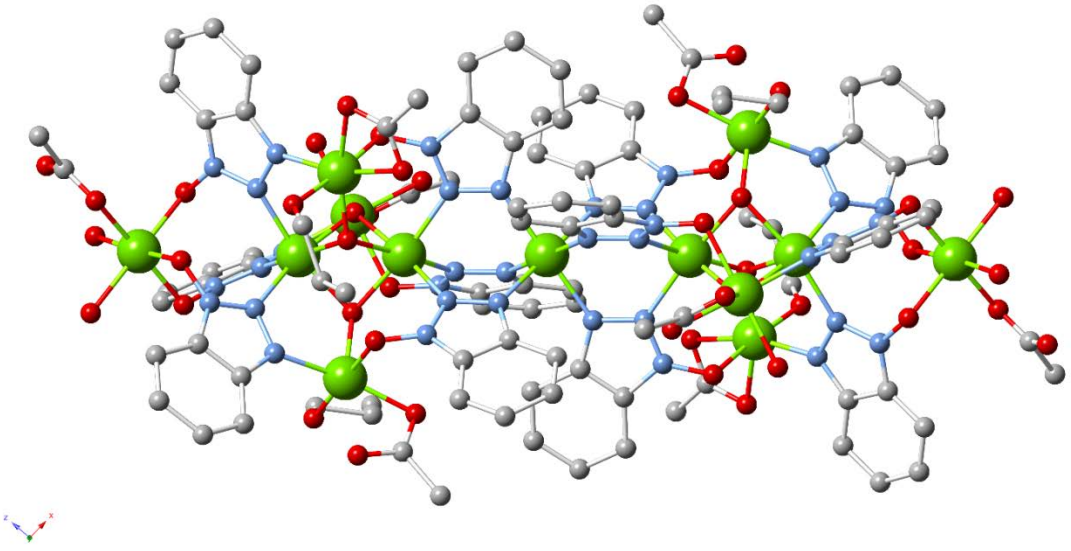

Figure 25. The structure of the tridecanuclear complex **157**. Hydrogen atoms are omitted for clarity. Colour code Ni (dark green), C (grey), N (light blue), O (red).

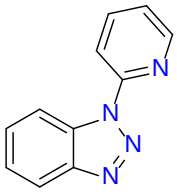

pbta

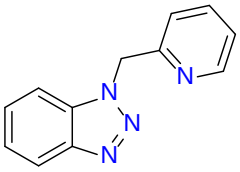

pmbta

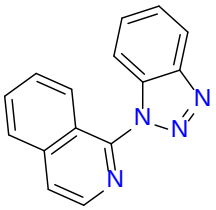

ibta

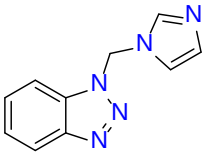

imbta

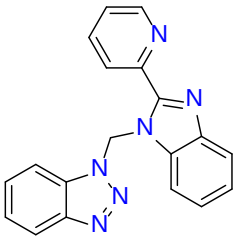

pbmb

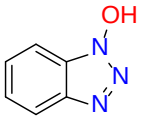

btaOH

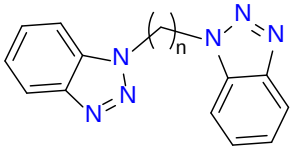

bbtm (n = 1)
bbte (n = 2)
bbtp (n = 3)
bbtb (n = 4)
bbth (n = 6)

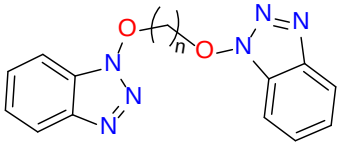

bbdp (n = 1)
bbdpt (n = 3)
bbdh (n = 4)

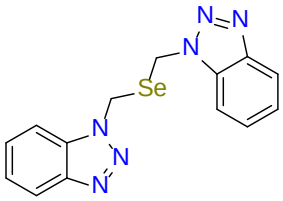

bbms

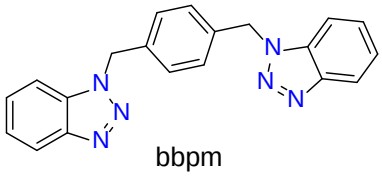

bbpm

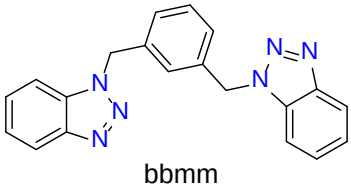

bbmm

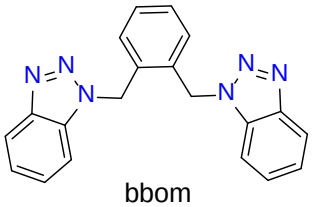

bbom

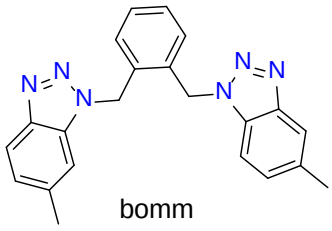

bomm

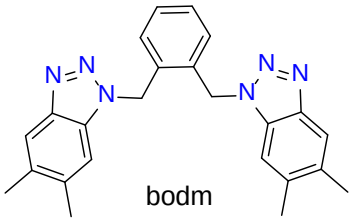

bodm

Scheme 8. The *N1*-substituted benzotriazole-based ligands mentioned in Section 4.2.1.

More intriguing, however, is the incorporation of a second benzotriazole unit to generate 1,1´-bis(benzotriazole) ligands with an increased number of potential coordination sites and provide controlled flexibility in the system. For this type of linkers, flexibility is typically introduced with the inclusion of alkyl chain spacer groups between the two benzotriazole units. Alkanes up to hexane have been a popular choice for these purposes, and several compounds have been reported with the respective ligands[121,130–139]. It is worth noting that the use of all linkers in this category mostly produced CPs with low dimensionalities, particularly one-dimensional. While several of these studies focus solely on the structural features of the compounds, the 1D CP $[Cu(bbtm)(NO_3)_2]$ (**162**, where bbtm = bis(benzotriazol-1-yl)methane, Figure 26) was further tested for its magnetic properties showing weak antiferromagnetic coupling between the Cu^{II} ions[135]. Moreover, a study by Meng *et al.* reported the third-order nonlinear optical (NLO) properties of 1D CPs $[Ni(bbtp)_2(NCS)_2]$ and $[Co(bbtp)_2(NCS)_2]$ (**163** – **164**, Figure 27), synthesized using 1,1'-(1,3-propylene)bis-1H-benzotriazole (bbtp) and KSCN with Ni^{II} or Co^{II} sources[131]. These isostructural ribbon-like compounds demonstrate strong NLO refractive behaviours with **164** exhibiting large NLO absorptive effects (nonlinear absorption coefficient $\alpha_2 = 1.4\ X\ 10^{-9}\ mW^{-1}$).

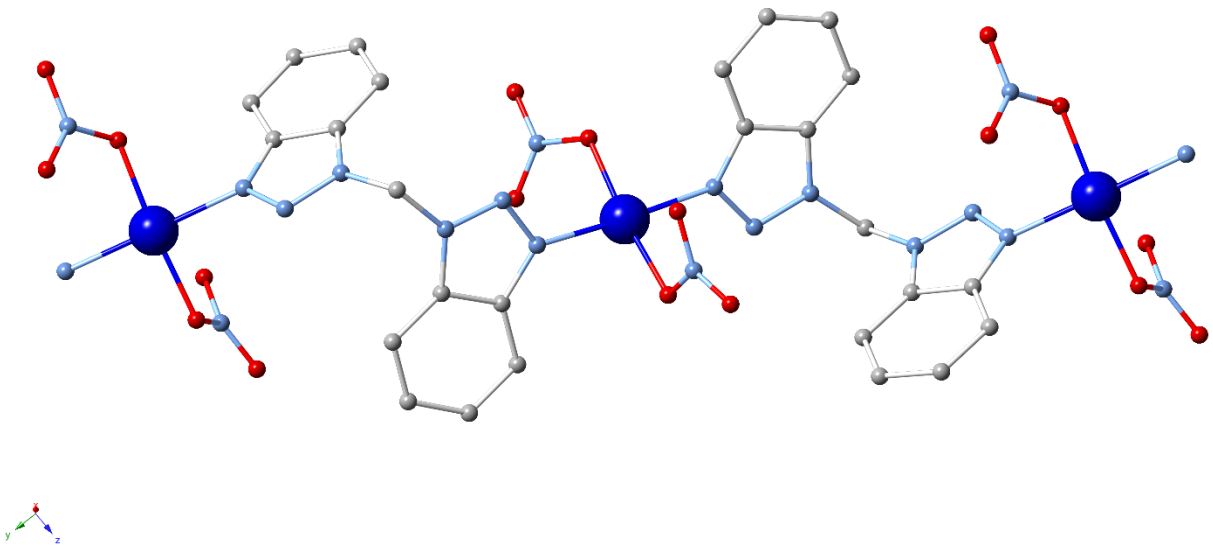

Figure 26. Part of the 1D framework in compound **162**. Hydrogen atoms are omitted for clarity. Colour code Cu (blue), C (grey), N (light blue), O (red).

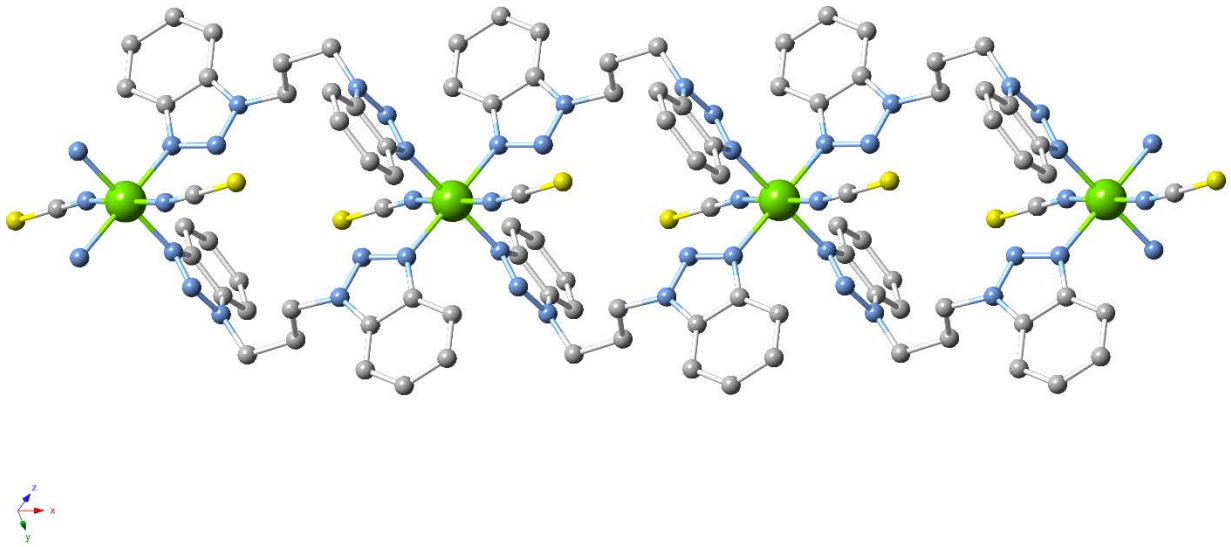

Figure 27. Part of the 1D framework in compound **163**. Hydrogen atoms are omitted for clarity. Colour code Ni (dark green), C (grey), N (light blue), S (yellow).

Analogous bis(benzotriazole)-dioxoalkane ligands have been employed using 1-hydroxybenzotriazole as the starting material, affording compounds similar to the above[140–142]. Notably, efforts[141] undertaken by Shit *et al*. resulted in the synthesis of isoskeletal polymeric compounds $[CuBr_2(bbdp)]_2$ and $[CuCl_2(bbdp)]_2$ (**165** – **166**, where bbdp = bis(benzotriazol-1-yl)-1,3-dioxapropane) which expand to two dimensions through halide bridging. **165** and **166** exhibited antiferromagnetic (J = -15.2 cm^{-1}, $\chi_M T$ = 0.79 cm^3 K mol^{-1} at 200 K, 0.09 cm^3 K mol^{-1} at 5 K) and ferromagnetic (J = +1.7 cm^{-1}, $\chi_M T$ = 0.91 cm^3 K mol^{-1} at 200 K, 1.00 cm^3 K mol^{-1} at 5 K) behaviour respectively. Magneto-structural correlation studies by the authors attributed this discrepancy to the different bridging halide atom in each case. Furthermore, Lu and co-workers introduce a similar selenium ether bis(benzotriazole) ligand to generate a ribbon-like 1D Co^{II} CP $[Co(bbms)_2(NCS)_2]$ (**167**, where bbms = bis((benzotriazol-1-yl)methyl)selane), during their attempts to utilize the biological activities typically found in selenium-based compounds[143]. For this reason, **167** and ligand bbms were tested for their superoxide dismutase activity to determine their performance in the conversion of superoxide to molecular oxygen using the pyrogallol autoxidation method. Interestingly, the former sample showed poorer activity, with the authors correlating this performance to the presence of the Co^{II} centres.

Another promising synthetic strategy in the field of bis(benzotriazole) ligands involves the incorporation of benzene-based spacers between the benzotriazole moieties, leading to 'semi-rigid' linkers with a smaller degree of flexibility[144]. This approach accounts for a middle-ground option that allows an amount of control over the resulting structure while retaining the advantages of flexible molecules, and can lead to a wide array of coordination motifs. The main ligands in this category are 1,4-bis((benzotriazol-1-yl)methyl)benzene (bbpm), 1,3-bis((benzotriazol-1-yl)methyl)benzene (bbmm), and 1,2-bis((benzotriazol-1-yl)methyl)benzene (bbom), which contain a flexible C-N bond in an otherwise rigid molecule and couple the benzotriazole units in respective *para*-, *meta*- and *ortho*-substitution on the benzene ring. Until recently the existing literature on these ligands was very scarce, simply consisting of a structural report on the 0D complex $[Ag_2(bbmm)_3]\cdot(NO_3)_2$ (**168**) and the POM-based CPs $[Cu(bbpm)_3(Mo_6O_{19})]$ and $[Ag_2(bbpm)_2(Mo_6O_{19})]$ (**169** and **170**)[145,146]. However, several studies by our group have since demonstrated that these ligands are indeed ideal candidates for the generation of functional low-dimensional CPs, producing dynamic architectures that can be easily manipulated and tuned to optimize their potential in magnetism and catalysis.

Initial systematic studies[147] with Co^{II} sources produced a series of 0D dimers, 1D and 2D CPs; this structural variety was shown to be owed to synthetic parameters (ratio, temperature and salt) as well as ligand selection, with the various conformations in each ligand being easily manipulated by temperature. In particular, a temperature-induced single-crystal to single-crystal transformation was found to take place, converting the 0D dimer $[Co(bbmm)Cl_2]\cdot MeCN$ (**171**) to a 2D coordination polymer $[Co(bbmm)Cl_2]$ (**172**) through a rotation of the non-rigid C-N bond in bbmm as seen in Scheme 9; alterations in crystallographic parameters as well as the coordination geometry of Co^{II} were also observed during this procedure. **172** was also investigated for its magnetic properties, along with selected compounds $[Co_2(bbom)_2Cl_4]\cdot 2MeCN$ (**173**, 1D CP, Figure 28) and $[Co_2(bbom)_2Br_4]$ (**174**, 0D dimer). Despite minor geometrical and structural variations in the complexes, the respective magnetic results showed considerable differences, suggesting that such Co^{II} nodes in CPs could function as sensitive signals of small changes in the local environment.

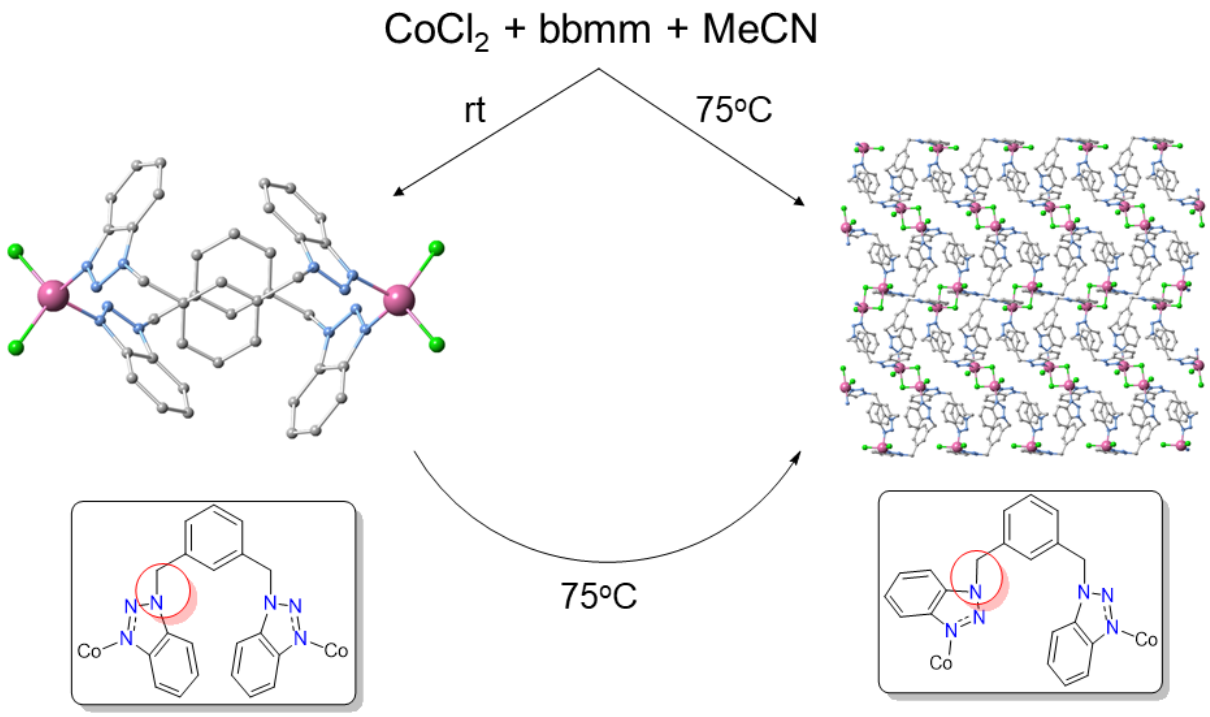

Scheme 9. A schematic representation of the temperature-induced single-crystal to single-crystal transformation of 0D dimer **171** (left) to 2D CP **172** (right).

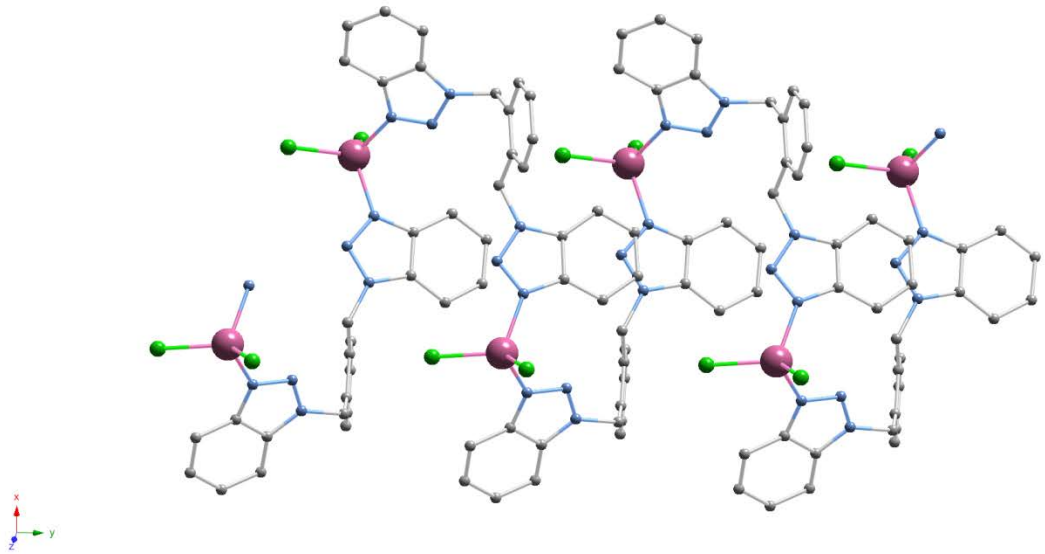

Figure 28. Part of the 1D framework of compound **173** along the *b* axis. Hydrogen atoms and solvent molecules are omitted for clarity. Colour code Co (pink), Cl (green), C (grey), N (light blue).

Having established a good initial understanding on the behaviour of these ligands in coordination chemistry, we then shifted our focus on the possible catalytic potential of such systems. Copper was a very attractive option for these purposes due to the many advantages (low cost, versatile chemistry, multiple oxidation states possible) it offers. As a result, subsequent studies demonstrated the use of various 1D Cu^{II} CPs as catalysts in a series of organic transformations. In these examples, the catalytic system was developed, optimized and evaluated through an "inorganic approach" that involved tuning of several coordination parameters in order to obtain important mechanistic information and refine the catalytic protocols. Furthermore, these results added an extensive amount of scientific input in the currently underutilized[148] field of 1D CPs in catalysis. The first of these reports demonstrated[149] the synthesis of $[Cu(bbom)_2(MeCN)_2]\cdot(ClO_4)_2$ (**175**), which presents a polymeric ribbon-like framework that extends to one dimension; each Cu^{II} centre presents a $\{N_6\}$ octahedral coordination environment in which the axial positions are occupied by acetonitrile nitrogens (Figure 29). **175** was then found to exhibit promising homogeneous catalytic activity in a new synthetic pathway towards the synthesis of substituted 1,4-dihydropyridines. These biologically interesting organic compounds and their derivatives have been found to show significant activity as calcium channel blockers; as a result, dihydropyridine analogues such as amlodipine, nifedipine and felodipine have been extensively used in pharmacology[150–152]. However, the known methodologies for the synthesis of such molecules typically include catalytic procedures with important disadvantages such as high reagent cost, high temperatures and tedious work up. Using mild catalytic conditions (2 mol% of catalyst, 24 hour stirring under refluxing MeOH), **175** was found to activate a previously unknown chemical transformation between symmetrical electron-rich aryl aldazines and alkyl propiolates to generate 5-aryl-1-(benzylideneamino)1,4-dihydropyridines in an efficient one-pot synthesis (Scheme 10, reaction A). The dihydropyridines were afforded in good isolated yields up to 68%, while Cu^{I} or Cu^{II} salts did not catalyse the reaction at all. During mechanistic investigations, polymeric compounds $[Cu(bbom)(NO_3)_2]$ (**176**) and $[Zn(bbom)_2(H_2O)_2]\cdot(ClO_4)_2$ (**177**) were also constructed but were found to be catalytically inactive; this big discrepancy in catalytic performance was attributed to the different coordination environment (**175** against **176**) as well as the different metal centre (**175** against **177**). Having these findings in mind, the proposed mechanism involved the formation of a Cu^{I}-acetylide intermediate, which undergoes a cyclization process followed by a [4 + 2] to produce the resulting dihydropyridine. Cyclic voltammetry

experiments on **175** further supported this hypothesis, revealing a reversible reduction process that was assigned to the [Cu^{II}]↔[Cu^{I}] couple.

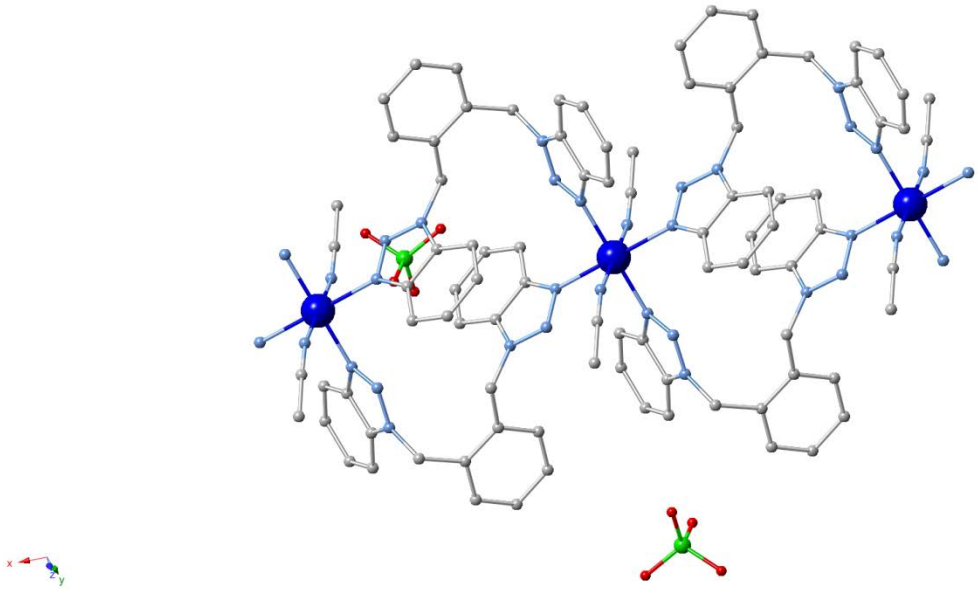

Figure 29. Part of the one-dimensional framework in **175** along the *a* axis. Lattice molecules and hydrogen atoms have been removed for clarity. Colour code Cu (blue), C (grey), N (light blue), Cl (green), O (red).

To carry on our investigations, we then sought to further optimize the catalytic potential of these Cu^{II} CPs. In particular, our studies were focused on already known organic transformations of significant importance, in which the proposed mechanism involved intermediates related to the suggested catalytic function of our system. Our selected reactions for these purposes, as shown in a number of subsequent reports[153–155], were (i) the multicomponent reaction (MCR) known as A^3 coupling of an aldehyde, an amine and an alkyne: this reaction yields propargylamines, which are important synthetic blocks towards *N*-containing biologically active compounds; (ii) the multicomponent synthesis of poly-substituted pyrroles from aldehydes, amines, and *β*-nitroalkenes, (iii) the azide-alkyne cycloaddition (“click” reaction), which affords 1,4-disubstituted 1,2,3-triazoles and requires the generation of Cu^{I} species in the reaction medium. These studies involved several fine-tuning and diagnostic experiments and established that the use of bbom with Cu^{II} sources that contain traditionally non-coordinating anions generates 1D CPs isoskeletal to **175** in high yields, using an easy two-step method and room temperature conditions.

These compounds retain their stability in solution and exhibit octahedral Cu^{II} centres that contain a symmetrical $\{N_4\}$ square plane with the nitrogen atoms belonging to ligand molecules. This coordination arrangement is crucial during catalytic experiments, as it accounts for adequate electron delocalization to further promote the reduction of Cu^{II} to Cu^{I}. The use of benzotriazole as the template *N*-donor molecule for these ligands was also found to be important: analogous ligands based on benzimidazole or imidazole provided similar 1D polymeric frameworks, however these compounds showed inferior catalytic activity due to second coordination sphere effect. Similarly, constructed ligands bomm and bodm (based on MebtaH and Me_2btaH respectively) were proven unsuitable for the generation of stable CPs and the respective compounds also showed little or no catalytic performance. As a result of the above, compound $[Cu(bbom)_2(CF_3SO_3)_2]$ (**178**, Figure 30) emerged as the optimal homogeneous catalytic precursor in all aforementioned reactions, avoiding any issues that would inhibit its performance. In more detail, good to excellent yields (57 – 100%) for a range of propargylamines were obtained when the reaction was carried out in 2-propanol, heated at 90°C and with 2 mol% of the catalyst (Scheme 10, reaction B) [153]. The use of **178** also provided efficient access to a series of tri-, tetra- and pentasubstituted pyrroles as seen in Scheme 10, reaction C, under mild catalytic conditions (stirring for 1 to 18 hours in refluxing MeOH) with low catalyst loading of 0.3 to 1 mol%. This method afforded very good to excellent (67 – 91%) conversions for a large scope (39 examples) of substrates[154]. Furthermore, the azide-alkyne cycloaddition reaction was activated by **178** through a protocol which employs either organic halides or phenylboronic acid as starting materials, along with sodium azide to generate the organic azides *in situ* and avoid the isolation of potentially unstable intermediates (Scheme 10, reaction D). Up to 99% yields of the resulting triazoles were afforded when the reaction mixture was stirred in EtOH for 24 hrs, under reflux and 5 mol% of catalyst; importantly, the presence of a reducing agent was not required under these conditions[155]. It is also worth noting that **178** exhibited superior catalytic activity and efficiency compared to Cu^{II} salts in all of the above reactions.

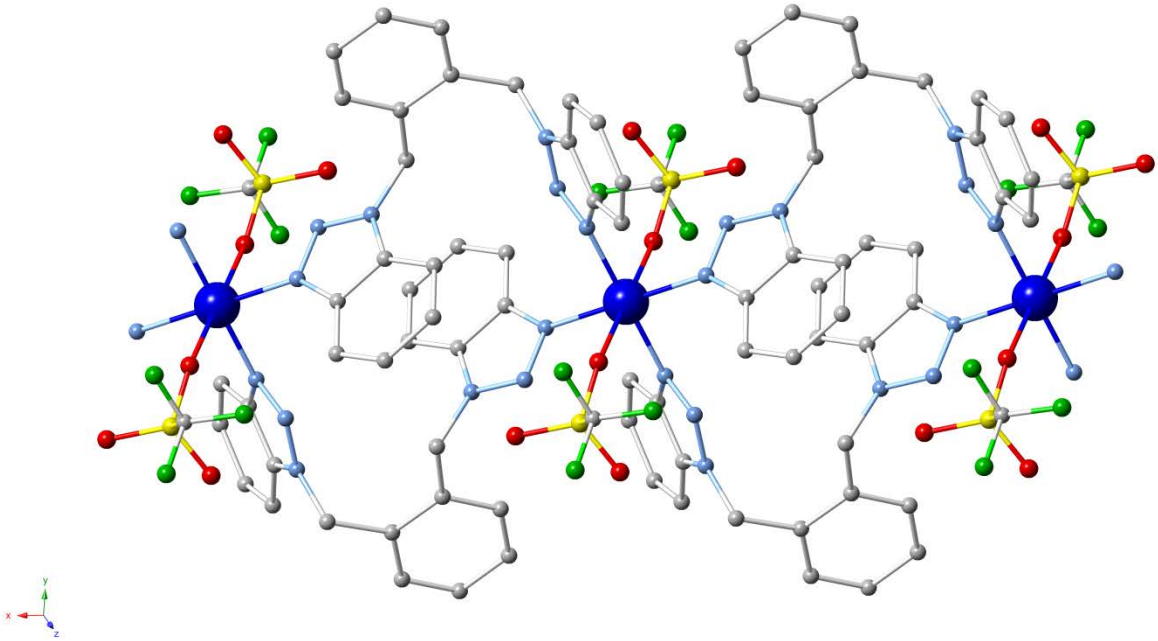

Figure 30. Part of the one-dimensional framework of **178** along the *a* axis. Hydrogen atoms are omitted for clarity. Colour code Cu (blue), C (grey), N (light blue), O (red), S (yellow), F (light green).

Having created a library of CPs with catalytic activity using these benzotriazole-based linkers, the next step in our research efforts was to combine this ligand system with the rich chemistry, unique coordination capabilities and superior alkynophilicity of Ag^{I} ions. These attempts are documented in a recent study which reports the synthesis of multiple new compounds using ligands bbpm, bbmm and bbom[156]. The complexes exhibit a large structural diversity of 0D dimers and 1D / 2D CPs with interesting topological features and architectures. Additionally, the 1D CP $[Ag(bbmm)(BF_4)(Et_2O)]$ (**179**) acts as an efficient homogeneous catalyst in A^3 coupling and alkyne hydration reactions, to produce the respective propargylamines and ketones in generally excellent yields (up to 99 and 93% in each case). The performance of **179** is attributed to its structural nature and coordination characteristics, and is comparable or superior to the ones of other reported Ag^{I}-based catalysts. As seen in Scheme 10, reactions B and E, both proposed protocols involve easy synthetic conditions without the use of inert atmosphere or environmentally harsh solvents.

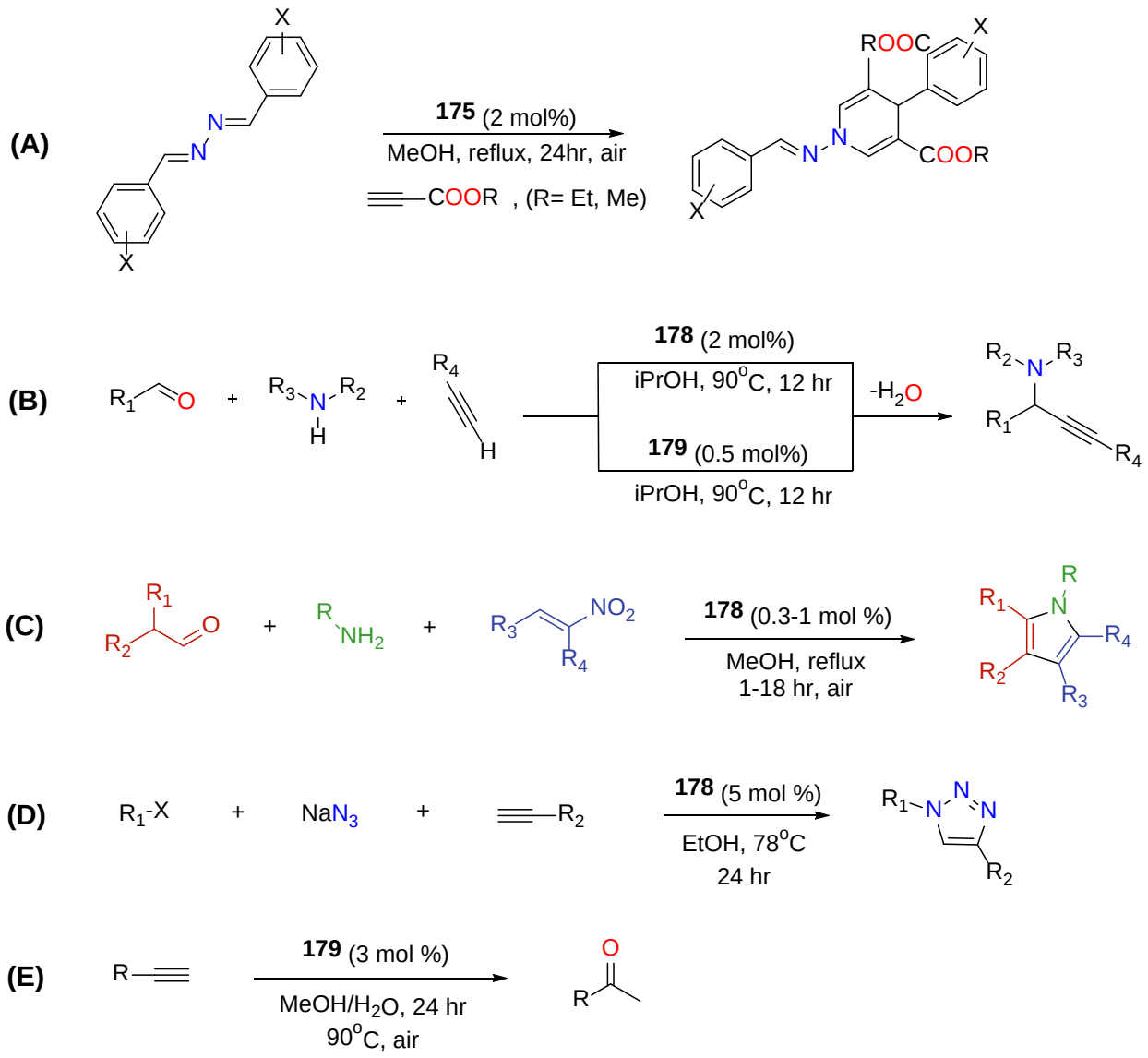

Scheme 10. Overview of our work on the use of benzotriazole-based 1D CPs as catalysts in organic transformations. Reactions: (**A**) formation of substituted 1,4-dihydropyridines from aldrazines and alkyl propiolates, (**B**) MCR synthesis of propargylamines from aldehydes, amines and alkynes, (**C**) MCR reaction of aldehydes, amines, and β-nitroalkenes to produce polysubstituted pyrroles, (**D**) MCR synthesis of 1,4-disubstituted 1,2,3-triazoles from organic halides or phenylboronic acid, (**E**) hydration of alkynes to ketones.

4.2.2. N2-substituted Benzotriazoles

In recent years there have been several studies that explore the coordination chemistry of ligands based on commercially available 2H-benzotriazol-2-yl phenolate (BTP) derivatives towards the

design of catalytic systems for ring-opening polymerization (ROP) reactions (Schemes 11 and 12). More specifically, it has been shown[157–159] that the ROP of cyclic esters, which affords biodegradable polyesters, is best promoted by well-defined metal complexes with a limited number of active sites, preventing any side reactions. BTP-type ligands are therefore ideal for these purposes, offering *N*,*O*-bidentate chelation which ensures the formation of stabilized and discreet 0D complexes. For example, Li and co-workers designed[160] the monomeric magnesium-based 0D compound [(^{TMCl}BTP)$_2$Mg(THF)$_2$] (**180**, ^{TMCl}BTPH = 2-tert-butyl-6-(5-chloro-2Hbenzotriazol-2-yl)-4-methylphenol, Figure 31) which was found to be an efficient catalyst in the ROP of L-lactide, generating polymers with conversions up to 97% when the reaction occurred in toluene at 80°C, in the presence of 9-anthracenemethanol (9-AnOH) and under 0.01 M of the catalyst. As shown by the same group, similar monomeric complexes based on lanthanide metals may also be derived through the use of other BTP analogues. Isostructural compounds [Dy(^{C1NN}BiBTP)(NO$_3$)(MeOH)$_2$] and [Y(^{C1NN}BiBTP)(NO$_3$)(MeOH)$_2$] (**181** and **182**, where ^{C1NN}BiBTPH$_2$ = 6,6'-(((2-(dimethylamino)ethyl)azanediyl)bis(methylene))bis(2-(2H-benzotriazol-2-yl)-4-methylphenol)) were synthesized and successfully tested for the ROP of L-lactide in analogous conditions as above, with **182** exhibiting the better overall catalytic performance (up to 98% conversions, no 9-AnOH required)[161].

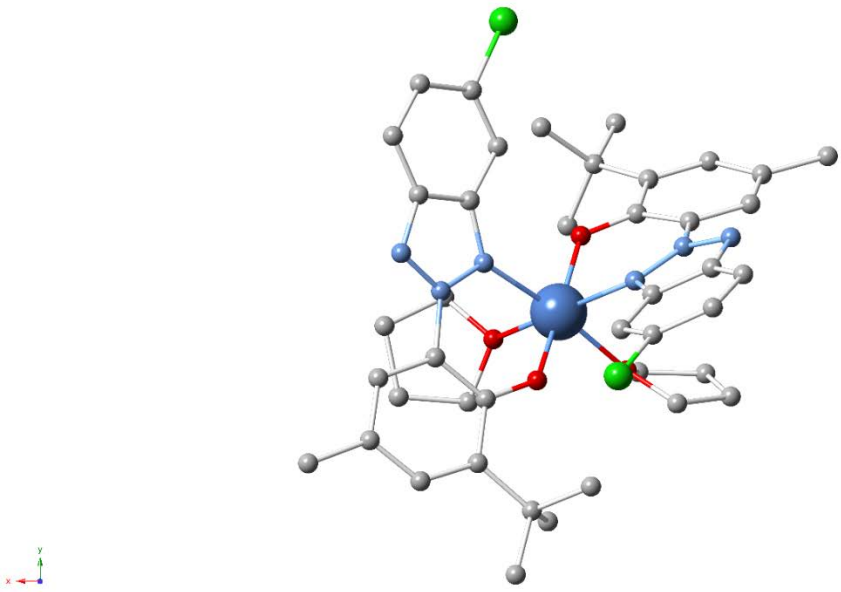

Figure 31. The structure of the monomeric compound **180**. Hydrogen atoms are omitted for clarity. Colour code Mg (blue), C (grey), N (light blue), O (red), Cl (green).

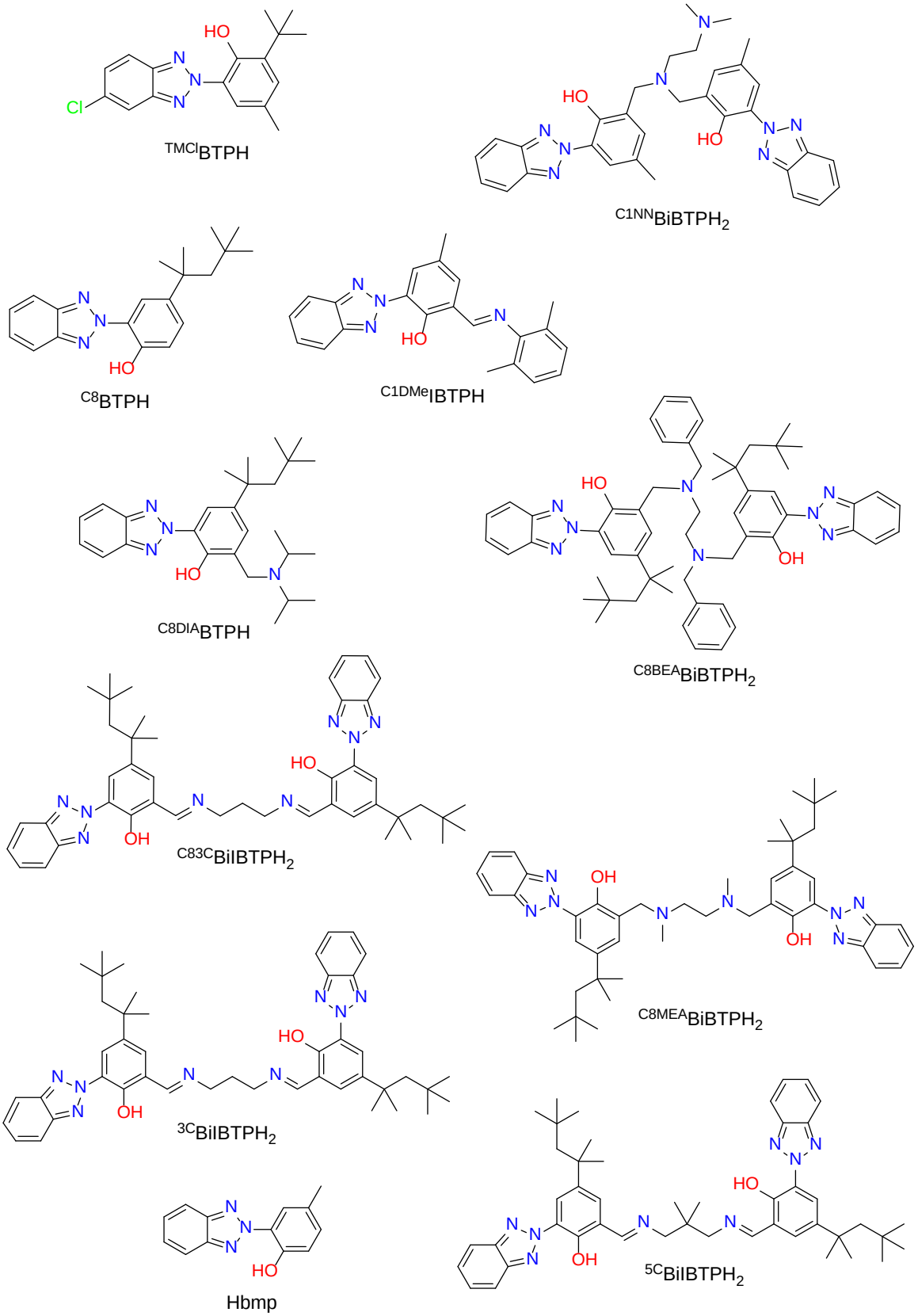

Scheme 11. The *N2*-substituted benzotriazole-based ligands mentioned in Section 4.2.2.

Expanding on these concepts, the development of well-defined catalysts with higher nuclearity can also be made possible through the introduction of strategically designed BTP-type ligands. Also reported[162] by Ko's group, the titanium-based dimeric compound [(μ-^{C8}BTP)Ti(O^{i}Pr)$_3$]$_2$ (**183**, ^{C8}BTPH = 2-(2H-benzotriazol-2-yl)-4-(2,4,4-trimethylpentan-2-yl)phenol, Figure 32), in which the Ti^{II} centres are bridged by phenol groups from ligand molecules, was found to catalyse the ROP of *ε*-caprolactone and L-lactide with excellent performance. Using under 0.01 M of the catalyst, the resulting polymers were afforded with conversions up to 99% when the reaction took place in toluene at 30°C. In similar fashion, Chang *et al*. constructed[163] a dinuclear zinc compound using the imino-based BTP ligand 2-(2H-benzotriazol-2-yl)-6-(((2,6-dimethylphenyl)imino)methyl)-4-methylphenol (^{C1DMe}IBTPH). [(μ-^{C1DMe}IBTP)ZnEt]$_2$ (**184**) catalyses the ROP of *ε*-caprolactone and *β*-butyrolactone in toluene at 55°C, as well as the ROP of L-lactide in CH_2Cl_2 at 30°C. In all cases the afforded conversions are excellent (up to 99%), while only 0.01 M of **184** is required.

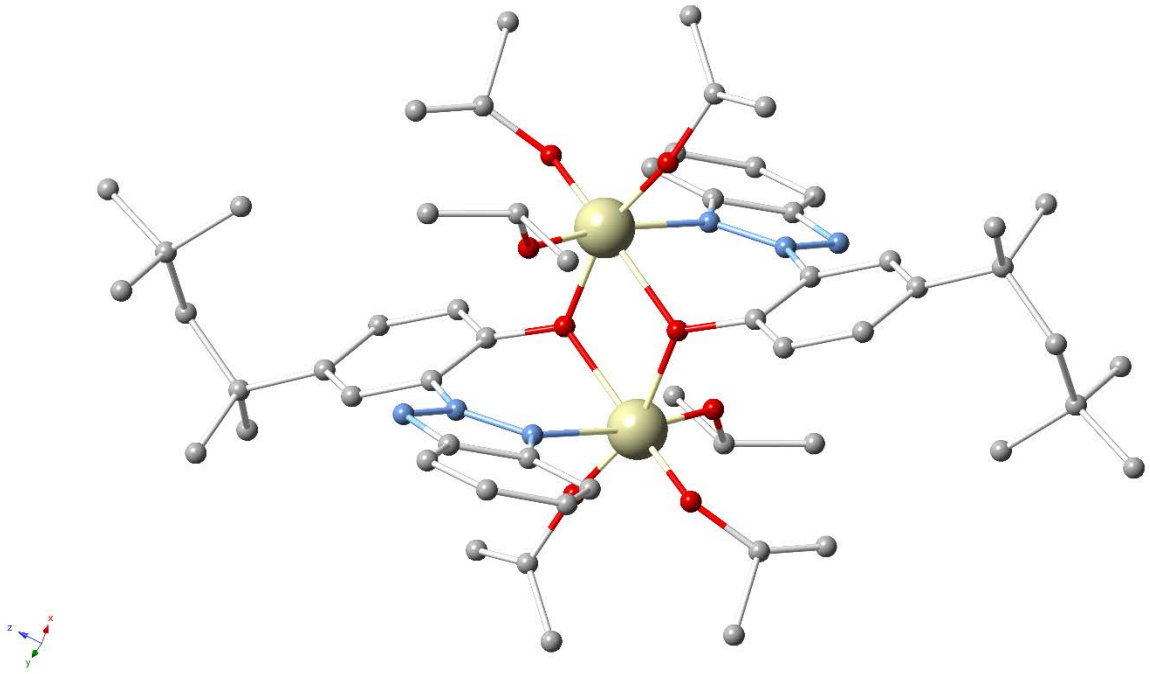

Figure 32. The structure of the dimeric compound **183**. Hydrogen atoms are omitted for clarity. Colour code Ti (white), C (grey), N (light blue), O (red).

A recent study[164] by the same group involved the use of 2-(2Hbenzotriazol-2-yl)-6-((diisopropylamino)methyl)-4-(2,4,4-trimethylpentan-2-yl)phenol (^{C8DIA}BTPH), another amino-modified BTP ligand, to generate 0D zinc compounds: The reaction of this ligand with $ZnEt_2$ led to the formation of the dimeric [(μ-^{C8DIA}BTP)ZnEt]$_2$ complex (**185**), in which the zinc centres are doubly bridged by two phenolate groups of the linker. Interestingly, further reaction of **185** with benzyl alcohol resulted in a tetranuclear zinc benzylalkoxide complex [(μ-^{C8DIA}BTP)Zn(OBn)]$_4$ (**186**) that exhibits a saddle-shaped Zn_4O_4 core as the zinc centres are linked by μ_2-bridging alkoxy groups (Figure 33). Under similar conditions as described in the case of **184**, both compounds were found to be efficient catalysts in the ROP reactions of *ε*-caprolactone and *β*-butyrolactone.

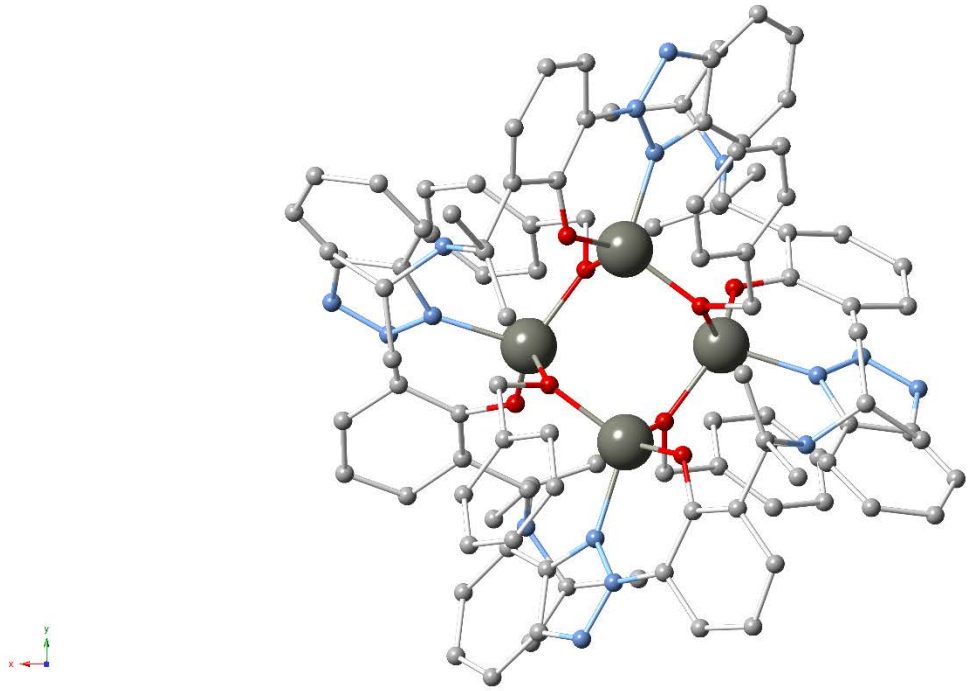

Figure 33. The structure of **186**. Hydrogen atoms and the ligand's *t*-Bu groups are omitted for clarity. Colour code Zn (dark grey), C (grey), N (light blue), O (red).

Incorporation of additional donor atoms in the ligands has been another design method towards similar high nuclearity compounds, with bis-BTP molecules being very useful in that department. This strategy recently yielded the dinuclear zinc complex [(^{C8BEA}BiBTP)Zn_2Et_2] (**187**, where ^{C8BEA}BiBTP = 6,6'-((ethane-1,2-diylbis(benzylazanediyl))bis(methylene))bis(2-(2H-benzo[d][1,2,3]triazol-2-yl)-4-(2,4,4-trimethylpentan-2-yl)phenol)) with considerable catalytic performance in the ROP of *ε*-caprolactone under favourable (0.005 M of **187**, 30^{o}C, 2 hrs stirring

in toluene, 9-AnOH as co-catalyst) reaction conditions, as reported[165] by Liu *et al.*. However, these ligands can also provide a possible waypoint towards the activation of other reactions: in addition to providing multiple pockets for metal coordination, their chelation modes resemble those of salen ligands; since salen-type metal complexes have been found to be good catalysts in CO_2/epoxide copolymerization reactions, compounds afforded with bis-BTP analogues could also be suitable candidates for these purposes.

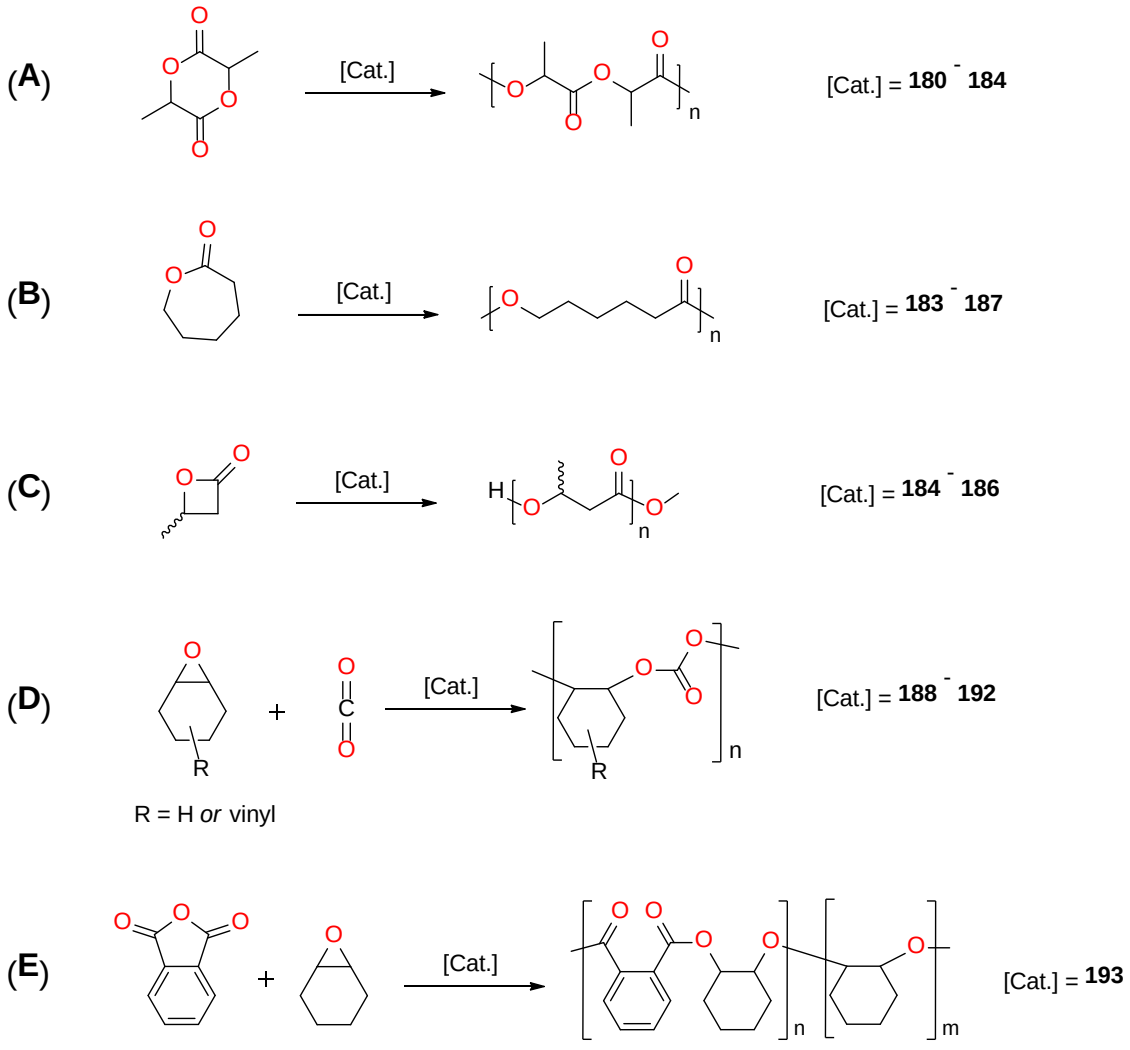

Scheme 12. The ring-opening (co)polymerization reactions of (**A**) lactide, (**B**) ε-caprolactone, (**C**) β-butyrolactone, (**D**) epoxide and CO_2, (**E**) phthalic anhydride and cyclohexene oxide, as mentioned in Section 4.2.2. Reported catalysts based on BTP ligand derivatives are also presented for each reaction.

Indeed, Li and co-authors reported the synthesis of isostructural dinuclear complexes [(^{C83C}BiIBTP)$Ni_2(OAc)_2$] and [(^{C83C}BiIBTP)$Co_2(OAc)_2$] (**188** and **189**, where ^{C83C}BiIBTPH_2 = 6,6'-((1E,1'E)-(propane-1,3-diylbis(azanylylidene))bis(methanylylidene))bis(2-(2H-benzotriazol-2-yl)-4-(2,4,4-trimethylpentan-2-yl)phenol)). These were found to be active catalysts for the copolymerization of cyclohexene oxide (CHO) and CO_2 without the use of other co-catalysts; **188** showed the better performance, affording poly(cyclohexene carbonate) of high molecular weight under the appropriate (120ºC, pCO_2^0 = 300 psi) conditions[166]. Similarly, compound [(^{C8MEA}BiBTP)$Ni_2(OAc)_2(H_2O)$] (**190**, where ^{C8MEA}BiBTPH_2 = 6,6'-((ethane-1,2-diylbis(methylazanediyl))bis(methylene))bis(2-(2H-benzotriazol-2-yl)-4-(2,4,4-trimethylpentan-2-yl)phenol) was also reported[167] by Lin *et al.* as an efficient catalyst in the above reaction, as well as the copolymerization of 4-vinyl-1,2-cyclohexene oxide (VCHO) and CO_2 when analogous conditions (140ºC, pCO_2^0 = 300 psi, 0.0625 mol% of **190**) were applied.

Another ligand system designed by the same group involved the bis(benzotriazole) iminophenolate derivatives ^{R}BiIBTP (where R = 3C for the propyl-bridged backbone, or 5C for the 2,2-dimethyl-1,3-propyl-bridged backbone). This led to the synthesis of dinuclear compounds [(^{3C}BiIBTP)$Ni_2(CF_3COO)_2$] and [(^{5C}BiIBTP)$Ni_2(OAc)_2$] (**191** and **192** respectively) reported in consecutive studies[168,169]. Both complexes exhibited comparable catalytic capabilities in the copolymerization of CHO and CO_2 with excellent selectivity under similar reaction conditions as above. In addition, **192** was tested successfully in the copolymerization of VCHO and CO_2, providing excellent (>99%) yields when only 0.03125 mol% of the catalyst was employed. Interestingly, isostructural compound [(^{5C}BiIBTP)$Co_2(OAc)_2$] (**193**) was also found to catalyse the ring-opening copolymerization of phthalic anhydride with CHO to produce a high-molecular weight polyester[169].

In addition to these works, more recent studies have demonstrated that the field of reactions that BTP-based complexes can catalyse extends beyond ROP reactions and copolymerizations. A 2017 article by Li and co-authors reports[170] the use of ligand ^{C1NN}BiBTP with M^{II} acetate sources to generate the isostructural trimetallic compounds [(^{C1NN}BiBTP)$_2Co_3(OAc)_2$] and [(^{C1NN}BiBTP)$_2Zn_3(OAc)_2$] (**194**, **195**). Both compounds showed considerable activity in the cycloaddition of cyclohexene oxide with CO_2, affording the corresponding *cis*-cyclohexene

carbonate in very high conversion and selectivity (up to 99% in both accounts) when the reaction took place in the presence of a co-catalyst (ammonium salt), at 80 °C and 300 psi pCO_2^0. The Co^{II} analogue (Figure 34) was further used for a range of epoxide substrates under the same reaction conditions, successfully producing the corresponding cyclic organic carbonates (Scheme 13) with high *cis*-isomer selectivity and conversions up to 98%. Furthermore, a 2018 article by Stanje *et al.* details[171] the use of ligand 2-(2H-benzotriazol-2-yl)-4-methylphenol (Hbmp) to generate a 0D mononuclear Fe^{III} complex formulated as $[FeCl(bmp)_2]$ (**196**). Interestingly, this compound was found to be an efficient catalyst for the oxidation of benzylic alcohols towards benzoic acids in a one-pot homogeneous procedure as seen in Scheme 14. Using 4 mol% of the catalyst, yields up to 95% for the corresponding acid were afforded when the reaction was performed in the presence of 30% aq. H_2O_2, at 70°C and for a period of 3 hours.

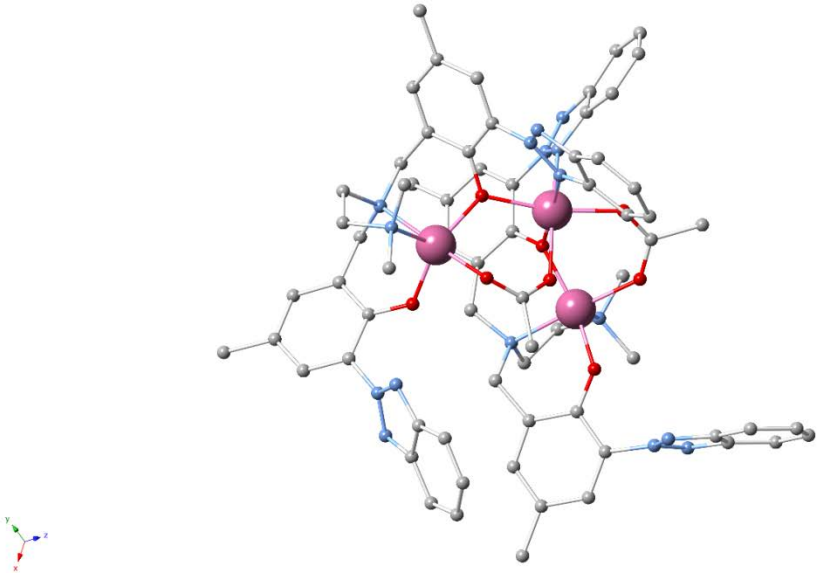

Figure 34. The structure of the trimetallic compound **194**. Hydrogen atoms are omitted for clarity. Colour code Co (pink), C (grey), N (light blue), O (red).

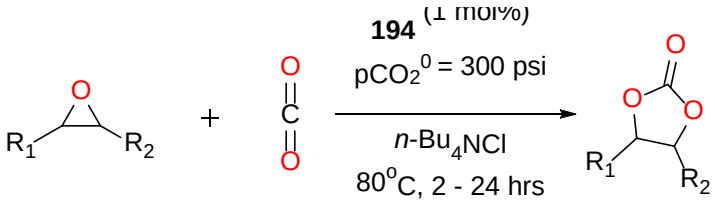

Scheme 13. Epoxide/CO_2 cycloaddition as catalysed by **194**.

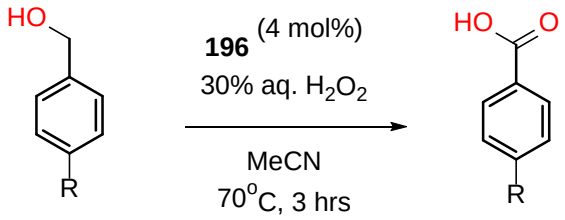

Scheme 14. Oxidation of benzylic alcohols as catalysed by **196**.

5. Benzotriazole Derivatives as co-Ligands

Having already mentioned the popularity and efficiency of the Hbta/carboxylates multi-ligand system, it is perhaps unsurprising that only a few examples of substituted benzotriazoles as co-linkers exist in the literature. Indeed, the addition of potential steric effects and increased unpredictability would be less wanted in a system which requires a second ligand that would simply need to act as a supporting pillar in the framework. An exception to this would be the H_2btca ligand, which can offer both the 1,2,3-triazole and the carboxylate group for coordination, allowing complete freedom when it comes to the choice of the second linker; for this reason, the majority of reported examples in this category contain this molecule. The first relevant study was presented by Lu and co-authors who reported[172] the structural details of [Zn(btca)(tatp)] (**197**), in which the *N*-donor bidentate molecule 1,4,8,9-tetraazatriphenylene (tatp) was employed as the second ligand. In this case, the main framework consists of a 2D [Zn(btca)] layer, as the btca ligand coordinates to three different zinc centres through $\mu_{1,3}$-triazole and *O*,*O*'-bidentate chelation. The tatp terminal ligand molecules participate in various weak interactions that influence the resulting supramolecular architecture.

Similar concepts were followed by Liu and co-workers, who examined the chemistry of Zn/btca using the *N*-donors imidazole (im) and 1,3-di(4-pyridyl)propane (tmdpy) as secondary linkers[173]. The resulting compounds [Zn_2(btca)$_2$(im)$_2$] and [Zn_2(btca)$_2$(tmdpy)] (**198**, **199**) possess a main 2D layer structure constructed by the same [Zn_2(btca)$_2$] building block, with similar coordination modes found in the btca linker. However, the resulting frameworks in **198** and **199** are 2D and 3D respectively, with im acting as a terminal ligand while tmdpy acts as a bridging ligand that connects the adjacent layers. The compounds also display solid-state luminescent emission assigned to ligand-ligand charge transfer. Isoquinoline (iqo), another *N*-donor molecule,

was recently tested[174] as the co-linker in the same system by Ning *et al*. The resulting polymeric compound [Zn(btca)(iqo)$_2$] (**200**) also extends to two dimensions with each btca molecule acting as tridentate ligand that coordinates through $\mu_{1,3}$-bridging N atoms and one carboxylic O atom. Interestingly, this water-stable compound exhibits strong fluorescence in aqueous solution and can be used for probing $Cr_2O_7^{2-}$/CrO_4^{2-} ions as well as detecting nitroaromatics based on fluorescence quenching effects.

In another report, Xin and co-authors demonstrate[175] a procedure towards 3d-4f heterometallic coordination polymers through the use of a copper-based macrocyclic oxamide metalloligand as the secondary node. The addition of lanthanide sources and H$_2$btca resulted in the isostructural complexes [GdCu$_2$(ddtpd)$_2$(Hbtca)(btca)(H$_2$O)] and [ErCu$_2$(ddtpd)$_2$(Hbtca)(btca)(H$_2$O)] (**201** and **202**, where H$_2$ddtpd = 2,3-dioxo-5,6,14,15-dibenzo-1,4,8,12-tetraazacyclo-pentadeca-7,13-dien). The compounds exhibit a double-strand meso-helical 1D chain structure that is built from trinuclear [LnCu$_2$(ddtpd)$_2$] units and extends through btca or Hbtca benzotriazolate ligands as seen in Figure 35. These act as bidentate connectors, bridging one Cu^{II} and one Ln^{III} ion; in addition, the uncoordinated NH group from Hbtca also participates in framework-stabilizing hydrogen bonding interactions. Magnetic experiments for **201** and **202** reveal the presence of ferromagnetic interactions in both compounds; it is also shown that the anisotropy of Er^{III} ions plays an important role in the magnetic behaviour of **202**. The same group also explored the capabilities of this ligand system using Ni^{II} sources to generate the isostructural tetranuclear 0D complexes [LnNi$_3$(ddtpd)$_3$(btca)(NO$_3$)], where Ln = Sm^{III} (**203**), Pr^{III} (**204**) or Eu^{III} (**205**); in this case the presence of an additional metalloligand in the building unit prevents the framework from extending to more dimensions (Figure 36) [176].

A different synthetic strategy in ligand incorporation was presented[177] by Werner *et al.*, who employed the pentanuclear compound [Co$_5$Cl$_4$(Me$_2$bta)$_6$] (**206**) as a precursor to generate [Co$_5$Tp*$_4$(Me$_2$bta)$_6$] (**207**) through a simple ligand exchange that replaced the Cl^- ions with the anionic *N*-donor tris(3,5-dimethyl-1-pyrazolyl)borate (Tp*) ligand, a molecule that has been used extensively in the design of scorpionate complexes. Interestingly, while **206** exhibits the pentanuclear motif seen in **90**, the introduction of capping ligands Tp* in **207** is accompanied with a change in coordination of the peripheral Co^{II} ions from tetrahedral to octahedral geometry. Magnetic susceptibility measurements in both compounds indicated the presence of weak anti-ferromagnetic exchange interactions between high-spin Co^{II} centres.

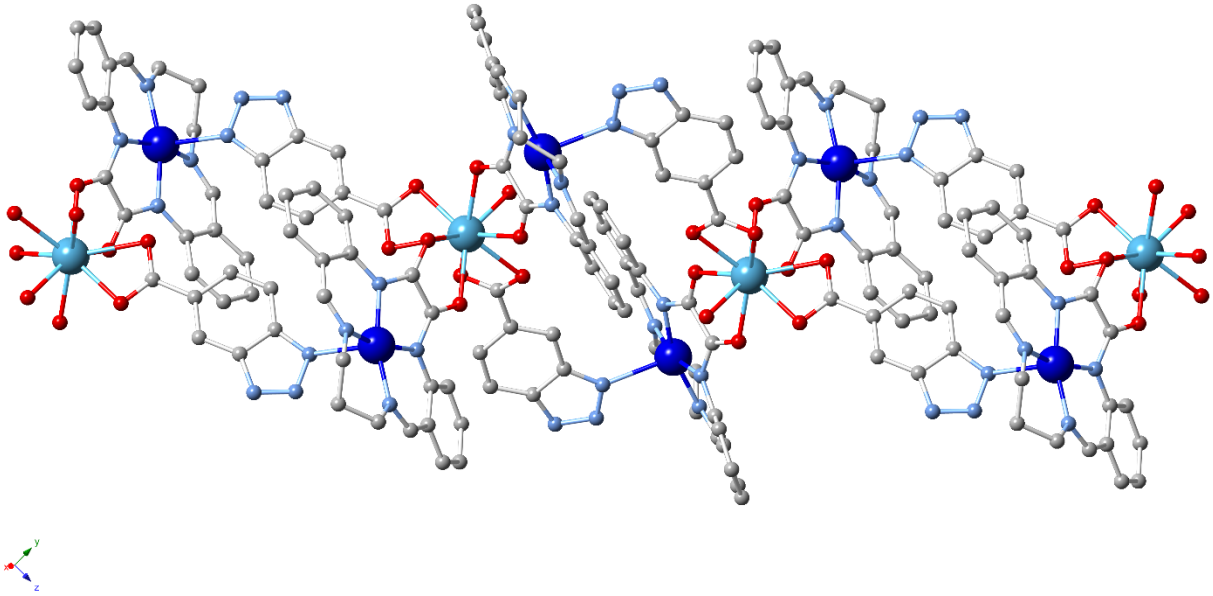

Figure 35. Part of the 1D framework in **201**. Hydrogen atoms have been omitted for clarity. Colour code Gd (cyan), Cu (dark blue), C (grey), N (light blue), O (red).

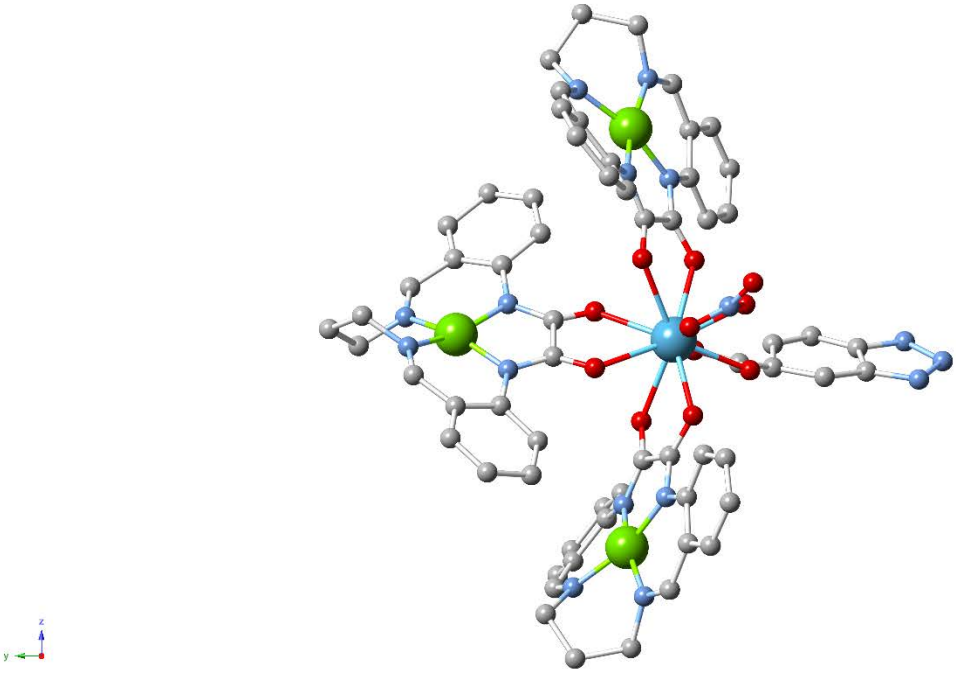

Figure 36. The tetranuclear complex **203**. Hydrogen atoms have been omitted for clarity. Colour code Sm (cyan), Ni (dark green), C (grey), N (light blue), O (red).

6. Conclusions and Future Directions

In the present review we have attempted to report recent advances in the use of benzotriazole and its derivatives as ligands in coordination chemistry through a series of highlighted examples. During the presentation of compounds in the above sections, large emphasis was paid towards displaying the role of benzotriazolates in the design and assembly of the structures, as well as the application potential of the resulting complexes. We feel that the reported examples clearly demonstrated these points.

From the studies mentioned in this review it is evident that such ligands are suitable for many research purposes that concern coordination chemists: Synthetic-wise, benzotriazolate linkers can provide (i) multiple *N*- (and in some cases, even *O*-) donor atoms, (ii) a variety of bridging and/or chelating coordination modes, (iii) the possibility to form weak interactions, (iv) a general ease of chemistry (e.g., solubility in common organic solvents, air and thermal stability) and (v) excellent efficiency either as main or as secondary ligands. This flexibility, along with their ease of preparation and low cost of starting material, has made these molecules very attractive for the construction of multiple networks and architectures that feature a range of metals (including main-group elements, transition metals and lanthanides) and, more importantly, the desired stability, dimensionality and applications. Indeed, the synthesis of stable polynuclear coordination clusters with noteworthy magnetic properties is easily achieved using Hbta or similar *C*-substituted derivatives. On the other hand, researchers interested in porous CPs and their sorption properties will be more intrigued by the potential of linkers such as H_2btca or the various Hbta/co-ligand systems and benzo(bis)triazole analogues. Lower-dimensionality, less-rigid frameworks that provide increased flexibility and easier manipulation are also possible through the use of *N*-substituted bis(benzotriazole) ligands, while BTP derivatives are instead ideal for the synthesis of well-defined 0D complexes; a series of remarkable catalytic systems has been developed using several compounds of both of these categories.

It is felt that great advances have been made in the design and understanding of such coordination compounds, as shown by the plethora of relevant studies. However, we believe that the field still has plenty of room for improvement in regards to developing and maximizing their application properties. The majority of the more recent studies described in this review include attempts to

exploit this potential and generate functional materials, rather than presenting simple structural reports; it is therefore expected that future research will continue that trend. Some of the possible directions could involve (i) efforts to expand the M^{II} and M^{III}/Hbta synthetic systems towards additional polynuclear coordination clusters; having the existing literature in mind, it can be hypothesized that the resulting motifs, nuclearities and magnetic properties might be influenced by the use of various metal sources, mixed metal systems or different synthetic conditions, (ii) the emergence of new, targeted benzo(bis)triazolate ligands in order to generate CPs with larger pores and explore their properties, (iii) deeper investigations into the catalytic potential of compounds containing relevant ligands, and further optimization of the performance of existing catalysts; this can be done refining parameters such as coordination environment, metal species and geometry. More organic reactions could also be explored, including the fields of asymmetric catalysis and photocatalysis, (iv) an increased focus on the biological applications of suitable complexes: targeted compounds may be tested for their antimicrobial activity or drug delivery capabilities. Finally, the design of coordination environments that mimic the behaviour of other known enzymes is certainly another intriguing approach with excellent potential. Having been used as a powerful synthetic auxiliary by organic chemists for several decades, benzotriazole is also proving to be an excellent tool for coordination chemists, offering exciting possibilities for the future. It is hoped that this review will provide inspiration to researchers during their efforts in the constant search and development of novel functional materials.

References

[1] D.S. Wofford, D.M. Forkey, J.G. Russell, ^{15}N NMR Spectroscopy: Prototropic Tautomerism of Azoles, J. Org. Chem. 47 (1982) 5132–5137. doi:10.1021/jo00147a018.

[2] F. Tomás, J.L.M. Abboud, J. Laynez, R. Notario, L. Santos, S.O. Nilsson, J. Catalán, R.M. Claramunt, J. Elguero, Tautomerism and Aromaticity in 1,2,3-Triazoles: The Case of Benzotriazole, J. Am. Chem. Soc. 111 (1989) 7348–7353. doi:10.1021/ja00201a011.

[3] J. Catalan, P. Perez, J. Elguero, Structure of benzotriazole in the gas phase: a UV experimental study, J. Org. Chem. 58 (1993) 5276–5277. doi:10.1021/jo00071a046.

[4] W. Roth, M. Schmitt, D. Spangenberg, C. Janzen, A. Westphal, The relative stabilities of benzotriazole tautomers determined by a rotational band contour analysis of the N–H stretching vibration, Chem. Phys. 248 (1999) 17–25. doi:10.1016/s0301-0104(99)00262-1.

[5] N. Jagerovic, M. Luisa Jimeno, I. Alkorta, J. Elguero, R. María Claramunt, An experimental (NMR) and theoretical (GIAO) study of the tautomerism of benzotriazole in solution, Tetrahedron. 58 (2002) 9089–9094. doi:10.1016/S0040-4020(02)01157-2.

[6] L.I. Larina, V. Milata, ^{1}H, ^{13C} and ^{15}N NMR spectroscopy and tautomerism of nitrobenzotriazoles, Magn. Reson. Chem. 47 (2009) 142–148. doi:10.1002/mrc.2366.

[7] F. Tomas, J. Catalan, P. Perez, J. Elguero, Influence of Lone Pair Repulsion vs Resonance Energy on the Relative Stabilities of Molecular Structures: A Theoretical Approach to the Equilibrium between 1H- and 2H-Benzotriazole Tautomers, J. Org. Chem. 59 (1994) 2799–2802. doi:10.1021/jo00089a026.

[8] A. Escande, J.L. Galigné, J. Lapasset, Structure cristalline et moléculaire du benzotriazole, Acta Crystallogr. Sect. B Struct. Crystallogr. Cryst. Chem. 30 (1974) 1490–1495. doi:10.1107/S0567740874005139.

[9] N. Zinin, Ueber einige Derivate des Azoxybenzids, Justus Liebigs Ann. Chem. 114 (1860) 217–227. doi:10.1002/jlac.18601140212.

[10] A. Werner, E. Stiasny, Ueber Nitroderivate des Azo-, Azoxy- und Hydrazo-Benzols, Berichte Der Dtsch. Chem. Gesellschaft. 32 (1899) 3256–3282. doi:10.1002/cber.18990320393.

[11] A. Wilh. Hofmann, Einwirkung der Salpetrigen Säure auf das Nitro-phenylendiamin, Ann. Der Chemie Und Pharm. 115 (1860) 249–260. doi:10.1002/jlac.18601150302.

[12] A. Ladenburg, Derivate von Diaminen, Berichte Der Dtsch. Chem. Gesellschaft. 9 (1876)

219–223. doi:10.1002/cber.18760090166.

[13] C.M.P. Pereira, H.A. Stefani, K.P. Guzen, A.T.G. Orfao, Improved Synthesis of Benzotriazoles and 1-Acylbenzotriazoles by Ultrasound Irradiation., ChemInform. 38 (2007) 43–46. doi:10.1002/chin.200731104.

[14] A.R. Katritzky, J.-C.M. Monbaliu, The chemistry of benzotriazole derivatives : a tribute to Alan Roy Katritzky, 1st ed., Springer International Publishing, 2016.

[15] E.F. V. Scriven, C.A. Ramsden, Heterocyclic chemistry in the 21st Century : a tribute to Alan Katritzky, 1st ed., Elsevier, 2017.

[16] L. Procter and Gamble, British Patent 652339, 652339, 1947.

[17] J.B. Cotton, I.R. Scholes, Benzotriazole and Related Compounds as Corrosion Inhibitors For Copper, Br. Corros. J. 2 (1967) 1–5. doi:10.1179/000705967798327235.

[18] J. Meunier-Piret, P. Piret, J.-P. Putzeys, M. Van Meerssche, Structure cristalline du complexe de l'hexakis-(benzotriazolyl)-hexakis(allylamine)-trisnickel(II) avec la triphénylphosphine oxyde, Acta Crystallogr. Sect. B Struct. Crystallogr. Cryst. Chem. 32 (1976) 714–717. doi:10.1107/S0567740876003853.

[19] J. Reedijk, G. Roelofsen, A.R. Siedle, A.L. Spek, Crystal structure of (benzotriazolato)thallium(I) and its relation with the mechanism of corrosion inhibition by benzotriazole, Inorg. Chem. 18 (1979) 1947–1951. doi:10.1021/ic50197a045.

[20] J. Reedijk, A.R. Siedle, R.A. Velapoldi, J.A.M. Van Hest, Coordination compounds of benzotriazole and related ligands, Inorg. Chim. Acta. 74 (1983) 109–118. doi:10.1016/S0020-1693(00)81414-0.

[21] B. Manna, A. V. Desai, S.K. Ghosh, Neutral N-donor ligand based flexible metal-organic frameworks, Dalton Trans. 45 (2016) 4060–4072. doi:10.1039/c5dt03443d.

[22] F.H. Allen, The Cambridge Structural Database: a quarter of a million crystal structures and rising, Acta Crystallogr. Sect. B-Structural Sci. 58 (2002) 380–388. doi:10.1107/s0108768102003890.

[23] A.A. Mohamed, Advances in the coordination chemistry of nitrogen ligand complexes of coinage metals, Coord. Chem. Rev. 254 (2010) 1918–1947. doi:10.1016/j.ccr.2010.02.003.

[24] G. Aromí, L.A. Barrios, O. Roubeau, P. Gamez, Triazoles and tetrazoles: Prime ligands to generate remarkable coordination materials, Coord. Chem. Rev. 255 (2011) 485–546. doi:10.1016/j.ccr.2010.10.038.

[25] J.-P. Zhang, Y.-B. Zhang, J.-B. Lin, X.-M. Chen, Metal Azolate Frameworks: From Crystal Engineering to Functional Materials, Chem. Rev. 112 (2012) 1001–1033. doi:10.1021/cr200139g.

[26] S. Zhang, W. Shi, P. Cheng, The coordination chemistry of N-heterocyclic carboxylic acid: A comparison of the coordination polymers constructed by 4,5-imidazoledicarboxylic acid and 1H-1,2,3-triazole-4,5-dicarboxylic acid, Coord. Chem. Rev. 352 (2017) 108–150. doi:10.1016/j.ccr.2017.08.022.

[27] J.H. Marshall, Preparation and characterization of tetrakis(2,4-pentanedionato)hexakis(benzotriazolato)pentacopper(II), Inorg. Chem. 17 (1978) 3711–3713. doi:10.1021/ic50190a081.

[28] J. Handley, D. Collison, C.D. Garner, M. Helliwell, R. Docherty, J.R. Lawson, P.A. Tasker, Hexakis(benzotriazolato)tetrakis(2,4-pentanedionato)pentacopper(II): A Model for Corrosion Inhibition, Angew. Chemie Int. Ed. English. 32 (1993) 1036–1038. doi:10.1002/anie.199310361.

[29] V. Tangoulis, C.P. Raptopoulou, A. Terzis, E.G. Bakalbassis, E. Diamantopoulou, S.P. Perlepes, Polynuclear Nickel(II) Complexes: Preparation, Characterization, Magnetic Properties, and Quantum-Chemical Study of $[Ni_5(OH)(Rbta)_5(Acac)4(H_2O)_4]$ (Rbtah = Benzotriazole and 5,6-Dimethylbenzotriazole), Inorg. Chem. 37 (1998) 3142–3153. doi:10.1021/ic9714091.

[30] S. Biswas, M. Tonigold, D. Volkmer, Homo- and heteropentanuclear coordination compounds with Td symmetry - The solid state structures of $[MZn_4(L)_4(L')_6]$ (M = CoII or Zn; L = chloride or acac; L′ = 1,2,3-benzotriazolate), Zeitschrift Fur Anorg. Und Allg. Chemie. 634 (2008) 2532–2538. doi:10.1002/zaac.200800296.

[31] C. Gkioni, V. Psycharis, C.P. Raptopoulou, Investigation of the zinc(II) acetylacetonate/benzotriazole reaction system in the presence of bridging N,N′-ligands: Pentanuclear, enneanuclear and polymeric complexes, Polyhedron. 28 (2009) 3425–3430. doi:10.1016/j.poly.2009.07.020.

[32] S. Biswas, M. Tonigold, M. Speldrich, P. Kögerler, D. Volkmer, Nonanuclear coordination compounds featuring $\{M_9L_{12}\}^{6+}$ cores (M = NiII, CoII, or ZnII; L = 1,2,3-benzotriazolate), Eur. J. Inorg. Chem. (2009) 3094–3101. doi:10.1002/ejic.200900156.

[33] S. Zhang, H. Chen, H. Tian, X. Li, X. Yu, A 3D supramolecular network constructed from

{Ni_9} cluster and benzotriazole, Inorg. Chem. Commun. 86 (2017) 87–89. doi:10.1016/j.inoche.2017.09.029.

[34] Y.X. Yuan, P.J. Wei, W. Qin, Y. Zhang, J.L. Yao, R.A. Gu, Combined studies on the surface coordination chemistry of benzotriazole at the copper electrode by direct electrochemical synthesis and surface-enhanced raman spectroscopy, Eur. J. Inorg. Chem. 2007 (2007) 4980–4987. doi:10.1002/ejic.200700436.

[35] S.A. Sulway, R.A. Layfield, M. Bodensteiner, S. Scheuermayer, M. Scheer, M. Zabel, Benzotriazolate cage complexes of tin(ii) and lithium: Halide-influenced serendipitous assembly, Dalton Trans. 40 (2011) 7559–7563. doi:10.1039/c1dt10400d.

[36] S.A. Sulway, D. Collison, J.J.W. McDouall, F. Tuna, R.A. Layfield, Iron(II) cage complexes of N-heterocyclic amide and bis(trimethylsilyl) amide ligands: Synthesis, structure, and magnetic properties, Inorg. Chem. 50 (2011) 2521–2526. doi:10.1021/ic102341a.

[37] L.F. Jones, E.K. Brechin, D. Collison, A. Harrison, S.J. Teat, W. Wernsdorfer, New routes to high nuclearity cages: a fluoride-based hexaicosametallic manganese cage, Chem. Commun. (2002) 2974–2975. doi:10.1039/b209445b.

[38] L.F. Jones, G. Rajaraman, J. Brockman, M. Murugesu, E.C. Sanudo, J. Raftery, S.J. Teat, W. Wernsdorfer, G. Christou, E.K. Brechin, D. Collison, New routes to polymetallic clusters: fluoride-based tri-, deca-, and hexaicosametallic MnIII clusters and their magnetic properties., Chem. Eur. J. 10 (2004) 5180–5194. doi:10.1002/chem.200400301.

[39] L.F. Jones, J. Raftery, S.J. Teat, D. Collison, E.K. Brechin, Manganese (III) fluoride as a new synthon in Mn cluster chemistry, Polyhedron. 24 (2005) 2443–2449. doi:10.1016/j.poly.2005.03.045.

[40] J. Tabernor, L.F. Jones, S.L. Heath, C. Muryn, G. Aromí, J. Ribas, E.K. Brechin, D. Collison, A centred, elongated ‘ferric tetrahedron’ with an S = 15/2 spin ground state, Dalton Trans. 4 (2004) 975–976. doi:10.1039/b403041a.

[41] R. Shaw, R.H. Laye, L.F. Jones, D.M. Low, C. Talbot-Eeckelaers, Q. Wei, C.J. Milios, S. Teat, M. Helliwell, J. Raftery, M. Evangelisti, M. Affronte, D. Collison, E.K. Brechin, E.J.L. McInnes, 1,2,3-Triazolate-bridged tetradecametallic transition metal clusters M-$_{14}$(L)$_6$O$_6$(OMe)$_{18}$X$_6$ (M = Fe-III, Cr-III and V-III/IV) and related compounds: Ground-state spins ranging from S=0 to S=25 and spin-enhanced magnetocaloric effect, Inorg. Chem. 46

(2007) 4968–4978. doi:10.1021/ic070320k.

[42] T. Mallah, A. Bell, E.J.L. McInnes, E. Rivière, L.F. Jones, S.J. Teat, E.K. Brechin, D.M. Low, Solvothermal Synthesis of a Tetradecametallic FeIII Cluster, Angew. Chemie Int. Ed. 42 (2003) 3781–3784. doi:10.1002/anie.200351865.

[43] R. Shaw, F. Tuna, W. Wernsdorfer, A.L. Barra, D. Collison, E.J.L. McInnes, Large spin, magnetically anisotropic, octametallic vanadium(III) clusters with strong ferromagnetic coupling, Chem. Commun. 0 (2007) 5161–5163. doi:10.1039/b710732c.

[44] R.A. Layfield, J.J.W. McDouall, S.A. Sulway, F. Tuna, D. Collison, R.E.P. Winpenny, Influence of the N-Bridging Ligand on Magnetic Relaxation in an Organometallic Dysprosium Single-Molecule Magnet, Chem. Eur. J. 16 (2010) 4442–4446. doi:10.1002/chem.201000158.

[45] M.A. Shestopalov, K.E. Zubareva, O.P. Khripko, Y.I. Khripko, A.O. Solovieva, N. V. Kuratieva, Y. V. Mironov, N. Kitamura, V.E. Fedorov, K.A. Brylev, The first water-soluble hexarhenium cluster complexes with a heterocyclic ligand environment: Synthesis, luminescence, and biological properties, Inorg. Chem. 53 (2014) 9006–9013. doi:10.1021/ic500553v.

[46] K.-Z. Shao, Y.-H. Zhao, Y. Xing, Y.-Q. Lan, X.-L. Wang, Z.-M. Su, R.-S. Wang, Assembly of a chiral bikitaite zeolite metal-organic framework based on the asymmetrical tetrahedral building blocks, Cryst. Growth Des. 8 (2008) 2986–2989. doi:10.1021/cg800103b.

[47] S.-D. Han, J.-P. Zhao, Y.-Q. Chen, S.-J. Liu, X.-H. Miao, T.-L. Hu, X.-H. Bu, A spin-canted polynuclear manganese complex comprised of alternating linkage of cyclic tetra-and mononuclear fragments, Cryst. Growth Des. 14 (2014) 2–5. doi:10.1021/cg401335n.

[48] J.J. Liu, Z.Y. Li, X. Yuan, Y. Wang, C.C. Huang, A Copper(I) coordination polymer incorporation the corrosion inhibitor 1H-benzotriazole: Poly[μ3-benzotriazolato-κ3 N1:N2:N3-copper(I)], Acta Crystallogr. Sect. C Struct. Chem. 70 (2014) 599–602. doi:10.1107/S2053229614010390.

[49] J.C. Rybak, I. Schellenberg, R. Pöttgen, K. Müller-Buschbaum, MOFs by transformation of 1D-coordination polymers II: The homoleptic divalent rare earth 3D benzotriazolate [Eu(Btz)$_2$] initiating from [Eu(Btz)$_2$(BtzH)$_2$], Zeitschrift Fur Anorg. Und Allg. Chemie. 636 (2010) 1720–1725. doi:10.1002/zaac.201000077.

[50] K. Müller-Buschbaum, Y. Mokaddem, MOFs by transformation of 1D-coordination

polymers: From ∞1[Ln(Btz)3BtzH] to the homoleptic rare earth 3D-benzotriazolate frameworks∞3 [Ln(Btz)3], Ln = La, Ce, Zeitschrift Fur Anorg. Und Allg. Chemie. 634 (2008) 2360–2366. doi:10.1002/zaac.200800287.

[51] J.-C. Rybak, K. Müller-Buschbaum, The Benzotriazolate Coordination Polymer[Eu(Btz)2(BtzH)2], Containing Divalent Europium, Zeitschrift Für Anorg. Und Allg. Chemie. 636 (2010) 126–131. doi:10.1002/zaac.200900382.

[52] K. Müller-Buschbaum, Y. Mokaddem, Rare earth benzotriazolates: Coordination polymers incorporating decomposition products from ammonia to 1,2-diaminobenzene in [Ln(BtZ)3(BtZH)] (Ln = Ce, Pr), [Ln(Btz)3{Ph(NH2)2}] (Ln = Nd, Tb, Yb), and [Ho2(Btz)6(BtzH)(NH3)], Eur. J. Inorg. Chem. 2006 (2006) 2000–2010. doi:10.1002/ejic.200600010.

[53] M. Ammam, Polyoxometalates: Formation, structures, principal properties, main deposition methods and application in sensing, J. Mater. Chem. A. 1 (2013) 6291–6312. doi:10.1039/c3ta01663c.

[54] D.L. Long, E. Burkholder, L. Cronin, Polyoxometalate clusters, nanostructures and materials: From self assembly to designer materials and devices, Chem. Soc. Rev. 36 (2007) 105–121. doi:10.1039/b502666k.

[55] H.N. Miras, J. Yan, D.-L. Long, L. Cronin, Engineering polyoxometalates with emergent properties., Chem. Soc. Rev. 41 (2012) 7403–30. doi:10.1039/c2cs35190k.

[56] M. Hutin, M.H. Rosnes, D.L. Long, L. Cronin, Polyoxometalates: Synthesis and Structure - From Building Blocks to Emergent Materials, Elsevier Ltd., 2013. doi:10.1016/B978-0-08-097774-4.00210-2.

[57] X. Wang, Y. Wang, G. Liu, A. Tian, J. Zhang, H. Lin, Novel inorganic-organic hybrids constructed from multinuclear copper cluster and Keggin polyanions: From 1D wave-like chain to 2D network, Dalton Trans. 40 (2011) 9299–9305. doi:10.1039/c1dt10776c.

[58] W.-L. Zhou, J. Liang, C. Qin, K.-Z. Shao, F.-M. Wang, Z.-M. Su, Syntheses, crystal structures and properties of inorganic-organic hybrids constructed from Keggin-type polyoxometalates and silver coordination compounds, CrystEngComm. 16 (2014) 7410–7418. doi:10.1039/c4ce00633j.

[59] D.-D. Wang, J. Peng, H.-J. Pang, P.-P. Zhang, X. Wang, M. Zhu, Y. Chen, M.-G. Liu, C.-L. Meng, Keggin polyoxometalate-templated chair-like heptanuclear silver complex, Inorg.

Chim. Acta. 379 (2011) 90–94. doi:10.1016/j.ica.2011.09.032.

[60] Y. Cao, J. Lv, K. Yu, C. Wang, Z. Su, L. Wang, B. Zhou, Synthesis and photo-/electro-catalytic properties of Keggin polyoxometalate inorganic–organic hybrid layers based on d10 metal and rigid benzo-diazole/-triazole ligands, New J. Chem. 41 (2017) 12459–12469. doi:10.1039/C7NJ02615C.

[61] C.-Z. Ruan, R. Wen, M.-X. Liang, X.-J. Kong, Y.-P. Ren, L.-S. Long, R.-B. Huang, L.-S. Zheng, Two triazole-based metal-organic frameworks constructed from nanosized Cu20 and Cu30 wheels, Inorg. Chem. 51 (2012) 7587–7591. doi:10.1021/ic3003299.

[62] Y. Bai, J. Tao, R. Huang, L. Zheng, The Designed Assembly of Augmented Diamond Networks From Predetermined Pentanuclear Tetrahedral Units, Angew. Chemie Int. Ed. 47 (2008) 5344–5347. doi:10.1002/anie.200800403.

[63] X.-L. Wang, C. Qin, S.-X. Wu, K.-Z. Shao, Y.-Q. Lan, S. Wang, D.-X. Zhu, Z.-M. Su, E.-B. Wang, Bottom-up synthesis of porous coordination frameworks: apical substitution of a pentanuclear tetrahedral precursor., Angew. Chem. Int. Ed. 48 (2009) 5291–5295. doi:10.1002/anie.200902274.

[64] J.J. Deng, B.Q. Song, J. Liang, Y.Q. Jiao, X.S. Wu, L. Zhao, K.Z. Shao, Z.M. Su, An interpenetrated framework based on pentanuclear tetrahedral cluster with four-connected mdf network, Inorg. Chem. Commun. 60 (2015) 82–86. doi:10.1016/j.inoche.2015.06.006.

[65] Z. Zhang, S. Xiang, Y.S. Chen, S. Ma, Y. Lee, T. Phely-Bobin, B. Chen, A robust highly interpenetrated metal-organic framework constructed from pentanuclear clusters for selective sorption of gas molecules, Inorg. Chem. 49 (2010) 8444–8448. doi:10.1021/ic1010083.

[66] Y.-Q. Lan, S.-L. Li, H.-L. Jiang, Q. Xu, Tailor-made metal-organic frameworks from functionalized molecular building blocks and length-adjustable organic linkers by stepwise synthesis, Chem. - A Eur. J. 18 (2012) 8076–8083. doi:10.1002/chem.201200696.

[67] Y.-Q. Chen, Y.-K. Qu, G.-R. Li, Z.-Z. Zhuang, Z. Chang, T.-L. Hu, J. Xu, X.-H. Bu, Zn(II)-Benzotriazolate Clusters Based Amide Functionalized Porous Coordination Polymers with High CO2 Adsorption Selectivity, Inorg. Chem. 53 (2014) 8842–8844. doi:10.1021/ic500788z.

[68] Y.X. Tan, Y. Zhang, Y.P. He, Y.J. Zheng, Microporous metal-organic layer built from pentanuclear tetrahedral units: Gas sorption and magnetism, New J. Chem. 38 (2014) 5272–

5275. doi:10.1039/c4nj00517a.

[69] D.C. Zhong, J.H. Deng, X.Z. Luo, H.J. Liu, J.L. Zhong, K.J. Wang, T.B. Lu, Two cadmium-cluster-based metal-organic frameworks with mixed ligands of 1,2,3-benzenetriazole (HBTA) and 1,4-benzenedicarboxylic acid (H_2BDC), Cryst. Growth Des. 12 (2012) 1992–1998. doi:10.1021/cg2016963.

[70] X.-L. Wang, C. Qin, Y.-Q. Lan, K.-Z. Shao, Z.-M. Su, E.-B. Wang, Metal-organic replica of γ-Pu: The first uninodal 10-connected coordination network based on pentanuclear cadmium clusters, Chem. Commun. 379 (2009) 410–412. doi:10.1039/b815629h.

[71] Y.W. Li, S.J. Liu, T.L. Hu, D.C. Li, J.M. Dou, Z. Chang, A new Co-based metal-organic framework constructed from infinite sinusoidal-like rod-shaped secondary building units, Inorg. Chem. Commun. 47 (2014) 67–70. doi:10.1016/j.inoche.2014.06.024.

[72] Y.Y. Qin, J. Zhang, Z.J. Li, L. Zhang, X.Y. Cao, Y.G. Yao, Organically templated metal-organic framework with 2-fold interpenetrated {33.59.63}-lcy net, Chem. Commun.(2008) 2532–2534. doi:10.1039/b800017d.

[73] Y.-W. Li, L.-F. Wang, K.-H. He, Q. Chen, X.-H. Bu, A sixfold interpenetrated microporous MOF constructed from heterometallic tetranuclear cluster exhibiting selective gas adsorption, Dalton Trans. 40 (2011) 10319–10321. doi:10.1039/c1dt10554j.

[74] L. Kan, L. Xu, J. Cai, Z. Jin, G. Li, Y. Liu, Two Stable Zn-Cluster-Based Metal–Organic Frameworks with Breathing Behavior: Synthesis, Structure, and Adsorption Properties, Inorg. Chem. 58 (2018) 391–396. doi:10.1021/acs.inorgchem.8b02507.

[75] Z.-W. Fan, L. Li, K. Cui, S.-S. Yang, F.-Q. Han, Structure and Luminescent Property of a New Cd(II) Coordination Polymer With (3,6)-Connected *ant* Topology, Synth. React. Inorganic, Met. Nano-Metal Chem. 46 (2016) 1701–1704. doi:10.1080/15533174.2015.1136962.

[76] Z.-Q. Jiang, G.-Y. Jiang, F. Wang, Z. Zhao, J. Zhang, Ring-size controllable metallamacrocycles as building blocks for the construction of microporous metal-organic frameworks, Chem. Commun. 48 (2012) 3653–3655. doi:10.1039/c2cc17256a.

[77] K.Z. Shao, Y.H. Zhao, X.L. Wang, Y.Q. Lan, D.J. Wang, Z.M. Su, R.S. Wang, Construction of a three-dimensional polynuclear zinc compound based on unique metallophthalocyanine-like subunits, Inorg. Chem. 48 (2009) 10–12. doi:10.1021/ic801439q.

[78] G.X. Liu, L.F. Huang, X.J. Kong, R.Y. Huang, H. Xu, Hydrothermal synthesis of two novel

three-dimensional cobalt(II) metal-organic frameworks based on polycarboxylate and benzotriazole, Inorganica Chim. Acta. 362 (2009) 1755–1760. doi:10.1016/j.ica.2008.08.025.

[79] E.-C. Yang, H.-K. Zhao, B. Ding, X.-G. Wang, X.-J. Zhao, Four Novel Three-Dimensional Triazole-Based Zinc(II) Metal−Organic Frameworks Controlled by the Spacers of Dicarboxylate Ligands: Hydrothermal Synthesis, Crystal Structure, and Luminescence Properties, Cryst. Growth Des. 7 (2007) 2009–2015. doi:10.1021/cg070356n.

[80] K. Zhu, H. Chen, S. Nishihara, G.-X. Liu, X.-M. Ren, Cobalt(II) coordination polymers assembled from polycarboxylate and benzotriazole: Syntheses, structures and physical properties, Inorg. Chim. Acta. 362 (2009) 4780–4784. doi:10.1016/j.ica.2009.06.048.

[81] Y. Dong, G. Xing, Two New Cadmium(II) Compounds based on Distinct Second Building Subunits: Solvothermal Syntheses, Crystal Structures, and Luminescent Properties, Zeitschrift Für Anorg. Und Allg. Chemie. 641 (2015) 1679–1683. doi:10.1002/zaac.201500061.

[82] F. Luo, Y. Ning, M.-B. Luo, G.-L. Huang, Chiral or achiral camphorate-based complexes controlled by the conformational rigidity of N-donor co-ligands, CrystEngComm. 12 (2010) 2769–2774. doi:10.1039/c000734j.

[83] J.-Y. Zou, L. Li, S.-Y. You, K.-H. Chen, X.-N. Dong, Y.-H. Chen, J.-Z. Cui, A usf Zinc(II) Metal-Organic Framework as a Highly Selective Luminescence Probe for Acetylacetone Detection and Its Postsynthetic Cation Exchange, Cryst. Growth Des. 18 (2018) 3997–4003. doi:10.1021/acs.cgd.8b00344.

[84] R. Herchel, Z. Indelá, Z. Trávníek, R. Zboil, J. Vančo, Novel 1D chain Fe(III)-salen-like complexes involving anionic heterocyclic N-donor ligands. Synthesis, X-ray structure, magnetic,57Fe Mössbauer, and biological activity studies, Dalton Trans. 0 (2009) 9870–9880. doi:10.1039/b912676g.

[85] B. Shankar, P. Elumalai, S. Deval Sathiyashivan, M. Sathiyendiran, Spheroid metallocavitands with eight calixarene-shaped receptors on the surface, Inorg. Chem. 53 (2014) 10018–10020. doi:10.1021/ic5014895.

[86] S.-D. Han, Y.-Q. Chen, J.-P. Zhao, S.-J. Liu, X.-H. Miao, T.-L. Hu, X.-H. Bu, Solvent-induced structural diversities from discrete cup-shaped Co_8 clusters to Co_8 cluster-based chains accompanied by in situ ligand conversion, CrystEngComm. 16 (2014) 753–756.

doi:10.1039/c3ce42007h.

[87] S. Biswas, M. Tonigold, M. Speldrich, P. Kögerler, M. Weil, D. Volkmer, Syntheses and magnetostructural investigations on kuratowski-type homo-and heteropentanuclear coordination compounds $[MZn_4Cl_4(L)_6]$ (M^{II} = Zn, Fe, Co, Ni, or Cu; L = 5,6-Dimethyl-1,2,3- benzotriazolate) represented by the nonplanar K 3,3 graph, Inorg. Chem. 49 (2010) 7424–7434. doi:10.1021/ic100749k.

[88] Y.Y. Liu, M. Grzywa, M. Tonigold, G. Sastre, T. Schüttrigkeit, N.S. Leeson, D. Volkmer, Photophysical properties of Kuratowski-type coordination compounds $[M^{II}Zn_4Cl_4(Me_2bta)_6]$ (M^{II}= Zn or Ru) featuring long-lived excited electronic states, Dalton. Trans. 40 (2011) 5926–5938. doi:10.1039/c0dt01750g.

[89] S. Biswas, M. Tonigold, M. Speldrich, P. Kögerler, D. Volkmer, Nonanuclear coordination compounds featuring $\{M_9L_{12}\}^{6+}$cores (M = Ni^{II}, Co^{II}, or Zn^{II}; L = 1,2,3-benzotriazolate), Eur. J. Inorg. Chem. 2009 (2009) 3094–3101. doi:10.1002/ejic.200900156.

[90] S. Biswas, M. Tonigold, H. Kelm, H.J. Krüger, D. Volkmer, Thermal spin-crossover in the $[M_3Zn_6Cl_6L_{12}]$ (M = Zn, Fe^{II}; L = 5,6-dimethoxy-1,2,3- benzotriazolate) system: Structural, electrochemical, Mössbauer, and UV-Vis spectroscopic studies, Dalton Trans. 39 (2010) 9851–9859. doi:10.1039/c0dt00556h.

[91] L.F. Jones, E.K. Brechin, D. Collison, J. Raftery, S.J. Teat, New Routes to High Nuclearity Clusters: Fluoride-Based Octametallic and Tridecametallic Clusters of Manganese, Inorg. Chem. 42 (2003) 6971–6973. doi:10.1021/ic034979b.

[92] R.H. Laye, Q. Wei, P. V. Mason, M. Shanmugam, S.J. Teat, E.K. Brechin, D. Collison, E.J.L. McInnes, A highly reduced Vanadium(III/IV) polyoxovanadate comprising an octavanadyl square-prism surrounding a dimetallic Vanadium(III) fragment, J. Am. Chem. Soc. 128 (2006) 9020–9021. doi:10.1021/ja062723+.

[93] A. Lanza, L.S. Germann, M. Fisch, N. Casati, P. Macchi, Solid-State Reversible Nucleophilic Addition in a Highly Flexible MOF, J. Am. Chem. Soc. 137 (2015) 13072–13078. doi:10.1021/jacs.5b09231.

[94] C. Qiao, L. Sun, S. Zhang, P. Liu, L. Chang, C. Zhou, Q. Wei, S. Chen, S. Gao, Pore-size-tuned host-guest interactions in Co-MOFs via in situ microcalorimetry: adsorption and magnetism, J. Mater. Chem. C. 5 (2017) 1064–1073. doi:10.1039/c6tc05082d.

[95] H.Y. Ren, X.M. Zhang, Enhanced Selective CO2 Capture upon Incorporation of

Dimethylformamide in the Cobalt Metal-Organic Framework [$Co_3(OH)_2(btca)_2$], Energy and Fuels. 30 (2016) 526–530. doi:10.1021/acs.energyfuels.5b02393.

[96] J. Xiao, Y. Wu, M. Li, B.Y. Liu, X.C. Huang, D. Li, Crystalline structural intermediates of a breathing metal-organic framework that functions as a luminescent sensor and gas reservoir, Chem. - A Eur. J. 19 (2013) 1891–1895. doi:10.1002/chem.201203515.

[97] Z.-B. Han, R.-Y. Lu, Y.-F. Liang, Y.-L. Zhou, Q. Chen, M.-H. Zeng, Mn(II)-based porous metal-organic framework showing metamagnetic properties and high hydrogen adsorption at low pressure., Inorg. Chem. 51 (2012) 674–679. doi:10.1021/ic2021929.

[98] J. Xiao, B.-Y. Liu, G. Wei, X.-C. Huang, Solvent induced diverse dimensional coordination assemblies of cupric benzotriazole-5-carboxylate: Syntheses, crystal structures, and magnetic properties, Inorg. Chem. 50 (2011) 11032–11038. doi:10.1021/ic201571n.

[99] W. Uhl, M. Voß, M. Layh, F. Rogel, Gallium-gallium bonds as efficient templates for the generation of a large cage containing twelve gallium atoms, Dalton Trans. 39 (2010) 3160–3162. doi:10.1039/c001032b.

[100] S. Biswas, M. Grzywa, H.P. Nayek, S. Dehnen, I. Senkovska, S. Kaskel, D. Volkmer, A cubic coordination framework constructed from benzobistriazolate ligands and zinc ions having selective gas sorption properties, Dalton Trans. 9226 (2009) 6487–6495. doi:10.1039/b904280f.

[101] H. Bunzen, M. Grzywa, M. Hambach, S. Spirkl, D. Volkmer, From Micro to Nano: A Toolbox for Tuning Crystal Size and Morphology of Benzotriazolate-Based Metal-Organic Frameworks, Cryst. Growth Des. 16 (2016) 3190–3197. doi:10.1021/acs.cgd.6b00038.

[102] P.-Q. Liao, X.Y. Li, J. Bai, C.T. He, D.D. Zhou, W.-X. Zhang, J.-P. Zhang, X.M. Chen, Drastic enhancement of catalytic activity via post-oxidation of a porous MnII triazolate framework, Chem. Eur. J. 20 (2014) 11303–11307. doi:10.1002/chem.201403123.

[103] P.-Q. Liao, H. Chen, D.-D. Zhou, S.-Y. Liu, C.-T. He, Z. Rui, H. Ji, J.-P. Zhang, X.-M. Chen, Monodentate hydroxide as a super strong yet reversible active site for CO_2 capture from high-humidity flue gas, Energy Environ. Sci. 8 (2015) 1011–1016. doi:10.1039/c4ee02717e.

[104] X.-F. Lu, P.-Q. Liao, J.-W. Wang, J.-X. Wu, X.-W. Chen, C.-T. He, J.-P. Zhang, G.-R. Li, X.-M. Chen, An Alkaline-Stable, Metal Hydroxide Mimicking Metal-Organic Framework for Efficient Electrocatalytic Oxygen Evolution, J. Am. Chem. Soc. 138 (2016) 8336–8339.

doi:10.1021/jacs.6b03125.

[105] A.J. Rieth, M. Dincă, Controlled Gas Uptake in Metal-Organic Frameworks with Record Ammonia Sorption, J. Am. Chem. Soc. 140 (2018) 3461–3466. doi:10.1021/jacs.8b00313.

[106] D. Denysenko, M. Grzywa, M. Tonigold, B. Streppel, I. Krkljus, M. Hirscher, E. Mugnaioli, U. Kolb, J. Hanss, D. Volkmer, Elucidating gating effects for hydrogen sorption in MFU-4-type triazolate-based metal-organic frameworks featuring different pore sizes, Chem. - A Eur. J. 17 (2011) 1837–1848. doi:10.1002/chem.201001872.

[107] D. Denysenko, T. Werner, M. Grzywa, A. Puls, V. Hagen, G. Eickerling, J. Jelic, K. Reuter, D. Volkmer, Reversible gas-phase redox processes catalyzed by Co-exchanged MFU-4l(arge), Chem. Commun. 48 (2012) 1236–1238.

[108] C.K. Brozek, M. Dincă, Thermodynamic parameters of cation exchange in MOF-5 and MFU-4l, Chem. Commun. 51 (2015) 11780–11782. doi:10.1039/c5cc04249f.

[109] A.M. Wright, A.J. Rieth, S. Yang, E.N. Wang, M. Dincă, Precise control of pore hydrophilicity enabled by post-synthetic cation exchange in metal-organic frameworks, Chem. Sci. 9 (2018) 3856–3859. doi:10.1039/c8sc00112j.

[110] R.J. Comito, E.D. Metzger, Z. Wu, G. Zhang, C.H. Hendon, J.T. Miller, M. Dincă, Selective Dimerization of Propylene with Ni-MFU-4l, Organometallics. 36 (2017) 1681–1683. doi:10.1021/acs.organomet.7b00178.

[111] R.J. Comito, K.J. Fritzsching, B.J. Sundell, K. Schmidt-Rohr, M. Dincă, Single-Site Heterogeneous Catalysts for Olefin Polymerization Enabled by Cation Exchange in a Metal-Organic Framework, J. Am. Chem. Soc. 138 (2016) 10232–10237. doi:10.1021/jacs.6b05200.

[112] R.J.C. Dubey, R.J. Comito, Z. Wu, G. Zhang, A.J. Rieth, C.H. Hendon, J.T. Miller, M. Dincă, Highly Stereoselective Heterogeneous Diene Polymerization by Co-MFU-4l: A Single-Site Catalyst Prepared by Cation Exchange, J. Am. Chem. Soc. 139 (2017) 12664–12669. doi:10.1021/jacs.7b06841.

[113] A.J. Rieth, Y. Tulchinsky, M. Dincă, High and Reversible Ammonia Uptake in Mesoporous Azolate Metal-Organic Frameworks with Open Mn, Co, and Ni Sites, J. Am. Chem. Soc. 138 (2016) 9401–9404. doi:10.1021/jacs.6b05723.

[114] A.J. Rieth, S. Yang, E.N. Wang, M. Dincă, Record Atmospheric Fresh Water Capture and Heat Transfer with a Material Operating at the Water Uptake Reversibility Limit, ACS Cent.

Sci. 3 (2017) 668–672. doi:10.1021/acscentsci.7b00186.

[115] A.J. Rieth, A.M. Wright, S. Rao, H. Kim, A.D. LaPotin, E.N. Wang, M. Dincă, Tunable Metal-Organic Frameworks Enable High Efficiency Cascaded Adsorption Heat Pumps, J. Am. Chem. Soc. 140 (2018) 17591–17596. doi:10.1021/jacs.8b09655.

[116] D.A. Reed, B.K. Keitz, J. Oktawiec, J.A. Mason, T. Runčevski, D.J. Xiao, L.E. Darago, V. Crocellà, S. Bordiga, J.R. Long, A spin transition mechanism for cooperative adsorption in metal-organic frameworks, Nature. 550 (2017) 96–100. doi:10.1038/nature23674.

[117] A.M. Wright, Z. Wu, G. Zhang, J.L. Mancuso, R.J. Comito, R.W. Day, C.H. Hendon, J.T. Miller, M. Dincă, A Structural Mimic of Carbonic Anhydrase in a Metal-Organic Framework, Chem. 4 (2018) 2894–2901. doi:10.1016/j.chempr.2018.09.011.

[118] P. Schmieder, M. Grzywa, D. Denysenko, M. Hambach, D. Volkmer, CFA-7: an interpenetrated metal–organic framework of the MFU-4 family, Dalton Trans. 44 (2015) 13060–13070. doi:10.1039/C5DT01673H.

[119] P. Schmieder, D. Denysenko, M. Grzywa, O. Magdysyuk, D. Volkmer, A structurally flexible triazolate-based metal–organic framework featuring coordinatively unsaturated Copper(i) sites, Dalton Trans. 45 (2016) 13853–13862. doi:10.1039/C6DT02672A.

[120] P. Schmieder, D. Denysenko, M. Grzywa, B. Baumgärtner, I. Senkovska, S. Kaskel, G. Sastre, L. Van Wüllen, D. Volkmer, CFA-1: The first chiral metal-organic framework containing Kuratowski-type secondary building units, Dalton Trans. 42 (2013) 10786–10797. doi:10.1039/c3dt50787d.

[121] C. Richardson, P.J. Steel, Benzotriazole as a structural component in chelating and bridging heterocyclic ligands; ruthenium, palladium,copper and silver complexes, Dalton Trans. (2003) 992–1000. doi:10.1039/b206990c.

[122] C.-X. An, X.-L. Han, P.-B. Wang, Z.-H. Zhang, H.-K. Zhang, Z.-J. Fan, Synthesis, crystal structures, and biological activities of silver(I) and cobalt(II) complexes with an azole derivative ligand, Transit. Met. Chem. 33 (2008) 835–841. doi:10.1007/s11243-008-9119-2.

[123] J. Hu, Y. Zhao, F. Yang, C. Liao, J. Zhao, Ag/Cd coordination architecture and photoluminescence behaviors, J. Coord. Chem. 71 (2018) 1368–1379. doi:10.1080/00958972.2018.1467008.

[124] Z. Xu, D.S. Wang, X. Yu, Y. Yang, D. Wang, Tunable Triazole-Phosphine-Copper

Catalysts for the Synthesis of 2-Aryl-1H-benzo[d]imidazoles from Benzyl Alcohols and Diamines by Acceptorless Dehydrogenation and Borrowing Hydrogen Reactions, Adv. Synth. Catal. 359 (2017) 3332–3340. doi:10.1002/adsc.201700179.

[125] R. Huang, Y. Yang, D.S. Wang, L. Zhang, D. Wang, Where does Au coordinate to N-(2-pyridiyl)benzotriazole: Gold-catalyzed chemoselective dehydrogenation and borrowing hydrogen reactions, Org. Chem. Front. 5 (2018) 203–209. doi:10.1039/c7qo00756f.

[126] Q. Wu, L. Pan, G. Du, C. Zhang, D. Wang, Preparation of pyridyltriazole ruthenium complexes as effective catalysts for the selective alkylation and one-pot C-H hydroxylation of 2-oxindole with alcohols and mechanism exploration, Org. Chem. Front. 5 (2018) 2668–2675. doi:10.1039/c8qo00725j.

[127] C. Papatriantafyllopoulou, E. Diamantopoulou, A. Terzis, V. Tangoulis, N. Lalioti, S.P. Perlepes, High-nuclearity nickel(II) clusters: Ni_{13} complexes from the use of 1-hydroxybenzotriazole, Polyhedron. 28 (2009) 1903–1911. doi:10.1016/j.poly.2008.10.036.

[128] C.C. Stoumpos, E. Diamantopoulou, C.P. Raptopoulou, A. Terzis, S.P. Perlepes, N. Lalioti, A two-dimensional manganese(II) coordination polymer containing 1-hydroxybenzotriazolate and acetate bridging ligands: Preparation, structural characterization and magnetic study, Inorganica Chim. Acta. 361 (2008) 3638–3645. doi:10.1016/j.ica.2008.03.071.

[129] A.D. Katsenis, N. Lalioti, V. Bekiari, P. Lianos, C.P. Raptopoulou, A. Terzis, S.P. Perlepes, G.S. Papaefstathiou, Initial use of 1-hydroxybenzotriazole in the chemistry of group 12 metals: An 1D zinc(II) coordination polymer and a mononuclear cadmium(II) complex containing the deprotonated ligand in a novel monodentate ligation mode, Inorg. Chem. Commun. 12 (2009) 92–96. doi:10.1016/j.inoche.2008.11.010.

[130] P. Børsting, P.J. Steel, Synthesis and X-ray Crystal Structures of Cobalt and Copper Complexes of 1,3-Bis(benzotriazolyl)propanes, Eur. J. Inorg. Chem. 2004 (2004) 376–380. doi:10.1002/ejic.200300271.

[131] X. Meng, J. Li, H. Hou, Y. Song, Y. Fan, Y. Zhu, Double helix chain frameworks constructed from bis-benzotriazole building blocks: Syntheses, crystal structures and third-order nonlinear optical properties, J. Mol. Struct. 891 (2008) 305–311. doi:10.1016/j.molstruc.2008.03.058.

[132] Y. Wang, M.C. Hu, Q.G. Zhai, S.N. Li, Y.C. Jiang, W.J. Ji, Synthesis, structure and

luminescent properties of an organic-inorganic hybrid solid based on unprecedented flower-basket-shaped [Cu_4I_4] clusters with 1,2-bis(benzotriazole)ethane ligands, Inorg. Chem. Commun. 12 (2009) 281–285. doi:10.1016/j.inoche.2009.01.003.

[133] E. V. Lider, D.A. Piryazev, A. V. Virovets, L.G. Lavrenova, A.I. Smolentsev, E.M. Uskov, A.S. Potapov, A.I. Khlebnikov, Structure and luminescent properties of the cadmium(II) chloride complex with bis(benzotriazole-1-yl)methane, J. Struct. Chem. 51 (2010) 514–518. doi:10.1007/s10947-010-0074-3.

[134] Q.-G. Zhai, X. Gao, S.-N. Li, Y.-C. Jiang, M.-C. Hu, Solvothermal synthesis, crystal structures and photoluminescence properties of the novel Cd/X/α,ω-bis(benzotriazole)alkane hybrid family (X = Cl, Br and I), CrystEngComm. 13 (2011) 1602–1616. doi:10.1039/c0ce00581a.

[135] E. V. Peresypkina, E. V. Lider, A.I. Smolentsev, J. Sanchiz, B. Gil-Hernández, A.S. Potapov, A.I. Khlebnikov, N.A. Kryuchkova, L.G. Lavrenova, Bis(benzotriazol-1-yl)methane as a linker in the assembly of new copper(II) coordination polymers: Synthesis, structure and investigations, Polyhedron. 48 (2012) 253–263. doi:10.1016/j.poly.2012.08.072.

[136] X. Zhou, X. Meng, W. Cheng, H. Hou, M. Tang, Y. Fan, Crystal structural, electrochemical and computational studies of two Cu(II) complexes formed by benzotriazole derivatives, Inorganica Chim. Acta. 360 (2007) 3467–3474. doi:10.1016/j.ica.2007.03.008.

[137] X.-L. Tang, W. Dou, J.-A. Zhou, G.-L. Zhang, W.-S. Liu, L.-Z. Yang, Y.-L. Shao, Metallomacrocycle or coordination polymer: Spacer-directed self-assembly of transition-metal complexes based on flexible bis(benzotriazole) ligands, CrystEngComm. 13 (2011) 2890–2898. doi:10.1039/c0ce00847h.

[138] X. Gao, Q.-G. Zhai, X. Dui, S.-N. Li, Y.-C. Jiang, M.-C. Hu, Synthesis, crystal structure, and characterizations of a 3-D Cu(I) complex with 1,6-bi(benzotriazole)hexane, J. Coord. Chem. 63 (2010) 214–222. doi:10.1080/00958970903383863.

[139] M.-C. Hu, Y. Wang, Q.-G. Zhai, S.-N. Li, Y.-C. Jiang, Y. Zhang, Synthesis, crystal structures, and photoluminescent properties of the Cu(I)/X/α,ω-bis(benzotriazole)alkane hybrid family (X = Cl, Br, I, and CN), Inorg. Chem. 48 (2009) 1449–1468. doi:10.1021/ic801574k.

[140] X.-L. Tang, W. Dou, J.-A. Zhou, G.-L. Zhang, W.-S. Liu, L.-Z. Yang, Y.-L. Shao,

Metallomacrocycle or coordination polymer: Spacer-directed self-assembly of transition-metal complexes based on flexible bis(benzotriazole) ligands, CrystEngComm. 13 (2011) 2890–2898. doi:10.1039/c0ce00847h.

[141] A. Sasmal, S. Shit, C. Rizzoli, H. Wang, C. Desplanches, S. Mitra, Framework solids based on copper(II) halides (Cl/Br) and methylene- bridged bis(1-hydroxybenzotriazole): Synthesis, crystal structures, magneto-structural correlation, and density functional theory (DFT) studies, Inorg. Chem. 51 (2012) 10148–10157. doi:10.1021/ic300629v.

[142] S. Saha, A. Sasmal, G. Pilet, A. Bauzá, A. Frontera, S. Mitra, An unusual nitroso···nitroso interaction in the coordination polymer structures of Ni(ii) and Co(ii) complexes with the α,ω- bis(benzotriazoloxy)alkane system, CrystEngComm. 16 (2014) 654–666. doi:10.1039/c3ce41765d.

[143] Y. Lu, Y. Tang, H. Gao, Z. Zhang, H. Wang, The synthesis, crystal structures and SOD activities of a new ligand (Lse) and Co(Lse)2(SCN)2 complex [Lse = selenium ether bis-(N-1-methyl- benzotriazole)], Appl. Organomet. Chem. 21 (2007) 211–217. doi:10.1002/aoc.1210.

[144] G.E. Kostakis, P. Xydias, E. Nordlander, J.C. Plakatouras, The first structural determination of a copper (II) complex containing the ligand [1-(4-((1H-benzo[d][1,2,3]triazol-2(3H)-yl)methyl)benzyl)-1H-benzo[d][1,2,3]triazole], Inorg. Chim. Acta. 383 (2012) 327–331. doi:10.1016/j.ica.2011.10.063.

[145] B.J. O'Keefe, P.J. Steel, Self-assembly and X-ray structure of a triple helicate with two trigonal silver(I) termini, Inorg. Chem. Commun. 3 (2000) 473–475. doi:10.1016/S1387-7003(00)00120-9.

[146] M. Sun, W.-Z. Zhou, Y.-H. Wang, H.-Q. Tan, Y.-F. Qi, H.-Y. Zang, Y.-G. Li, Luminescent hybrid metal-organic coordination polymers based on Cu/Ag-bis(benzotriazole) units and polyoxometalates, J. Coord. Chem. 69 (2016) 1769–1779. doi:10.1080/00958972.2016.1146258.

[147] E. Loukopoulos, N.F. Chilton, A. Abdul-Sada, G.E. Kostakis, Exploring the Coordination Capabilities of a Family of Flexible Benzotriazole-Based Ligands Using Cobalt(II) Sources, Cryst. Growth Des. 17 (2017) 2718–2729. doi:10.1021/acs.cgd.7b00200.

[148] E. Loukopoulos, G.E. Kostakis, Recent advances of one-dimensional coordination polymers as catalysts, J. Coord. Chem. 71 (2018) 1–40.

doi:10.1080/00958972.2018.1439163.

[149] M. Kallitsakis, E. Loukopoulos, A. Abdul-Sada, G.J. Tizzard, S.J. Coles, G.E. Kostakis, I.N. Lykakis, A Copper-Benzotriazole-Based Coordination Polymer Catalyzes the Efficient One-Pot Synthesis of (N' -Substituted)-hydrazo-4-aryl-1,4-dihydropyridines from Azines, Adv. Synth. Catal. 359 (2017) 138–145. doi:10.1002/adsc.201601072.

[150] C.B. Toal, P.A. Meredith, H.L. Elliott, Long-acting dihydropyridine calcium-channel blockers and sympathetic nervous system activity in hypertension: a literature review comparing amlodipine and nifedipine GITS., Blood Press. 21 Suppl 1 (2012) 3–10. doi:10.3109/08037051.2012.690615.

[151] F.-V. Lauro, D.-C. Francisco, G.-C. Elodia, P.-G. Eduardo, R.-N. Marcela, H.-H. Lenin, S.A. Betty, Design and synthesis of new dihydrotestosterone derivative with positive inotropic activity, Steroids. 95 (2015) 39–50.

[152] K. Tanaka, T. Niino, T. Ishihara, A. Takafuji, T. Takayama, Y. Kanda, T. Sugizaki, F. Tamura, S. Kurotsu, M. Kawahara, T. Mizushima, Protective and therapeutic effect of felodipine against bleomycin-induced pulmonary fibrosis in mice, Sci. Rep. 7 (2017) 3439. doi:10.1038/s41598-017-03676-y.

[153] E. Loukopoulos, M. Kallitsakis, N. Tsoureas, A. Abdul-Sada, N.F. Chilton, I.N. Lykakis, G.E. Kostakis, Cu(II) coordination polymers as vehicles in the A3 coupling, Inorg. Chem. 56 (2017) 4898–4910. http://pubs.acs.org/doi/abs/10.1021/acs.inorgchem.6b03084.

[154] D. Andreou, M. Kallitsakis, E. Loukopoulos, C. Gabriel, G.E. Kostakis, I.N. Lykakis, Copper-promoted regioselective synthesis of polysubstituted pyrroles from aldehydes, amines and nitroalkenes via 1,2-phenyl/alkyl migration, J. Org. Chem. 83 (2018) 2104–2113. doi:10.1021/acs.joc.7b03051.

[155] E. Loukopoulos, A. Abdul-Sada, G. Csire, C. Kallay, A. Brookfield, G.J. Tizzard, S. Coles, I. Lykakis, G.E. Kostakis, Copper(II)-benzotriazole coordination compounds in click chemistry: A diagnostic reactivity study, Dalton Trans. 47 (2018) 10491–10508. doi:10.1039/C8DT01256C.

[156] E. Loukopoulos, A. Abdul-Sada, E.M.E. Viseux, I.N. Lykakis, G.E. Kostakis, Structural Diversity and Catalytic Properties in a Family of Ag(I)-Benzotriazole Based Coordination Compounds, Cryst. Growth Des. 18 (2018) 5638–5651. doi:10.1021/acs.cgd.8b00960.

[157] B.J. O'Keefe, M.A. Hillmyer, W.B. Tolman, Polymerization of lactide and related cyclic

esters by discrete metal complexes, J. Chem. Soc. Dalton Trans. (2001) 2215–2224. doi:10.1039/b104197p.

[158] J. Wu, T.L. Yu, C.T. Chen, C.C. Lin, Recent developments in main group metal complexes catalyzed/initiated polymerization of lactides and related cyclic esters, Coord. Chem. Rev. 250 (2006) 602–626. doi:10.1016/j.ccr.2005.07.010.

[159] C.Y. Li, C.Y. Tsai, C.H. Lin, B.T. Ko, Synthesis, structural characterization and reactivity of aluminium complexes supported by benzotriazole phenoxide ligands: Air-stable alumoxane as an efficient catalyst for ring-opening polymerization of l-lactide, Dalton Trans. 40 (2011) 1880–1887. doi:10.1039/c0dt01108h.

[160] C.Y. Li, J.K. Su, C.J. Yu, Y.E. Tai, C.H. Lin, B.T. Ko, Synthesis and structural characterization of magnesium complexes bearing benzotriazole phenoxide ligands: Photoluminescent properties and catalytic studies for ring-opening polymerization of l-lactide, Inorg. Chem. Commun. 20 (2012) 60–65. doi:10.1016/j.inoche.2012.02.017.

[161] K.-C. Lee, H.-J. Chuang, B.-H. Huang, B.-T. Ko, P.-H. Lin, Structurally diverse dysprosium and yttrium complexes containing an amine-bis(benzotriazole phenolate) ligand: Synthesis, characterization and catalysis for lactide polymerization, Inorg. Chim. Acta. 450 (2016) 411–417. doi:10.1016/j.ica.2016.06.033.

[162] C.Y. Li, C.J. Yu, B.T. Ko, Facile synthesis of well-defined titanium alkoxides based on benzotriazole phenoxide ligands: Efficient catalysts for ring-opening polymerization of cyclic esters, Organometallics. 32 (2013) 172–180. doi:10.1021/om300962k.

[163] C.H. Chang, H.J. Chuang, T.Y. Chen, C.Y. Li, C.H. Lin, T.Y. Lee, B.T. Ko, H.Y. Huang, Di-nuclear zinc complexes containing tridentate imino-benzotriazole phenolate derivatives as efficient catalysts for ring-opening polymerization of cyclic esters and copolymerization of phthalic anhydride with cyclohexene oxide, J. Polym. Sci. Part A Polym. Chem. 54 (2016) 714–725. doi:10.1002/pola.27902.

[164] B.-T. Ko, J.-K. Su, C.-C. Lin, B.-H. Huang, J.-H. Wang, C.-Y. Tsai, Mono-, di- and tetra-zinc complexes derived from an amino-benzotriazole phenolate ligand containing a bulkier N-alkyl pendant arm: synthesis, structure and catalysis for ring-opening polymerization of cyclic esters, Dalton Trans. 44 (2015) 12401–12410. doi:10.1039/c4dt02906b.

[165] J.-D. Chen, B.-T. Ko, C.-Y. Li, C.-Y. Tsai, Z.-T. Liu, W.-L. Liu, Titanium, aluminum and zinc complexes containing diamine-bis(benzotriazole phenolate) ligands: Synthesis,

structural characterization and catalytic studies for ring-opening polymerization of ε-caprolactone, J. Mol. Struct. 1134 (2016) 395–403. doi:10.1016/j.molstruc.2016.12.081.

[166] C.-H. Li, H.-J. Chuang, C.-Y. Li, B.-T. Ko, C.-H. Lin, Bimetallic nickel and cobalt complexes as high-performance catalysts for copolymerization of carbon dioxide with cyclohexene oxide, Polym. Chem. 5 (2014) 4875–4878. doi:10.1039/c4py00528g.

[167] P.-M. Lin, C.-H. Chang, H.-J. Chuang, C.-T. Liu, B.-T. Ko, C.-C. Lin, Bimetallic Nickel Complexes that Bear Diamine-Bis(Benzotriazole Phenolate) Derivatives as Efficient Catalysts for the Copolymerization of Carbon Dioxide with Epoxides, ChemCatChem. 8 (2016) 984–991. doi:10.1002/cctc.201501280.

[168] L.-S. Huang, C.-Y. Tsai, H. Chuang, B.-T. Ko, Copolymerization of Carbon Dioxide with Epoxides Catalyzed by Structurally Well-Characterized Dinickel Bis(benzotriazole iminophenolate) Complexes: Influence of Carboxylate Ligands on the Catalytic Performance, Inorg. Chem. 56 (2017) 6141–6151. doi:10.1021/acs.inorgchem.7b00090.

[169] C.-Y. Yu, H.-J. Chuang, B.-T. Ko, Bimetallic bis(benzotriazole iminophenolate) cobalt, nickel and zinc complexes as versatile catalysts for coupling of carbon dioxide with epoxides and copolymerization of phthalic anhydride with cyclohexene oxide, Catal. Sci. Technol. 6 (2016) 1779–1791. doi:10.1039/c5cy01290b.

[170] C.-Y. Li, Y.-C. Su, C.-H. Lin, H.-Y. Huang, C.-Y. Tsai, T.-Y. Lee, B.-T. Ko, Synthesis and characterization of trimetallic cobalt, zinc and nickel complexes containing amine-bis(benzotriazole phenolate) ligands: Efficient catalysts for coupling of carbon dioxide with epoxides, Dalton Trans. 46 (2017) 15399–15406. doi:10.1039/c7dt02841e.

[171] B. Stanje, P. Traar, J.A. Schachner, F. Belaj, N.C. Mösch-Zanetti, Iron catalyzed oxidation of benzylic alcohols to benzoic acids, Dalton Trans. 47 (2018) 6412–6420. doi:10.1039/c8dt00819a.

[172] R.-Y. Lu, G.-Y. Luan, Z.-B. Han, A two-dimensional Zn^{II} coordination polymer constructed by benzotriazole-5-carboxylate and 1,4,8,9-tetraazatriphenylene, Acta Crystallogr. Sect. C Cryst. Struct. Commun. 66 (2010) 283–285. doi:10.1107/S0108270110033998.

[173] J. Liu, H.-B. Zhang, Y.-X. Tan, F. Wang, Y. Kang, J. Zhang, Structural Diversity and Photoluminescent Properties of Zinc Benzotriazole-5-carboxylate Coordination Polymers, Inorg. Chem. 53 (2014) 1500–1506. doi:10.1021/ic402467g.

[174] S. Ning, H. Chen, S. Zhang, P. Cheng, A 2D water-stable metal–organic framework for

fluorescent detection of nitroaromatics, Polyhedron. 155 (2018) 457–463. doi:10.1016/j.poly.2018.09.001.

[175] N. Xin, Y.-Q. Sun, Y.N. Han, D.Z. Gao, Two 3d-4f Heterometallic Coordination Polymers of Macrocyclic Oxamide with Benzotriazole-5-carboxylate Co-ligand: Syntheses, Crystal Structures and Magnetic Properties, Zeitschrift Fur Anorg. Und Allg. Chemie. 642 (2016) 1460–1465. doi:10.1002/zaac.201600377.

[176] G.Z. Deng, N. Xin, Y.N. Han, Y.Q. Sun, Hydrothermal Synthesis, Crystal Structures, and Fluorescence Properties of Ni(II)–Ln(III) Complexes (Ln = Sm, Pr, Eu), Russ. J. Coord. Chem. 44 (2018) 365–371. doi:10.1134/S1070328418050019.

[177] T.W. Werner, S. Reschke, H. Bunzen, H.-A.K. Von Nidda, J. Deisenhofer, A. Loidl, D. Volkmer, [$Co_5Tp*4(Me_2bta)_6$]: A Highly Symmetrical Pentanuclear Kuratowski Complex Featuring Tris(pyrazolyl)borate and Benzotriazolate Ligands, Inorg. Chem. 55 (2016) 1053–1060. doi:10.1021/acs.inorgchem.5b01982.

Recent advances in the coordination chemistry of benzotriazole-based ligands